

NUREG/CR-2966

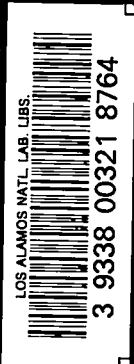
LA-9536-MS

C.3

CIC-14 REPORT COLLECTION
REPRODUCTION
COPY

Los Alamos National Laboratory is operated by the University of California for the United States Department of Energy under contract W-7405-ENG-36.

*Buckling Investigation of Ring-Stiffened
Cylindrical Shells Under Unsymmetrical
Axial Loads*



Los Alamos Los Alamos National Laboratory
Los Alamos, New Mexico 87545

An Affirmative Action/Equal Opportunity Employer

NOTICE

This report was prepared as an account of work sponsored by an agency of the United States Government. Neither the United States Government nor any agency thereof, or any of their employees, makes any warranty, expressed or implied, or assumes any legal liability or responsibility for any third party's use, or the results of such use, of any information, apparatus, product or process disclosed in this report, or represents that its use by such third party would not infringe privately owned rights.

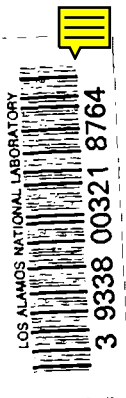
NUREG/CR-2966
LA-9536-MS

RF

Buckling Investigation of Ring-Stiffened Cylindrical Shells Under Unsymmetrical Axial Loads

William Baker
Joel Bennett
Charles Babcock

Manuscript submitted: September 1982
Date published: October 1982



Prepared for
Mechanical/Structural Engineering Branch
Division of Engineering Technology
Office of Nuclear Regulatory Research
US Nuclear Regulatory Commission
Washington, DC 20555

NRC FIN No. A7222

Los Alamos Los Alamos National Laboratory
Los Alamos, New Mexico 87545

CONTENTS

ABSTRACT.	1
INTRODUCTION.	1
DESCRIPTION OF MODELS AND LOADING METHOD.	4
IMPERFECTION MEASUREMENTS AND RESULTS	6
TEST PROCEDURE AND RESULTS.	9
SUPPORTING ANALYSIS.	13
REFERENCES	19
APPENDICES	
A. CHORD GAGE DATA AND RESULTS FOR MODEL 1.	54
B. CHORD GAGE DATA AND RESULTS FOR MODEL 2.	62
C. COMPARISON OF LVDT AND CHORD GAGE RESULTS.	70

BUCKLING INVESTIGATION OF RING-STIFFENED CYLINDRICAL SHELLS UNDER UNSYMMETRICAL AXIAL LOADS

by

William Baker, Joel Bennett, and Charles Babcock

ABSTRACT

Two buckling experiments are described in detail. The first purpose of these experiments is to establish baseline values for the buckling loads and modes for ring-stiffened cylindrical shells that have geometric parameters characteristic of the ring-stiffened cylindrical section of a typical nuclear steel containment vessel. A series of follow-on experiments on nominally identical ring-stiffened cylinders that have framed and reinforced penetrations typical of nuclear industry practice are planned and will be described in a separate report. This report is issued separately because of the volume of detail included on methods, measurements, and data reduction techniques. In addition, a second purpose of these experiments is to serve as a set of benchmark experiments for computer codes that can predict buckling loads for axisymmetric geometries, and in this respect this work stands alone. Complete material stress-strain curves are described and complete geometric imperfection data for the shells are given. These data are also available in digitized form on tape. Typical load-strain information is reported, as well as the distribution of load around the cylinder at buckling. A method for taking and reducing chord gage measurements to characterize the out-of-roundness imperfections is also examined in detail and comparisons to actual imperfection sweep measurements are made.

INTRODUCTION

Steel containments are currently in use on many nuclear power stations. Several future power plants in various stages of planning will also utilize steel containments. The steel containments are essentially large pressure vessels. One common type consists of a vertical cylindrical section with a

hemispherical or torispherical dome. Generally, the cylindrical section is reinforced with several ribs. Figure 1 is a cross section of a reactor plant with this type of steel containment.

The primary function of the containment is that of safety in the event of accidental release of radioactive material from the reactor. Therefore, it must maintain its integrity as a pressure vessel throughout the life of the plant. This includes conditions such as normal operating loads, loads imposed due to operating accidents and loads imposed due to seismic activity. Because of the complexity of these operating loads and the various required combinations and the complexity of the problem itself, it is generally accepted that use of a computer and selected large codes is advantageous in the design phase, as well as in subsequent analyses made on the containment.

The loads on the containment invariably result in compressive stresses in the containment, and under certain conditions these stresses could result in a buckling type of failure. While the analysis for buckling loads for the idealized problems is quite direct and easily handled by closed form solutions or numerical solutions to the governing equations, there can be large differences between these solutions and the results of what appear to be simple experiments, which apparently closely match the conditions of the analysis. The predicted buckling load using the closed form solution is always higher than the experimentally determined buckling. Similarly, the predicted buckling load from numerical solutions may vary substantially from those determined from carefully planned experiments. However, recent improvements in buckling computer codes have led some users and developers of the codes to believe that they are now adequately accurate for better understanding the structural response of steel containments to the myriad of inputs to which they may be subjected. This study has been conducted to aid in verifying the validity of this belief, and the work is being carried out under the "Margins to Failure" program of the Nuclear Regulatory Commission at their request.

The classical buckling load, P_{c1} , for a cylindrical shell loaded uniformly in the axial direction on the edge has been shown to be

$$P_{c1} = \frac{2\pi Et^2}{\sqrt{3(1-\nu^2)}} .$$

where E = modulus of elasticity,
 t = wall thickness, and
 ν = Poisson's ratio.

Results of tests on actual cylinders always give buckling loads less than this value, sometimes as much as 80 to 85% less. The reasons for this discrepancy are clearly differences in the idealized analytical model and the test conditions. The test conditions generally recognized as being the significant ones may be broadly classified as follows:

1. Imperfections in the shell geometry.
2. Boundary conditions at the loaded ends.
3. Material properties and condition.

The imperfection effect of these test conditions has been the subject of extensive studies, both experimental and analytical in the past. The initial work was done by Donnell.¹ Subsequently, numerous investigators have studied this problem both analytically and experimentally. Examples include work by von Karman and Tsien,² Donnell and Wan,³ Horton and Durham,⁴ Hutchinson and Amazigo,⁵ Arbocz and Babcock,⁶ and Singer.⁷ These and the many works not mentioned have contributed much to the understanding of the nature of imperfections occurring in shells and their effect on the buckling load. One conclusion for which investigators are in general agreement is that the imperfections are the single greatest factor causing the reduction of the actual buckling load from classical.

The second factor mentioned above is that of boundary conditions at the loaded ends, and this includes both the fixity at the ends as well as the load distribution around the edges. This factor has also been studied in some detail, with works by Weller, Baruch and Singer,⁸ Weller,⁹ and Singer and Rosen,¹⁰ being examples. One conclusion that may be drawn from these studies is that the fixity at the ends does have an effect on the buckling loads, but it is not significant enough to explain the wide scatter in experimental results.

The last category, shell material properties, is used in a broad sense, to include factors such as nonlinearity of the stress-strain curve, anisotropy, residual stresses, and nuclei of plastic strain. Of these only the effect of nonlinearities has been the subject of much study, and some current analysis techniques do include nonlinear material model capability.

The significant differences between the predicted and actual buckling loads have led to use of a "knockdown factor" in the American Society of Mechanical Engineering (ASME) Boiler and Pressure Vessel Code for the design of containments. The knockdown factor may be defined as the ratio of the desired (or actual) buckling load to the classical value. It is always less than one, and the values in the codes are generally determined from the results of experimental investigations. Normally, these knockdown factors are conservative.

Several of the current shell computer codes, such as BOSOR,¹¹ STAGS,¹² and ADINA¹³ have the capability to include the effects of factors which cause the actual buckling load to be less than the classical buckling load. They can also handle complications, such as imperfections in ring stiffeners, penetrations, and reinforcing, that invariably appear on steel containments. However, there have been no buckling tests conducted on shells designed to approximate steel containments for reactors and possessing these complications to check or evaluate the accuracy of these refined codes.

The specific purpose of this study was to conduct an experimental program for which buckling tests would be conducted on two steel "containment-like" cylinders to determine buckling loads and other data as required for use in evaluating the accuracy of numerical codes for buckling predictions.

Activities undertaken in the course of this work included:

1. Design and fabrication of the cylinders,
2. Design and fabrication of the loading fixtures,
3. Measurement of imperfections in the cylinder,
4. Collection of required material property data,
5. Analysis with certain numerical codes in support of the design and test planning, and
6. Conduction of the buckling tests.

One specific numerical solution to which the results of the buckling tests were to be compared was carried out by the Lockheed Palo Alto Research Laboratory.

DESCRIPTION OF MODELS AND LOADING METHOD

A sketch of the models designed and fabricated for these tests is shown in Fig. 2. The design of these cylinders was based upon inputs received from

D. Bushnell, Lockheed Palo Alto Research Laboratory, and R. B. Grove, Chicago Bridge and Iron Company. Values for the significant parameters are given below:

Radius (R), in.	13.75	(34.93 cm)
Thickness (t), in.	0.030	(0.76 mm)
R/t	458	
Stiffener area (A_r) in. ²	0.191	(12.32 mm ²)
Maximum stiffener spacing (λ), in.	2.5	(6.35 cm)
λ/\sqrt{Rt}	3.89	
$A_r/\lambda t$	0.255	(0.255)
Stiffener moment of inertia ($I_{E\theta}$), in. ⁴	1.485×10^{-4}	(6.18×10^{-3} cm ⁴)

The size of the stiffeners was based in part upon requirements given in Code Case N-284 for Section III, Class MC constructions, NE-3222 of the ASME Boiler and Pressure Vessel Code. This code case places the following lower bounds on size parameters for the stiffeners.

$$A_r/\lambda t \geq .06$$

$$I_{E\theta} > .31 \times 10^{-4} \text{ in}^4 \text{ (} 1.29 \times 10^{-3} \text{ cm}^4 \text{) .}$$

Both of these requirements are exceeded in these models. It should be pointed out that $I_{E\theta}$ is the moment of inertia of the combined cross section of the stiffener and the effective width of the shell about the centroidal axis of the two and is calculated as specified in the code case. No attempt was made to have $I_{E\theta}$ and $A_r/\lambda t$ equal to the code requirements, only to insure that the values exceed these requirements.

The material used for the shell was ASTM A366 steel, since it is a common deep drawing structural steel with a smooth stress-strain curve to failure. The material used for the ring stiffener was a low-carbon (1010) steel. Fabrication of the cylinder was accomplished by rolling the sheet into a cylinder and welding the joint. The weld at the joint was ground flush on both the inside and outside. The ring stiffeners were turned from sheet stock. Assembly of the shell and ring stiffener was done by spot welding initially and

then soft soldering. The spot welding was done with a low capacity unit at approximately 6-in. spacings (10 cm) and functioned primarily to hold the rings in position for soldering.

The large rings at each end of the cylinder served to give additional radial stability and to aid in obtaining a uniform load distribution at the ends. They were made of steel. Figure 3 shows one of the completed cylinders.

The material for the cylinders was purchased in two thicknesses, 0.030 in. (0.76 mm) and 0.116 in. (2.95 mm). Tests were run on specimens cut from each of these thicknesses to determine the modulus of elasticity and the 0.2% offset yield. Table I shows the results of these tests, and Fig. 4 shows typical stress-strain curves for each of these stock thicknesses.

The testing machine used to load the cylinders was a 50,000-lb (222,400-N) servohydraulic MTS unit. Figure 5 describes the hardware used to apply the load. This figure shows the load as applied, i.e., with an eccentricity of $R/2$. The same hardware was used for the axisymmetric loading tests done prior to the buckling test.

IMPERFECTION MEASUREMENTS AND RESULTS

As part of the test program, imperfection measurements were made on the shells. Knowledge of the initial imperfections is necessary to access qualitatively the severity of deviation from perfect and quantitatively to assess expected effect of the imperfection on the buckling load. For this work, the measurements were made using two separate techniques, one with a "chord gage" and the second involved collection of digital data on the variation in the radius to the outside surface of the shell at many axial stations on the shell.

The chord gage measurements simulate a technique which may be used during or after construction of actual containments, and these measurements were made at the suggestion of R. Grove of Chicago Bridge and Iron Co. The digital data more precisely define the contour of the shell, and they were taken to permit inclusion of imperfections in subsequent numerical analyses and for development of imperfection measurement methods for steel containments.

Prior to a discussion of these measurements, it is advantageous to describe the location identification scheme used on the cylinder. The same scheme will be used to specify locations for all phases of this report. The

angular position is specified by the angle in degrees measured counterclockwise around the cylinder looking down from the top. The welded seam was taken as angular position zero. The axial position, or level, is given in terms of the station number at which measurements were made. These stations are on 0.50-in. (12.7-mm) spacings with station 1 being 0.25 in. (6.4 mm) from the bottom end ring. Reference to a reinforcing ring is by the ring number, with ring one being the lowest and the others numbered in sequential order. Figure 6 locates the levels and reinforcing rings for identification.

The chord gage measurements were taken with the gage described in Fig. 7. Figure 8 shows it in use. The dial indicator reading, Δ , was taken at 10^0 increments around the circumference at twelve levels on the shell surface and on the seven reinforcing rings. The data were taken at two levels between the reinforcing rings having the widest spacing [2.5 in. (6.3 cm)] and on the outside of each of the seven reinforcing rings adjacent to these bays. This measurement process resulted in 684 readings for each cylinder.

Reduction of these data included computation of the local radius of curvature at each datum point (ρ), average radii at each axial station, and differences between corresponding local and average radii. These values were determined for the reading taken with the chord gage on the shell surface and on the reinforcing rings.

The local radius of curvature at a datum point is actually an average radius over the arc spanned by the chord gage, and it is found from the equation

$$\rho = \frac{a^2 - 2r\Delta + \Delta^2}{2\Delta} ,$$

where the symbols are defined in Fig. 6.

Appendices A and B give the data and summarize the results for cylinders 1 and 2 respectively. Typical plots of data and results are shown in Fig. 9. A further study of data reduction techniques for chord gage data is described in the Supporting Analysis section.

The digital data on the imperfections in the shells were collected using a technique based, in principle, on a method first used by Arbocz and Babcock⁶. It involves collection of sufficient data to define the contour of the shell at the time of the measurements.

The presence of imperfections results in the test specimen not being cylindrical, and it is necessary then to refer to the "best fit cylinder." In Ref. (6), a priori knowledge of what the location and orientation of the axes of the best fit cylinder are not assumed, and it is subsequently determined from the data. This was considered necessary when the location of the reference axes and best fit axes differ by an amount that is the same order as or greater than the actual imperfections.

Because of the construction method for these shells, and care in establishing the orientation of the rotation axis for the imperfection measurements, it was not considered necessary to use the more complex data reduction scheme for establishing the best fit cylinder axis. The data collection scheme used in this work is based upon the following assumptions.

1. The axis of rotation of the rotary table used and the best fit cylinder axis are parallel.
2. The best fit cylinder axis is normal to the contact surface of the base ring.

Validity of these assumptions is supported by measurements of the maximum vertical runout at the periphery on the rotary table base plate [.001 in. (0.025 mm)] and on the top ring of the test shells [.002 in. (0.050 mm)].

The measurement system used is shown in Fig. 10. Linear variable differential transformers (LVDT) were used to obtain a voltage proportional to the change in the radial position of the shell surface as the cylinder was slowly turned by the rotary table. The voltages were recorded at selected increments of rotation. On completion of a revolution of the models, the carriage supporting the LVDT's was moved to a different vertical position for another sweep, and this process was repeated until data at all desired levels were obtained. The voltage measurements were made and recorded with a data acquisition system based upon a Hewlett Packard 9825 calculator.

At each sweep around a circumference, measurements for determining the radial displacement were made at increments of 2 degrees. The data acquisition system was triggered with appropriately spaced lobes on the drive wheel of the rotary table. Sweeps were made on each cylinder at 0.5-in. (12.70-mm) increments, starting 0.25 in. (6.35 mm) above the base ring. This gave imperfection data at 48 axial stations. The LVDT's were calibrated with a depth micrometer.

Additional data taken included an inside diameter measurement at one specific location, and a radial displacement measurement for each axial position at one specific angular station on the cylinder. The inside diameter was measured with an inside micrometer and was used in establishing a reference radius. The set of radial displacement measurements was made with a dial indicator, and they were used in relating the measurements made with the LVDT's at all axial stations to the reference radius.

Results determined from these imperfection measurements included the average radii for the cylinders and contour plots. The average radius for shell 1 was 13.753 and 13.751 for shell 2. The contour plots for shells 1 and 2 are shown in Figs. 11 and 12.

TEST PROCEDURE AND RESULTS

Upon completion of the imperfection measurements, strain gages were put on the shell at selected locations. Results of computations and the fact that the load was to be applied with an eccentricity of $R/2$ were used as a guide in determining gage locations. Figure 13 shows these locations. The identification numbers shown are the ones used throughout this report. All of the the strain gages used were single-element gages, mounted for measurement of axial strain, with the exception of locations 13 and 63. At locations 13 and 63, rectangular rosettes were used, oriented so one of the elements was axial and one was circumferential. Gages 9 and 9' were mounted as close to the base rings as possible.

At each location indicated on Fig. 13, there was a gage on the outside surface and a corresponding gage on the inside surface of the shell. Every gage was monitored individually during the tests. This arrangement was used so the bending strains could be separated from the membrane strains. There was a total of 102 strain gages on each cylinder. The reasons for the locations selected were as follows.

1. Gages 1 through 8 and 1' through 8' were used to determine the uniformity of loading (or lack of it) around the ends.
2. Gages 11 through 65 were applied to give coverage of the area where the first buckle would form, with the rosettes at 13 and 63 being used at the most likely position of the buckle (based upon analysis).

3. Gages 9 and 9' were used to monitor the strains at the discontinuity due to the end rings.

Shell 1 was tested first, and the initial test was with axisymmetric loading. The hardware shown in Fig. 5 was assembled on the testing machine. Initially, no filler was used in the gaps between the end plates and the end rings, so there were invariably air gaps between the end rings of the cylinder and the end plates because of manufacturing tolerances and distortion. A 10 000-lb (44.5-kN) load was slowly applied, and during the loading process all strain gage channels were repeatedly scanned. The 10-000 lb (44.5-kN) peak load was selected since it was well below the buckling load of the cylinder. A study of the load-strain plots for gages 1 through 8 and 1' through 8', both for the inside and outside gages showed that the load distribution around the ends was nonuniform to a large degree. The following table illustrates this nonuniformity.

		<u>Gages 1-8*</u>	<u>Gages 1'-8'*</u>
Membrane Strain ($\mu\epsilon$)	Maximum	142	260
	Minimum	69	49
	Average	113	128
	Standard Dev.	29	58
Bending Strain ($\mu\epsilon$)	Maximum	33	120
	Minimum	3	4
	Average	15	58
	Standard Dev.	10	57
% Bending to Membrane	Maximum	33	61
	Minimum	2	3
	Average	15	36
	Standard Dev.	11	25

*Based upon values at 10 000 lb (44.5 kN) load.

This nonuniformity of load distribution at the ends was considered excessive. To reduce this nonuniformity, the gaps between the end rings on the cylinder

and the loading plates were filled with an epoxy. A mold release was used to facilitate removal of the end plates, and a load of 2000 lb (8.9 kN) was applied to the assembly during the curing process to insure uniform distribution of the epoxy on the load bearing surfaces (see Fig. 14).

After curing of the epoxy, this assembly was once again tested with an axisymmetric load of 10 000 lb (44.5 kN). The signal from all strain gages was once again monitored at close intervals. A study of the data obtained showed that the uniformity of loading had been significantly improved. A comparison of values in the following table with the corresponding ones obtained without the epoxy filler demonstrates this improvement.

		<u>Gages 1-8*</u>	<u>Gages 1'-8'*</u>
Membrane Strain ($\mu\epsilon$)	Maximum	127	156
	Minimum	110	104
	Average	118	130
	Standard Dev.	7	18
Bending Strain ($\mu\epsilon$)	Maximum	37	35
	Minimum	0	0
	Average	10	17
	Standard Dev.	13	11
% Bending to Membrane	Maximum	33	27
	Minimum	0	0
	Average	8	13
	Standard Dev.	11	8

*Based upon values at 10 000 lb (44.5 kN) load.

Data are not presented in this report showing the effect of the epoxy filler on readings at gages other than 1-8 and 1'-8'. However, in general it also resulted in the membrane strains being more nearly uniform, and the bending strains reduced for the area covered by gages 11 through 65.

The unit was then moved from the axisymmetric loading position to the R/2 load position for the buckling test. Figures 15 and 16 are views of the test

configuration prior to the buckling test. The load was applied in a "controlled force" mode, with the maximum ram displacement limited to 0.5 in. (12.7 mm). The rate of loading was about 6 lb/s (26.7 N/S). The maximum force range was 25 000 lb (111 kN). Readings were taken from all of the strain gages on the cylinder.

At a load of 21 900 lb (97 kN), the hydraulic power supply for the loading machine cut out, terminating the test and removing the load. After correcting the equipment problem, the shell was reloaded. The loading rate was about 50 lb/s (220 N/s) to 20 000 lb (89 kN), and then it was reduced to about 8 lb/s (35.6 N/s).

The buckle occurred at a load of 24 744 lb (103.65 kN), including the tare weight of the top loading plate. The buckle apparently initiated at $\theta = 180^\circ$, and an axial position in the top 2-1/2" (63.5-mm) wide bay. Figures 17 and 18 show this buckle.

The buckle probably was initiated at or near strain gage location 63, the position where rosettes were located. Figures 19 through 24 show the data from these rosettes and the results of the rosette data reduction. For comparison, similar data and results are shown for location 13 (Figs. 25 through 30).

Figure 31 shows the axial strain distribution around the top and bottom at a load of 23 000 lb (102 kN). The data from most of these gages were linear up to 23 000 lb (102.3 kN). The gages that departed from linearity did so because their location was near the buckle. The strain in gages 5 inside, 6 inside, 7 inside, 8 inside, 5' inside, and 6' inside decreased significantly and the strain in gages 7' and 8' increased significantly. These changes signalled a definite change in load distribution at about 23 000 lb (102.3 kN).

Cylinder 2 was tested next. Because of the experience with cylinder 1, the epoxy gap filler was applied prior to any testing. After curing, an axisymmetric load of 5000 lb (22.2 kN) was applied to check all strain gage circuitry and the recording system. Then the cylinder was offset to R/2 in the testing machine and the buckling test conducted. As with cylinder 1, regular scans were made of all strain gage circuits, applied force, and ram displacement. In this test, the ram control was on displacement, not force. The load was applied at an average rate of about 9 lb/s (40 N/s), and it was monotonically increased to buckling.

Buckling occurred at 26 911 lb (119.70 kN). Failure was not dramatic, as with force control of the ram, but buckling was easily identified by the instantaneous drop in load supported by the cylinder. Ram displacement at buckling was 0.063 in. (1.60 mm), and the test was continued to 0.073 in. (1.85 mm) to produce an easily visible permanent deformation.

The location of the buckle was between reinforcing rings 1 and 3. It was basically an "elephant's foot" type of buckle, but with rotation of ring 2, and is shown in Figs. 32 and 33.

The axial strain distribution around the top of the cylinder is shown in Fig. 34. In Fig. 34, the plotted data marked with an asterisk were determined by extrapolation, that is, by extending the initial straight segment of the force-strain curves to the 26 900-lb (119.7-kN) load. This extrapolation better represents the initial force distribution at the boundary.

Gage locations 4, 5, and 6 were in the immediate vicinity of the location of the initial buckle, and data from these gages are shown in Figs. 35, 36, and 37. Three characteristics are observed in these graphs. First, moderate bending strain occurs from the very beginning of loading and it increases percentage-wise as the loading increases. Second, the largest measured plastic strains occurred at gage 5, which was nearest the initial buckle location. Third, the strains clearly grow at a much faster rate near the location of the initial buckle.

The load-strain graphs of the other gages in the pattern in the central area of the cylinder had characteristics similar to that of gage 5, though to a lesser degree. These included gages 13 axial, 14, 23, 33, and 43. Their behavior was indicative that the cylinder was close to buckling at additional locations.

SUPPORTING ANALYSIS

A. Axisymmetric Modeling of the BBM Specimens

Supporting analyses were carried out using the Los Alamos version of the finite element code ADINA. The code has several modifications that make it an effective tool for carrying out nonlinear collapse analysis. Among these modifications are the addition of a nonlinear axisymmetric shell element described in Ref. 14. Also, the material used in these tests is a "deep drawing" material with a uniaxial stress-strain curve that is best described

by a sequence of tangent moduli. This capability was added to the material model library of the shell element. Basically, this modification consists of having available a multilinear tabular description of the uniaxial stress-strain curve and implementing the logic for describing a load-increment dependent hardening modulus in the elastic-plastic state. The points plotted in Fig. 4 show the results of an ADINA modeling of the uniaxial stress-strain test for the A366 material using these modifications.

An axisymmetric finite element model of the baseline benchmark cylinders composed of 484 shell elements with 17 continuum elements to represent the rings was constructed as shown in Fig. 38. This model was used to predict the results of the axisymmetric prebuckling loading tests and to examine the adequacy of the end ring boundary conditions. In particular, one of the questions we investigated was the effect of having the first set of reinforcing rings be spaced 1 in. (25.4 mm) away from the end rings as opposed to 3/4 in. (19 mm), as was called for in the original design.

Figures 39 and 40 show the load vs strain curves calculated from the axisymmetric ADINA model for elements that correspond to gage locations 9' and 63 on the test cylinders. The calculation was carried to near "buckling" as indicated by a failure of the code to converge within a load step for 30 iterations. Figure 41 shows the deformed mesh at "buckling". It should be noted that the code was converging during the final load step so that the predicted axisymmetric buckling load is in excess of 44 988 lb (200.1 kN) or, 520 lb/in. Although the purpose of these calculations was not to predict the buckling load, comparison of the predicted axisymmetric "buckling" membrane strain of $674 \mu\epsilon$ to the average strains along the symmetry axis ($\theta = 180^\circ$) of Figs. 31 and 34, indicates that the axisymmetric model can indeed give some indication of the buckling load for this problem.

A further conclusion that was drawn from these computer runs was that the main effect of the 1-in. (25.4-mm) end ring spacing was to cause yielding in the first shell level to occur before it occurred in the wider spaced ring regions. This was not the case for the 3/4-in. (19-mm) spacing; for this case, yielding occurred in the wider spaced ring sections first. However, because the membrane strains for a given loading were still slightly larger in the wider space ring regions for both cases, it was judged that buckling should occur there. In this respect, the influence of the design change was regarded as minimal.

B. Reduction of the Chord Gage Data

One aspect of the imperfection measurements is to correlate the chord gage measurements with the direct displacement measurements. Indeed, while chord gage measurements give data in a form similar to that required by the ASME boiler and pressure vessel code (Ref. 16) for specifying the deviation from true circular form, the opportunity is seldom available to compare this method of measuring imperfections to direct data. In fact, if imperfection measurements are to be used in conjunction with analytical methods to predict buckling, several questions arise regarding the chord gage method. First, how many chord gage measurements are necessary to characterize the important components of the imperfections? Second, what method should be used to reduce the data and to put it into a usable form for analysis?

For use in an analysis, presumably an analytical model of the shell will incorporate the imperfections into the model geometry. There are several methods that can be used, and we will present two variations of one here. The chord gage measurement is based upon the assumption that the shell between the gage points is circular with radius ρ . The geometry of the measuring device is shown in Fig. 7. The rise height Δ is calculated as

$$\Delta = (r + \rho) - \sqrt{(r + \rho)^2 - a^2} .$$

Assuming that the measured radius ρ is only slightly different than the nominal radius ρ_n

$$\rho = \rho_n + \bar{\rho} = \rho_n \left[1 + \frac{\bar{\rho}}{\rho_n} \right] ,$$

where $\bar{\rho}/\rho_n \ll 1$ and Δ is the change in rise height

$$\Delta = \Delta_n + \bar{\Delta} ,$$

where Δ_n is the nominal rise height, then the change in rise height is calculated as

$$\bar{\Delta} = \bar{\rho} \left[1 - \frac{(r + \rho_n)}{(r + \rho_n)^2 - a^2} \right].$$

For the chord gage and shell values in this experiment, we have

$$\begin{aligned} r &= .250 \text{ in.} \\ \rho_n &= 13.75 \text{ in.} \\ a &= 2.431 \text{ in.} \end{aligned}$$

Therefore,

$$\begin{aligned} \bar{\Delta} &= - .01543 \bar{\rho} \quad \text{or} \\ \bar{\rho} &= - 64.83 \bar{\Delta} = -C \bar{\Delta} . \end{aligned}$$

Here, the change in radius was measured at 36 locations around the shell. In principal, the initial deviation from circular can be calculated from these data. The procedure is as follows.

The change in curvature can be calculated in terms of the normal displacement. Flugge's (Ref. 15) expression will be used in that it accounts for curvature changes because of uniform displacement.

$$\chi_\theta = \frac{1}{\rho_n^2} \frac{d^2 w}{d\theta^2} + \frac{w}{\rho_n^2} = \frac{1}{\rho} - \frac{1}{\rho_n} ,$$

where w = radial displacement (+ outward) and,

$$\frac{1}{\rho_n} - \frac{1}{\rho} = \frac{\bar{\rho}}{\rho_n^2} .$$

We have then

$$\frac{d^2 w}{d\theta^2} + w = \bar{p} = -C\bar{\Delta} = 64.83 (0.2127 - \Delta) . \quad (1)$$

Now assume that the data can be developed into a Fourier series so that Eq. (1) can be solved for $w(\theta)$. That is,

$$\bar{p}(\theta) = A_0 + \sum_{n=1}^N (A_n \cos n\theta + B_n \sin n\theta) .$$

we know that w is periodic of period 2π , and therefore we can also express w as

$$w(\theta) = w_0 + \sum_{m=1}^M (D_m \cos m\theta + E_m \sin m\theta) .$$

Substitute both expressions into Eq. (1) and obtain that,

$$\begin{aligned} w_0 + \sum_{m=1}^M [D_m(1-m^2) \cos m\theta + E_m(1-m^2) \sin m\theta] \\ = A_0 + \sum_{n=1}^N [A_n \cos n\theta + B_n \sin n\theta] . \end{aligned}$$

Clearly $w_0 = A_0$ and

$$D_m = \frac{A_n}{1-m^2} \quad E_m = \frac{B_n}{1-m^2} , \quad m, n = 1 \text{ or } m, n = 2, 3, \dots .$$

The case of $m = n = 1$ yields no useful information. This mode is a rigid body translation as shown in Fig. 42 and can be discarded. In fact when the

$n = 1$ harmonic is calculated from the chord gage data (ρ_i), the values of A_1 and B_1 should be zero. But in fact because the actual results are not zero, that is, there are probably rigid body components in the data, it should be discarded.

With this simplification

$$w = A_0 + \sum_{n=2}^N \frac{A_n}{1-n^2} \cos n\theta + \frac{B_n}{1-n^2} \sin n\theta \quad (2)$$

The chord gage data were used at each level to numerically obtain the Fourier coefficients A_n and B_n and Eq. (2) was evaluated at 36 points around the cylinder for each level. Appendix C shows the results of both chord gage and LVDT data on cylinder 1 and cylinder 2.

An alternate to performing the Fourier sum of Eq. (2) is to solve Eq. (1) numerically. Using a central difference scheme to represent the second derivative and evaluating Eq. (1) at each measured point, the following expression is found

$$\frac{1}{\Delta\theta^2} \begin{bmatrix} -2+\Delta\theta^2 & 1 & 0 & 0 & \cdot & \cdot & 1 \\ 1 & -2+\Delta\theta^2 & 1 & 0 & \cdot & \cdot & 0 \\ 0 & 1 & -2+\Delta\theta^2 & 1 & \cdot & \cdot & 0 \\ \cdot & \cdot & \cdot & \cdot & \cdot & \cdot & \cdot \\ \cdot & \cdot & \cdot & \cdot & \cdot & \cdot & \cdot \\ 0 & \cdot & \cdot & 0 & 1 & -2+\Delta\theta^2 & 1 \\ 1 & \cdot & \cdot & 0 & 0 & \cdot & -2+\Delta\theta^2 \end{bmatrix} \begin{bmatrix} w_1 \\ w_2 \\ w_3 \\ \cdot \\ \cdot \\ w_{35} \\ w_{36} \end{bmatrix} = C \begin{bmatrix} \bar{\Delta}_1 \\ \bar{\Delta}_2 \\ \bar{\Delta}_3 \\ \cdot \\ \cdot \\ \bar{\Delta}_{35} \\ \bar{\Delta}_{36} \end{bmatrix}$$

where for this experiment, $\Delta\theta = 10^0 = \pi/18$.

Although they are somewhat arbitrary, initial conditions must be supplied to remove the singularities from this matrix equation. To preserve the proper symmetry for the solution required by removal of the $n = 1$ mode from the data, we chose to set $w(\pi/2) - w(\pi) = 0$. Although this requirement will give the proper symmetry to the solution, the $n = 1$ mode must still be subtracted from the result. The $n = 1$ Fourier coefficients were obtained for the chord

gage data and subtracted from the solution of Eq. (3). Aside from any arbitrary constant, the results are identical. Because of the necessity of removing the $n = 1$ mode and also performing the Fourier analysis of the data combined with the requirement of solving the matrix equations for w , this variation is probably no more efficient, computationally, than the direct Fourier analysis.

A third method for reducing the chord gage data is to use it as a direct measure of the variations in the radius of curvature. By referring each measurement to a common coordinate system, and locating the center and radius of the best fit circle, the displacement of each measured point from this circle can be computed. Theoretically, this displacement will be the required imperfection. Although the conceptual details of the method have been worked out, we have not attempted to implement them computationally, and have not assessed the accuracy requirements for this method.

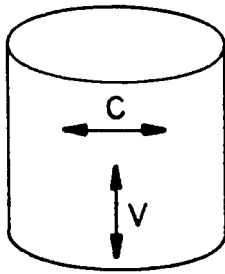
REFERENCES

1. L. H. Donnell, "A New Theory for the Buckling of Thin Cylinders under Axial Compression and Bending," *Trans. ASME*, Vol. 56, p. 795, 1934.
2. T. von Karman and H. S. Tsien, "The Buckling of Thin Cylindrical Shells Under Axial Compression," *Journal of Aeronautical Sciences*, Vol. 8, p. 303, June 1941.
3. L. H. Donnell and C. C. Wan, "Effect of Imperfections on Buckling of Thin Cylinders and Columns Under Axial Compression," *Journal of Applied Mechanics*, Vol. 17, No. 1, p. 73, 1950.
4. W. H. Horton and S. C. Durham, "Imperfections, A Main Contributor to Scatter in the Experimental Values of Buckling Load," *International Journal of Solids Structures*, Vol. 1, p. 59, 1965.
5. J. W. Hutchinson and J. C. Amazigo, "Imperfection Sensitivity of Eccentrically Stiffened Shells," *AIAA Journal*, Vol. 5, No. 3, p. 392, March 1967.
6. J. Arbocz and C. D. Babcock, "The Effect of General Imperfections on the Buckling of Cylindrical Shells," *Journal of Applied Mechanics*, Vol. 28, p. 28, 1969.
7. J. Singer, "Buckling of Integrally Stiffened Cylindrical Shells--a Review of Experiment and Theory," Contributions to the Theory of Aircraft Structures, Delft University Press, 1972.

8. T. Weller, M. Baruch, and J. Singer, "Influence of In-plane Boundary Conditions on Buckling of Ring Stiffened Cylindrical Shells," TAE Report 101, Technicon-Israel Institute of Technology, Haifa, Israel, October 1970.
9. T. Weller, "Further Studies on the Effect of In-plane Boundary Conditions on the Buckling of Stiffened Cylindrical Shells," TAE Report 120, Technicon-Israel Institute of Technology, Haifa, Israel, January 1974.
10. J. Singer and A. Rosen, "Influence of Boundary Conditions on the Buckling of Stiffened Cylindrical Shells," Buckling of Structures, Proc. of IVTAM Symposium, Harvard Univ., June 1974. Springer-Verlag, Berlin, 1976, p. 227.
11. D. Bushnell, "BOSORS, Program for Buckling of Elastic-Plastic Complex Shells of Revolution Including Large Deflections and Creep," Computers and Structures, Vol. 6, pp 221-239, 1976.
12. B. O. Almroth and F. A. Brogan, "The STAGS Computer Code," NASA CR 2950, February 1978.
13. K. J. Bathe, "ADINA, A Finite Element Program for Automatic Dynamic Incremental Nonlinear Analysis," MIT Dept. of Mech. Eng. report 82448-1, September 1975, Revised December 1, 1978.
14. W. A. Cook, "Linear and Nonlinear Symmetrically Loaded Shells of Revolution Approximated with the Finite Element Method," Los Alamos National Laboratory Report LA-7538-MS, October 1978.
15. W. Flugge, "Stresses in Shells," Springer-Verlag New York, Inc., 1966.
16. ASME Boiler and Pressure Vessel Code, Section III: Nuclear power plant components, Division 1, Subsection NE, Class MC Components, NE-3332 (1979) pp 68-70.

TABLE I
RESULTS OF α/ϵ TESTS ON ASTM A366 AND LOW-CARBON STOCK STEEL TO
BE USED IN RING-STIFFENED CYLINDER MODELS

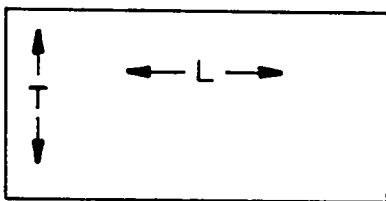
1. 30 mil. stock--cylinder wall--ASTM A366



$t = .0295 \text{ in.}$

<u>Specimen No.</u>	<u>Direction</u>	<u>E(psi)</u>	<u>σ_y (0.2% offset, psi)</u>
H	V	27.73×10^6	30,508
E	C	27.73×10^6	29,152
F	C	26.03×10^6	29,491

2. 116 mil. stock reinforcing rings--AISI 1010



$t = .116 \text{ in.}$

<u>Specimen No.</u>	<u>Direction</u>	<u>E(psi)</u>	<u>σ_y (0.2% offset, psi)</u>
N	T	29.84×10^6	40,000
M	T	30.52×10^6	
I	L	29.48×10^6	36,380
K	L	29.05×10^6	34,655

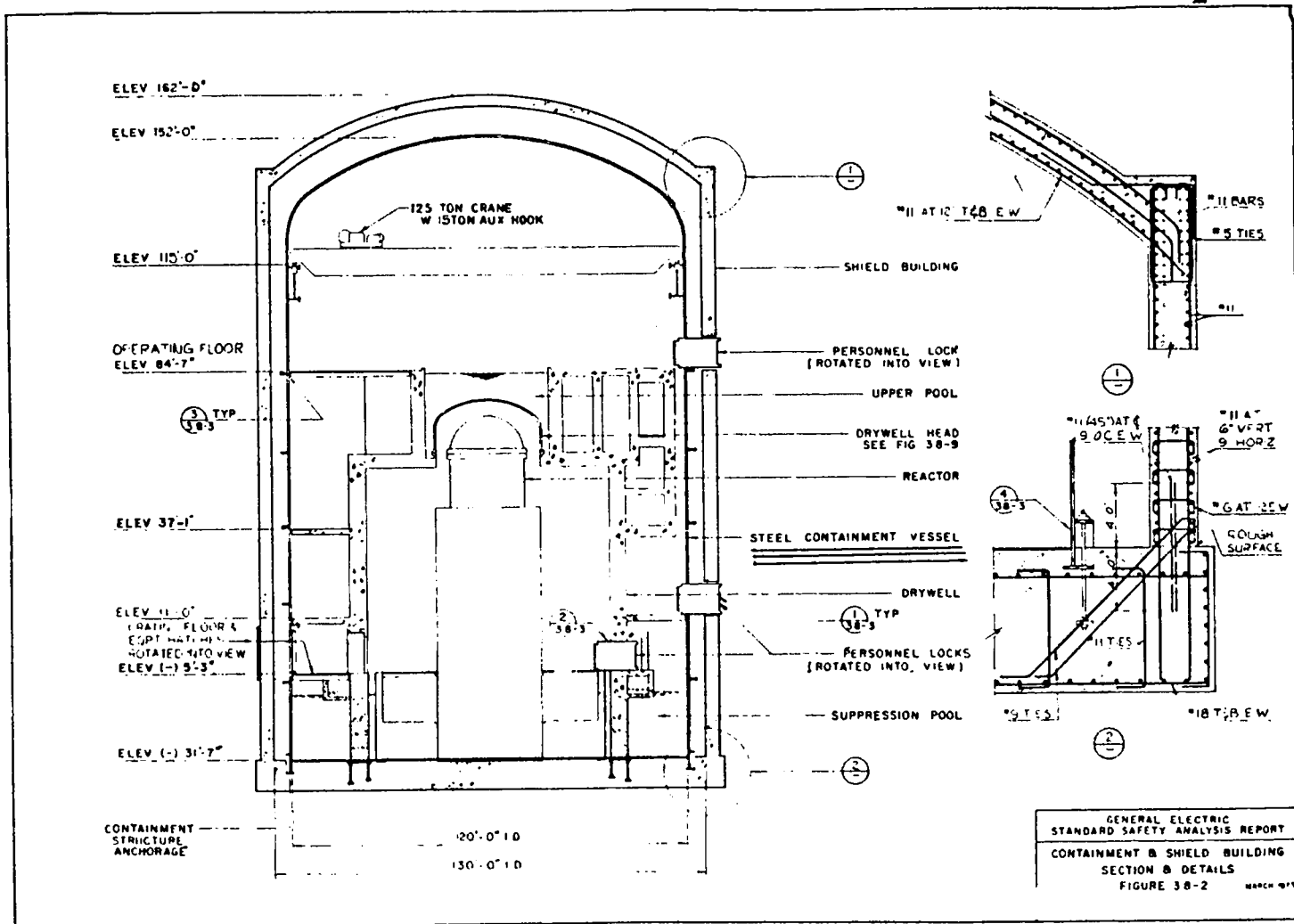
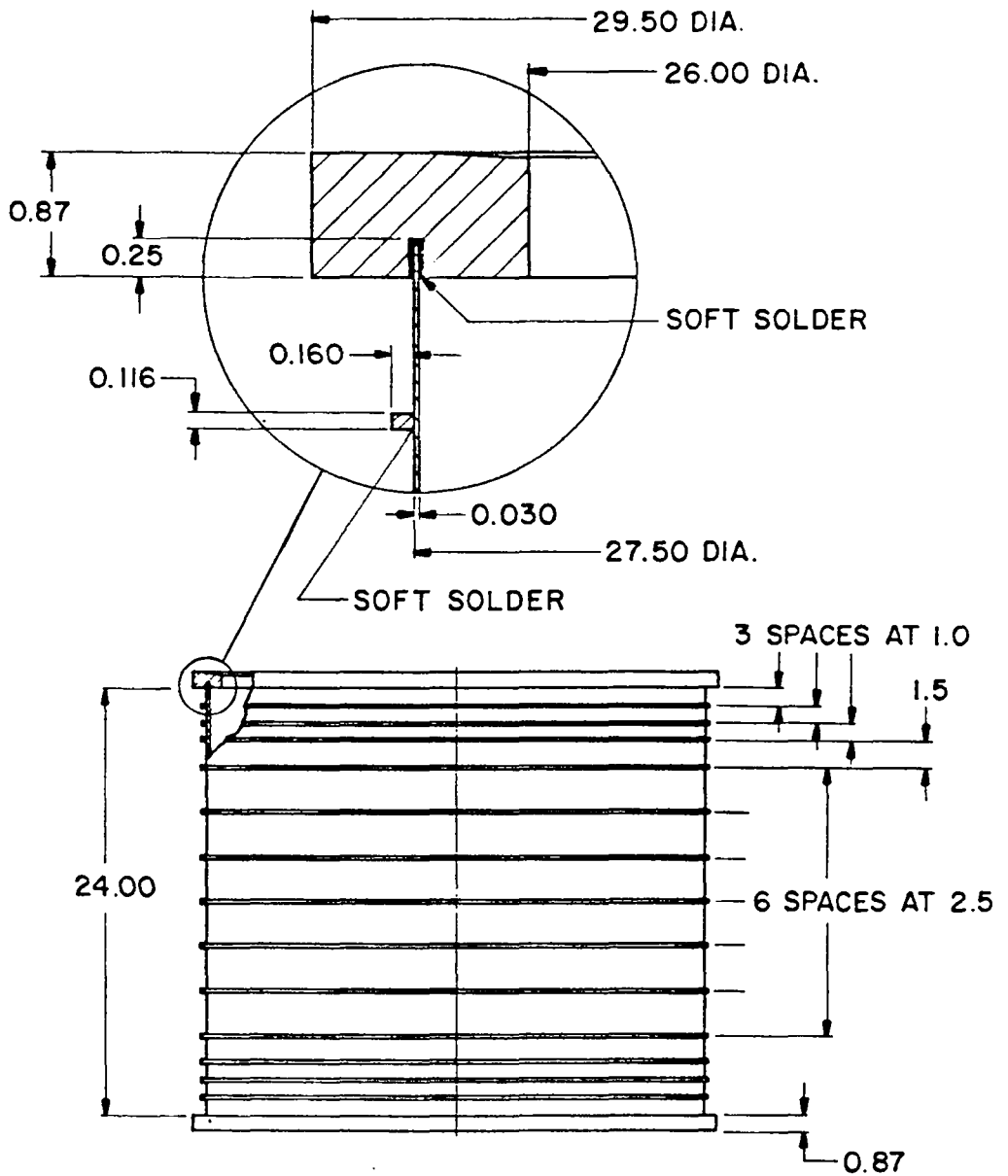


Fig. 1. Schematic of reactor with steel containment.



DIMENSIONS ARE IN INCHES
 MATERIAL: LOW CARBON STEEL

Fig. 2. Baseline benchmark model.

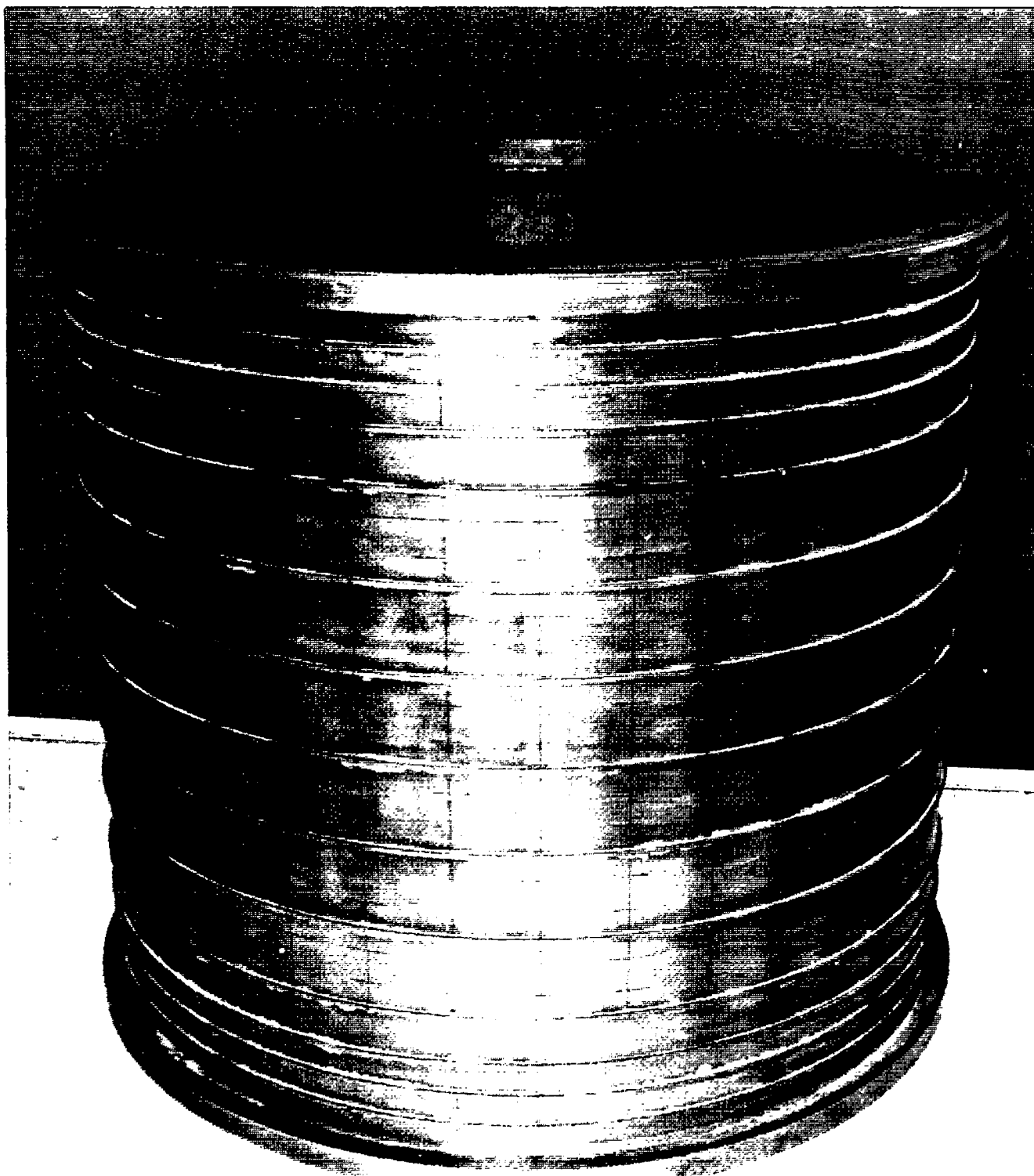


Fig. 3. Completed model No. 2.

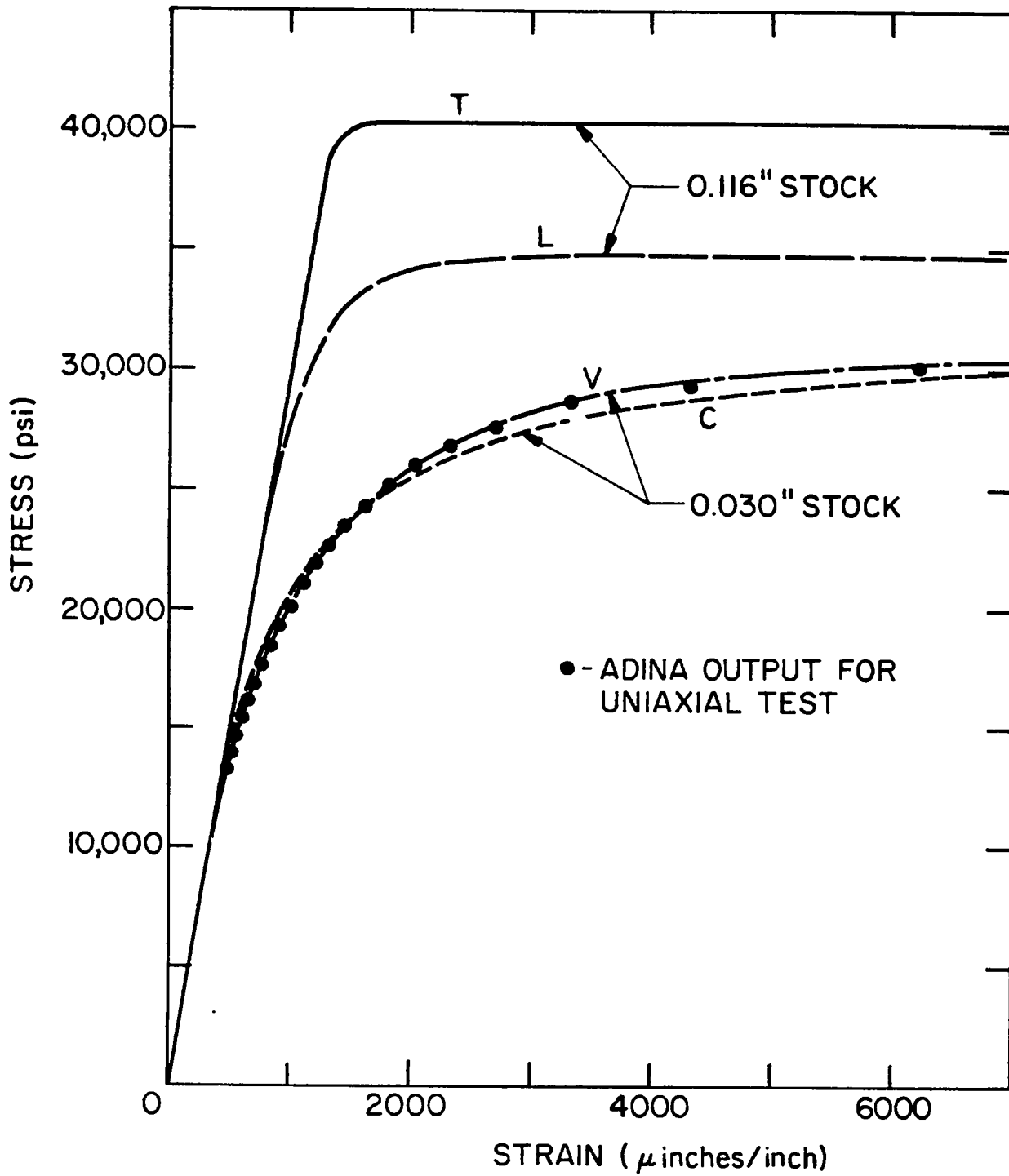


Fig. 4. Stress-strain curves for model materials.

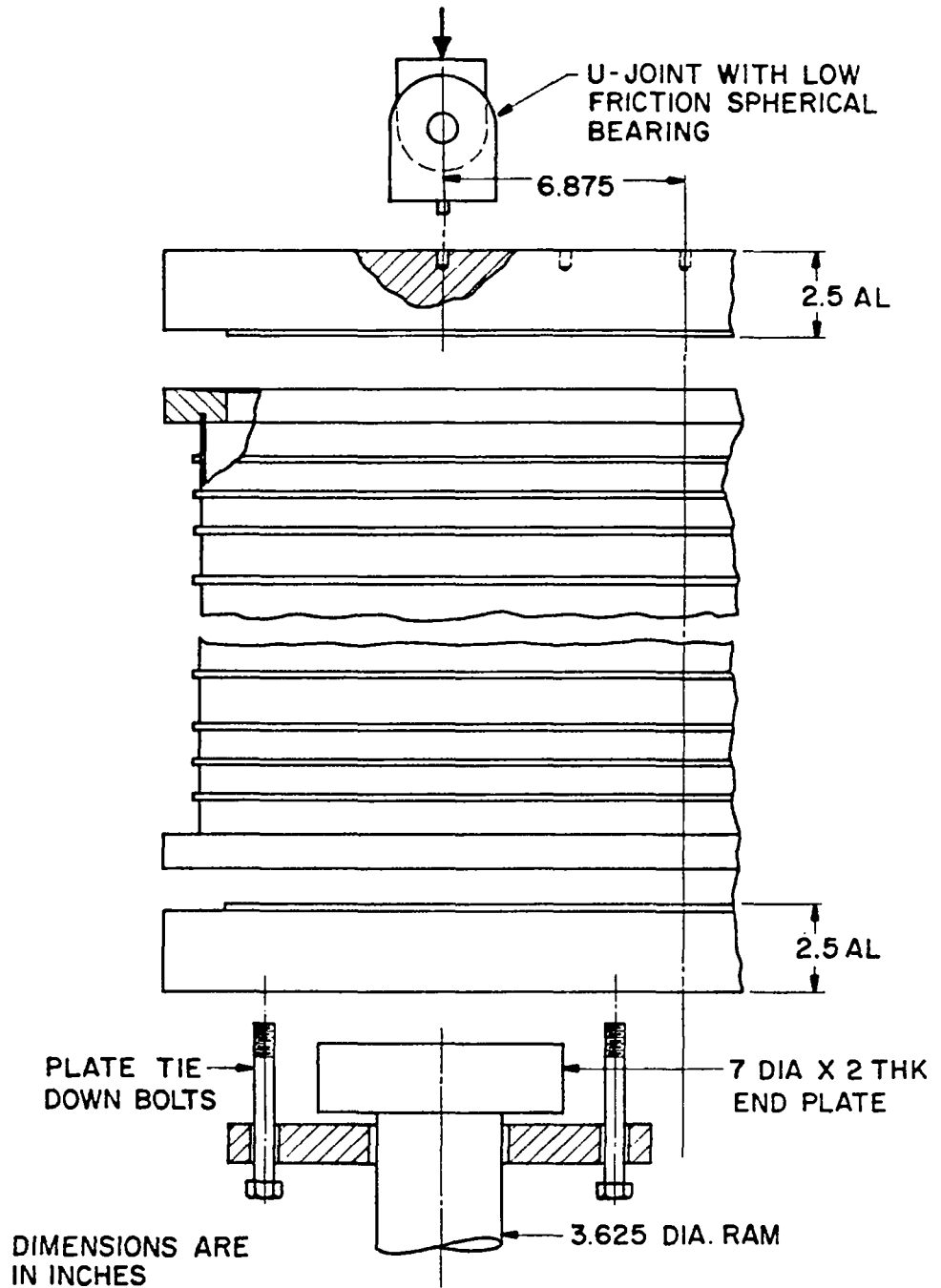


Fig. 5. Loading hardware.

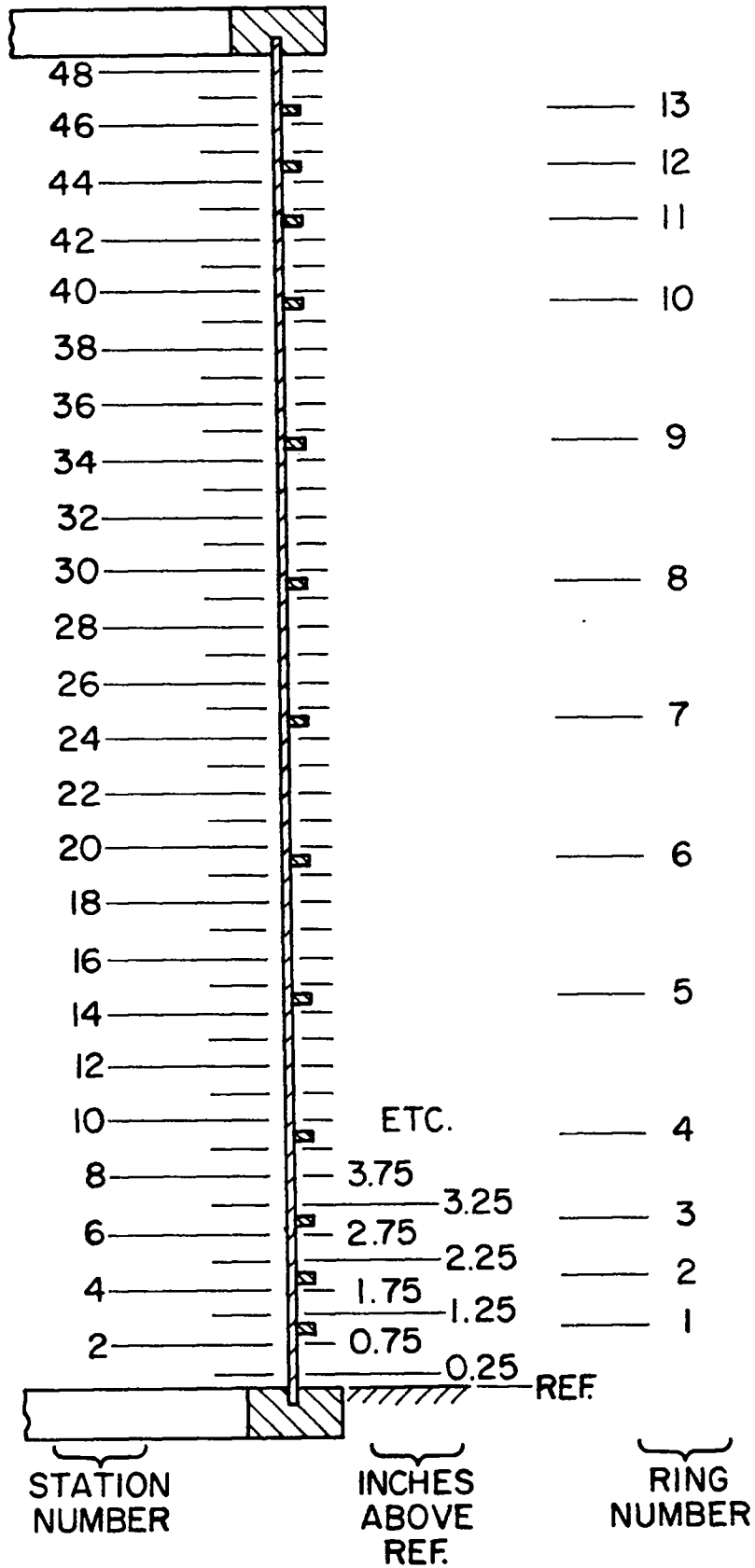


Fig. 6. Identification of axial stations and ring numbers.

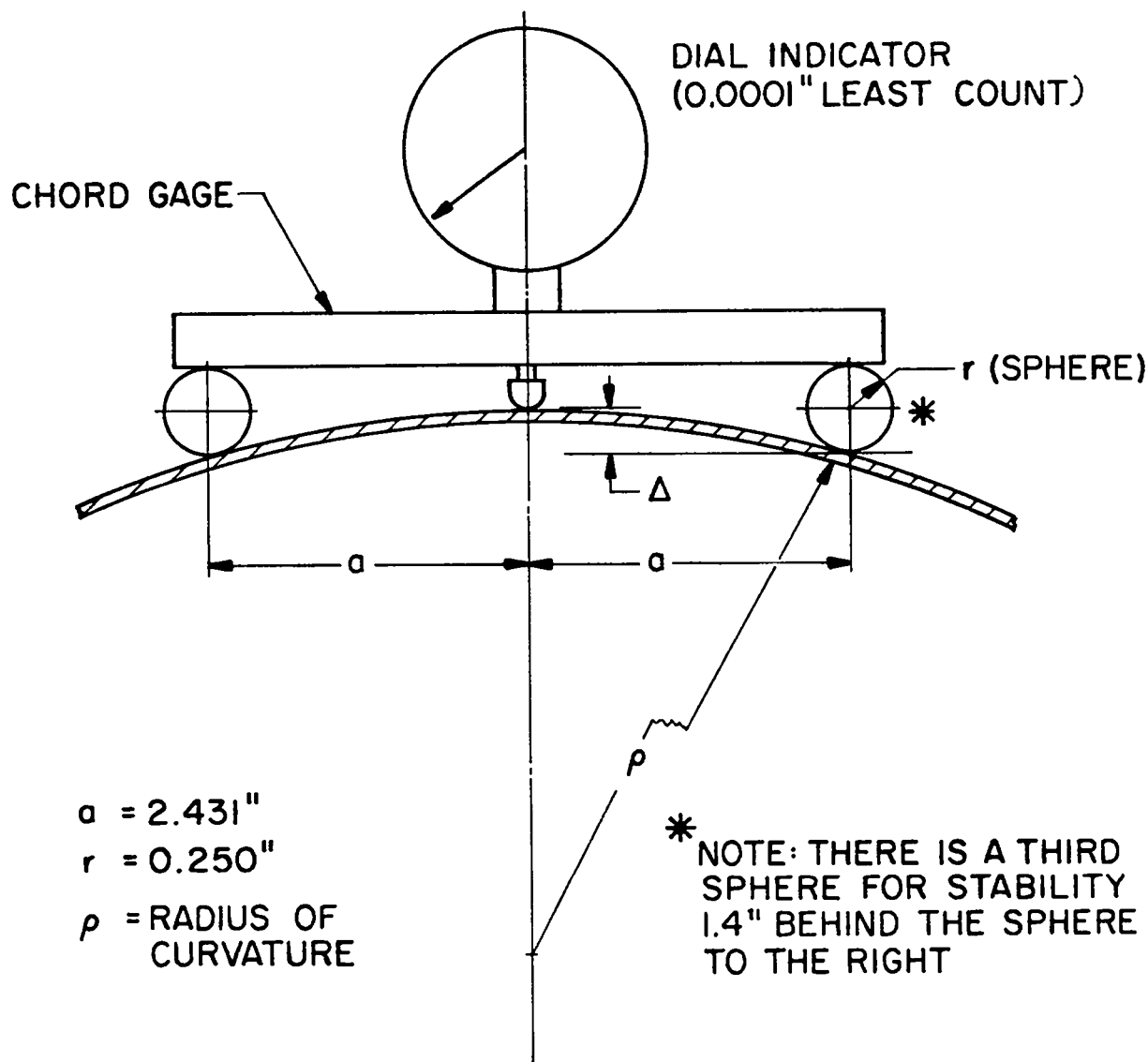


Fig. 7. Chord gage.

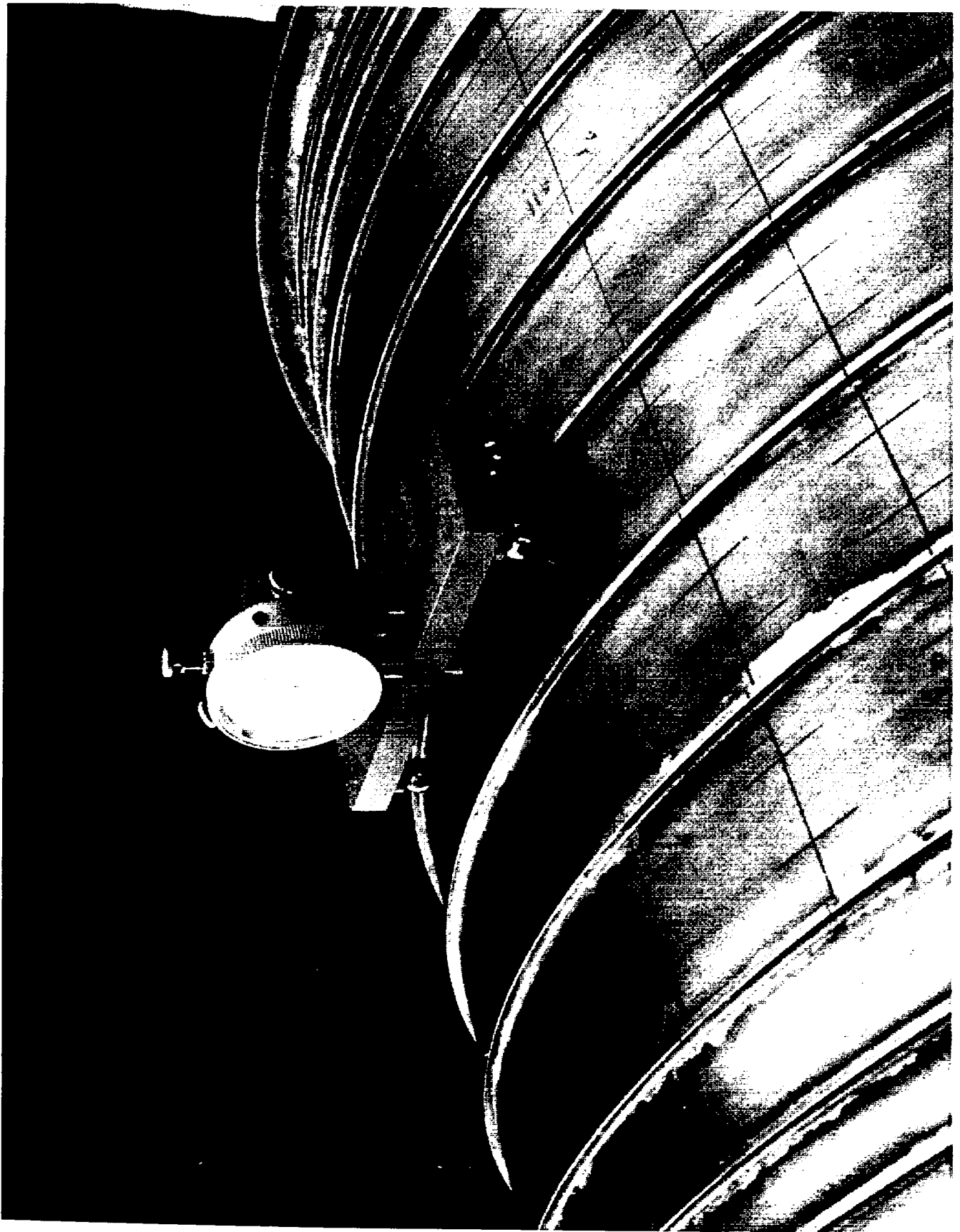


Fig. 8. Chord gage measurement.

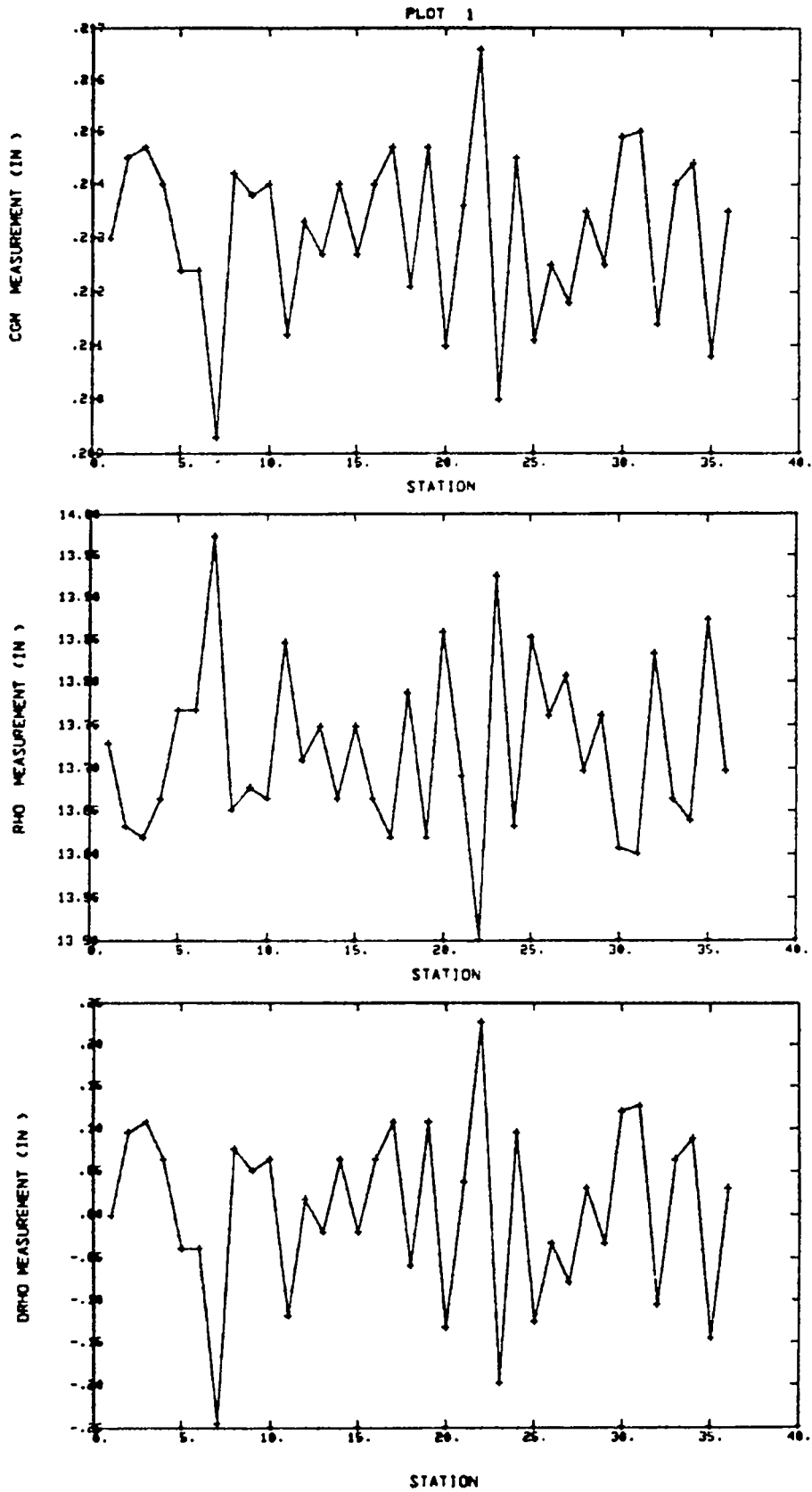


Fig. 9. Typical results of chord gage measurements for cylinder 1.

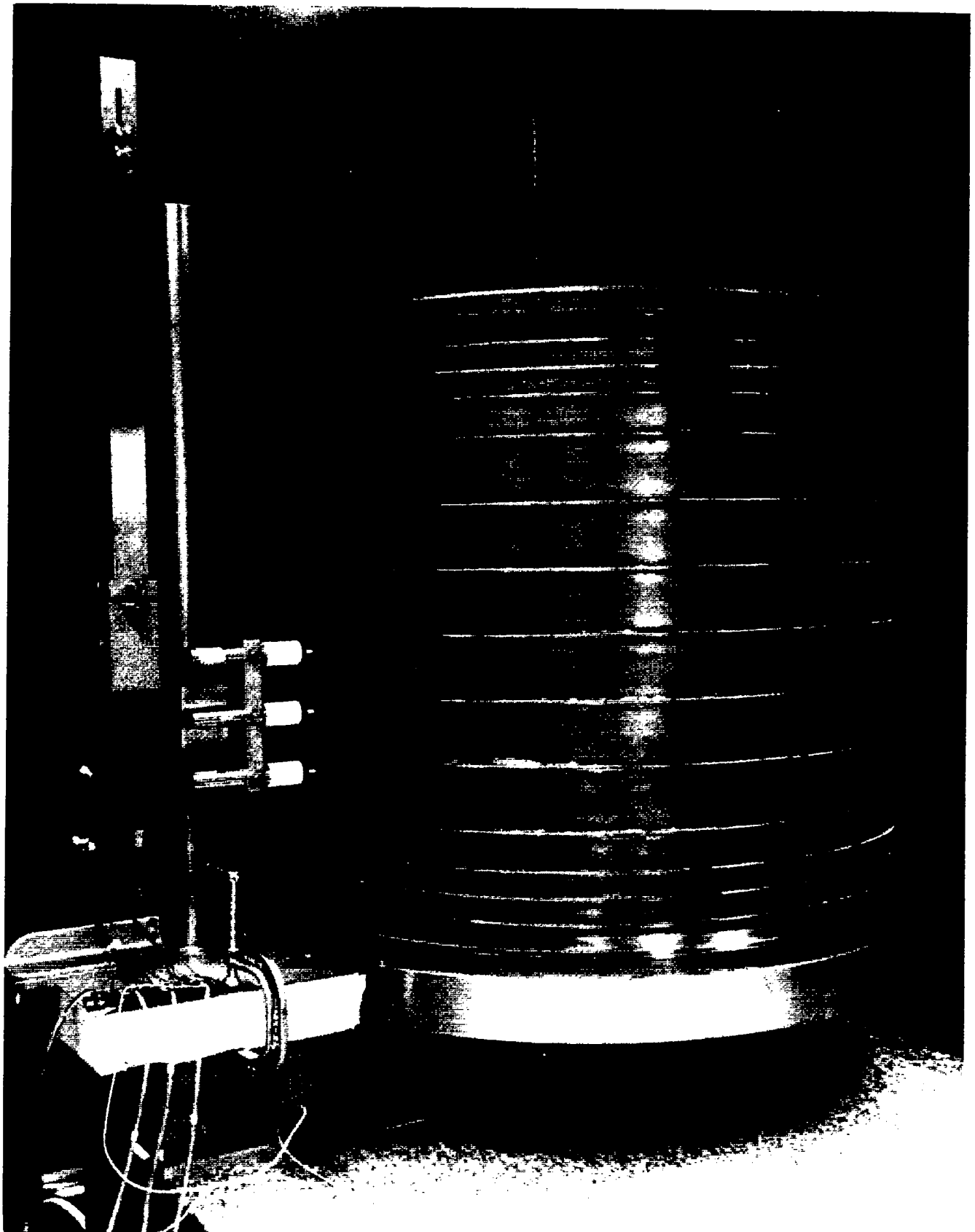


Fig. 10. Experimental setup for imperfection measurements.

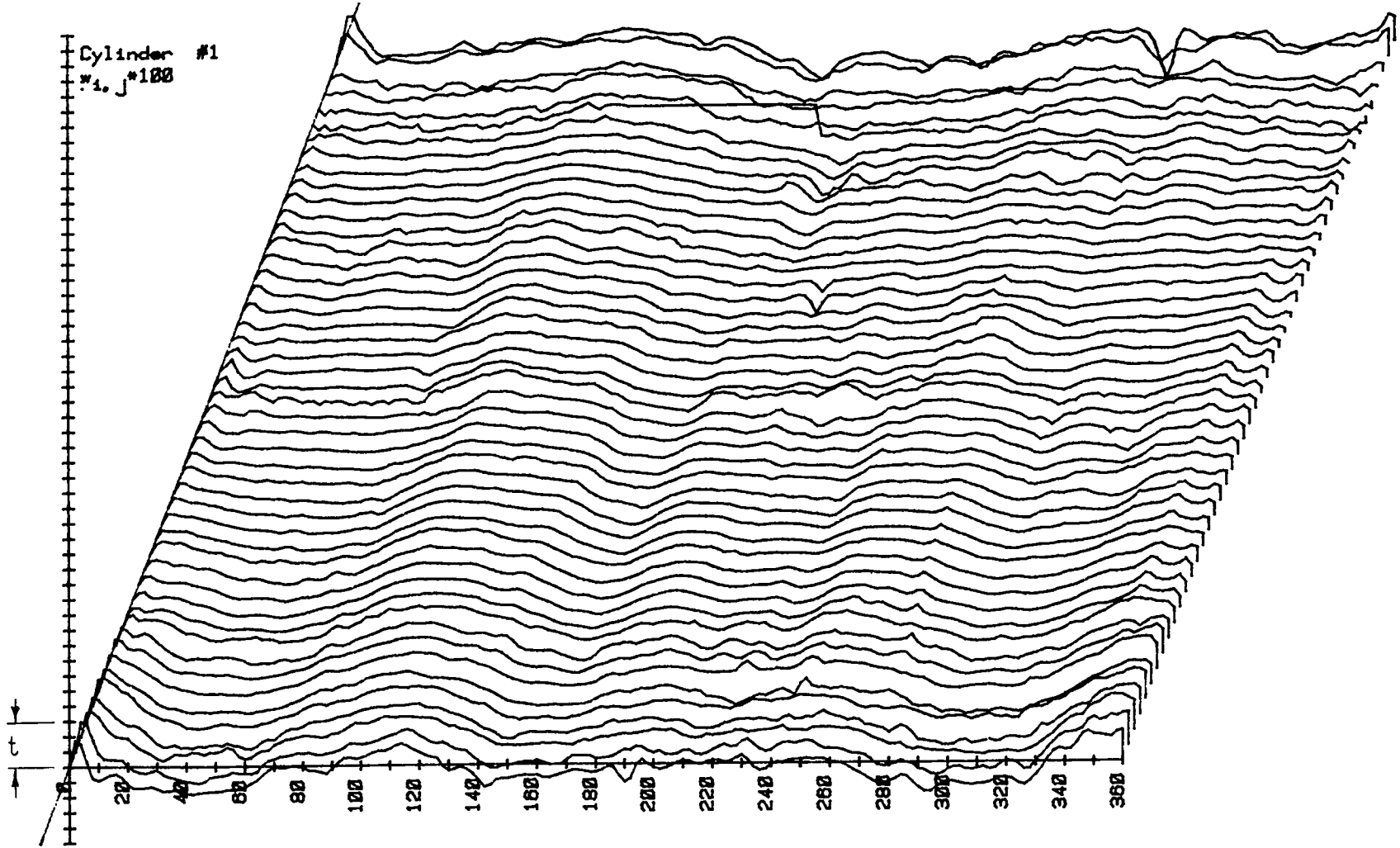


Fig. 11. Contour plot of imperfections in cylinder 1.

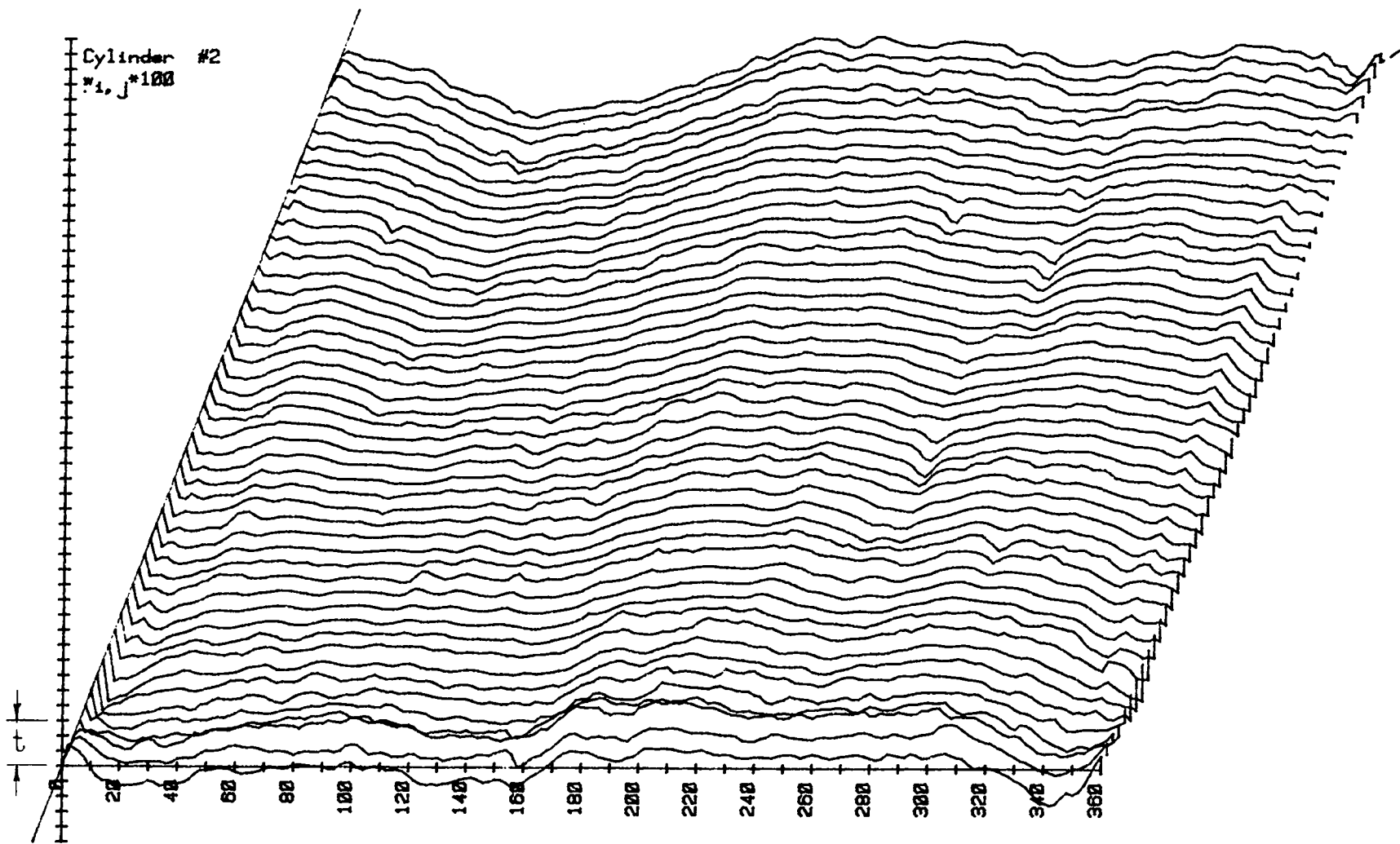


Fig. 12. Contour plot of imperfections in cylinder 2.

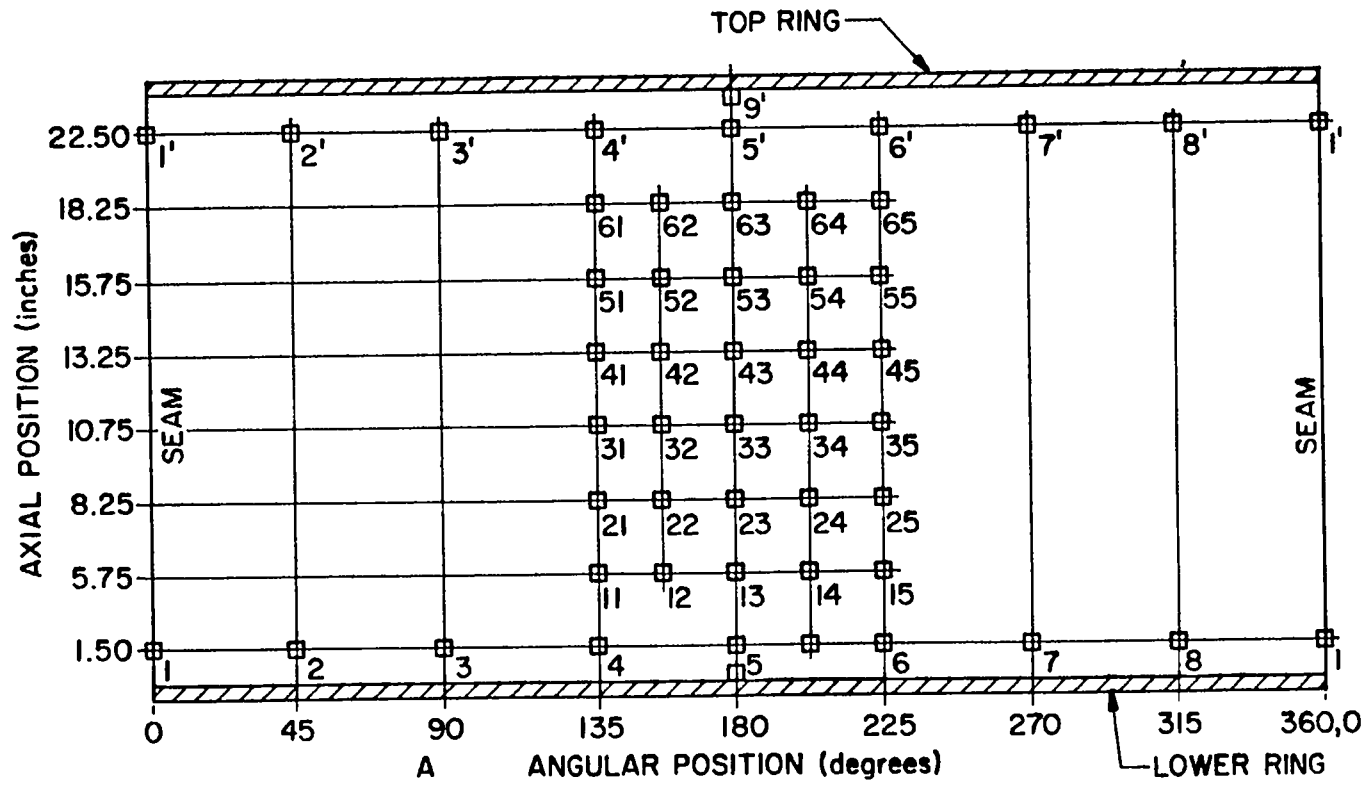


Fig. 13. Strain gage locations.



Fig. 14. Epoxy filler at junction of end ring and loading plate.

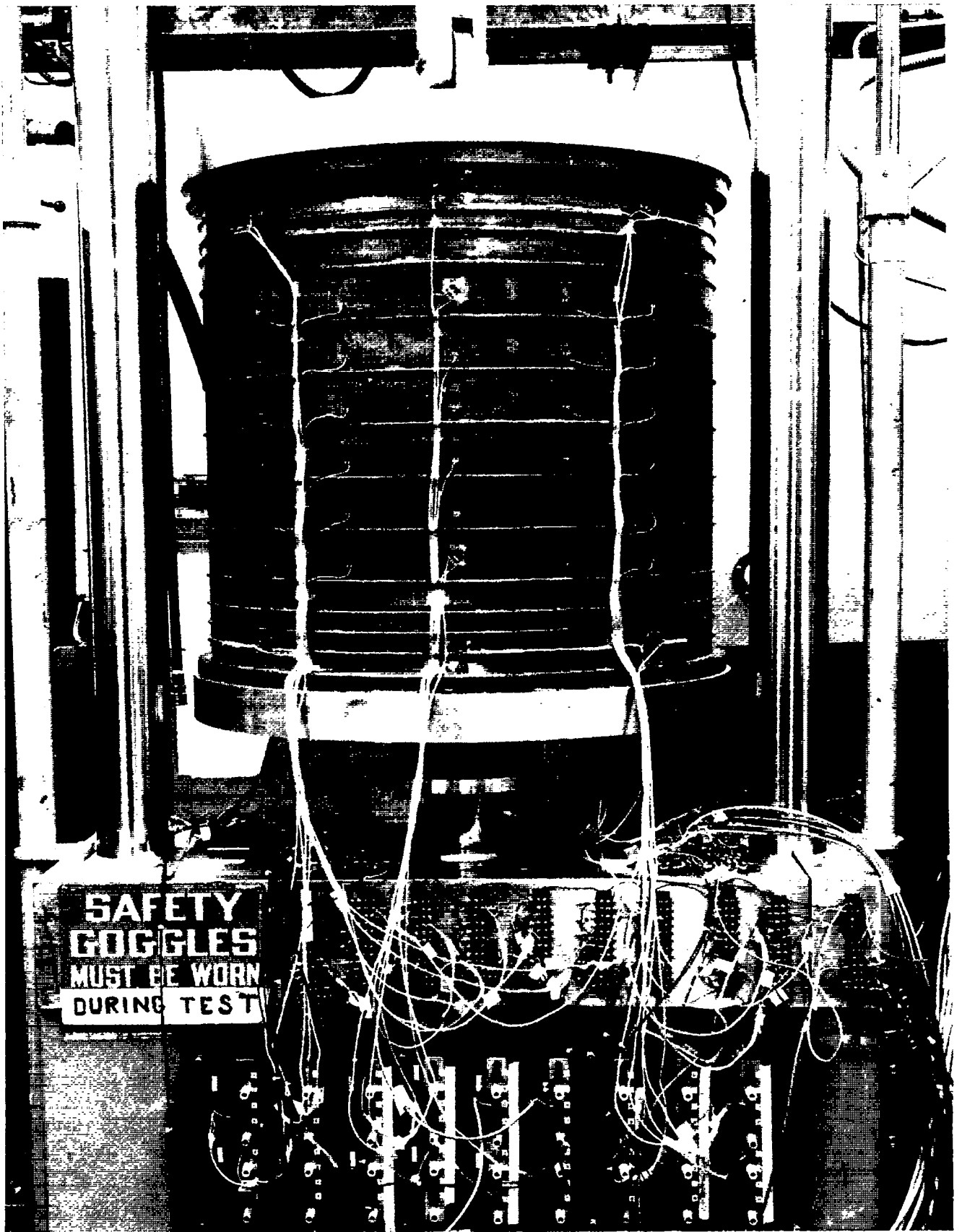


Fig. 15. Cylinder in testing machine for buckling test.

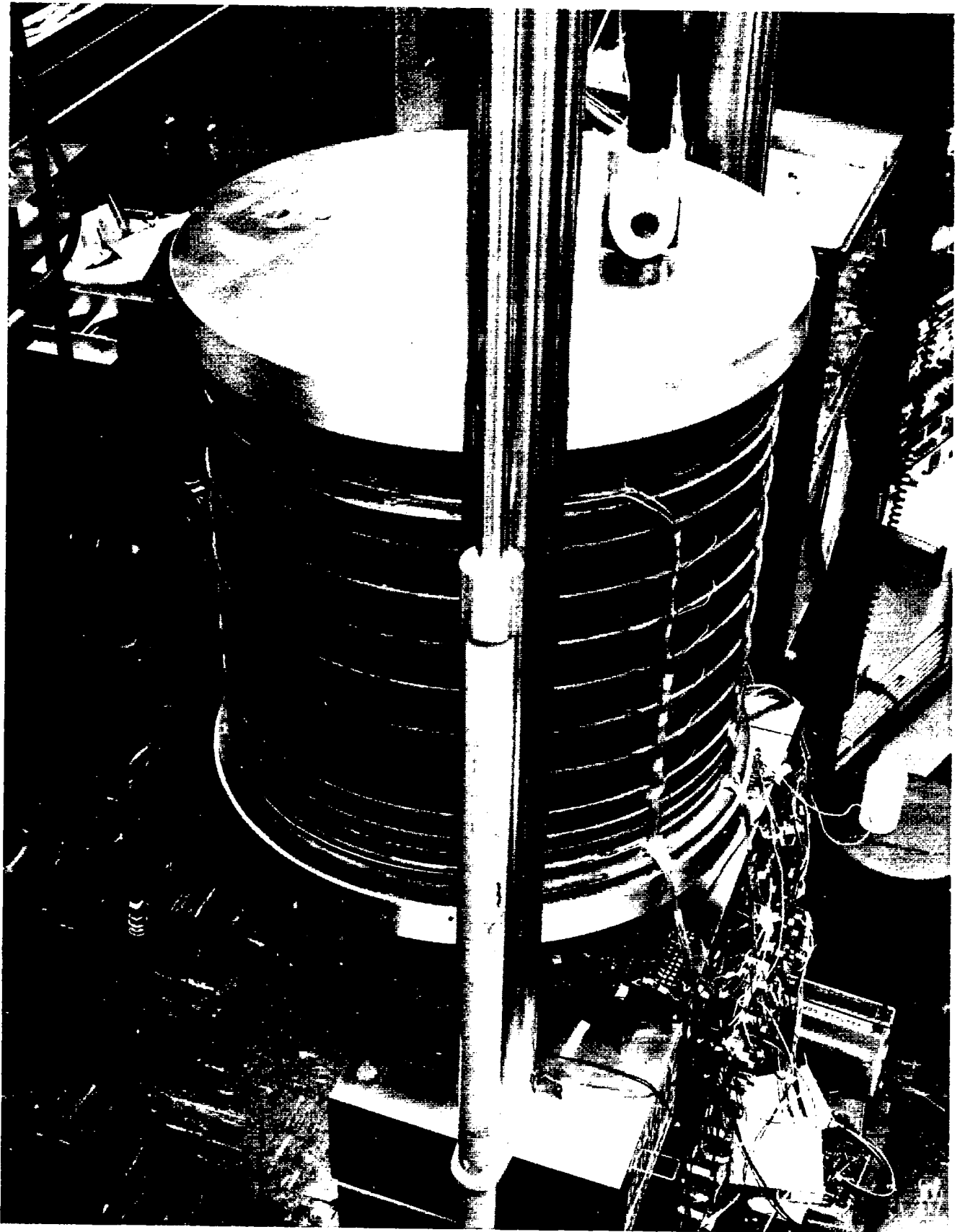


Fig. 16. Top view of cylinder in testing machine.



Fig. 17. Cylinder 1 buckle.

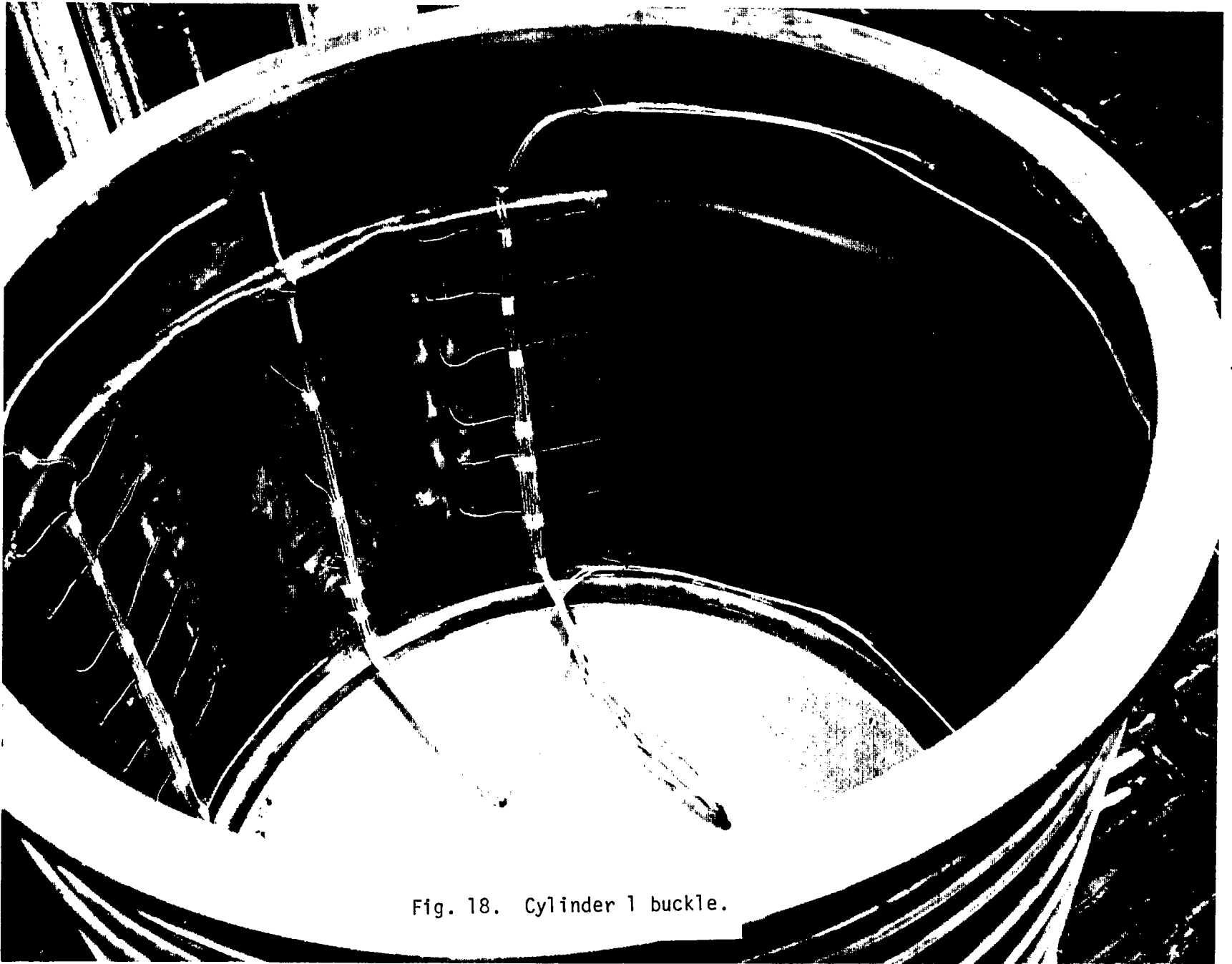


Fig. 18. Cylinder 1 buckle.

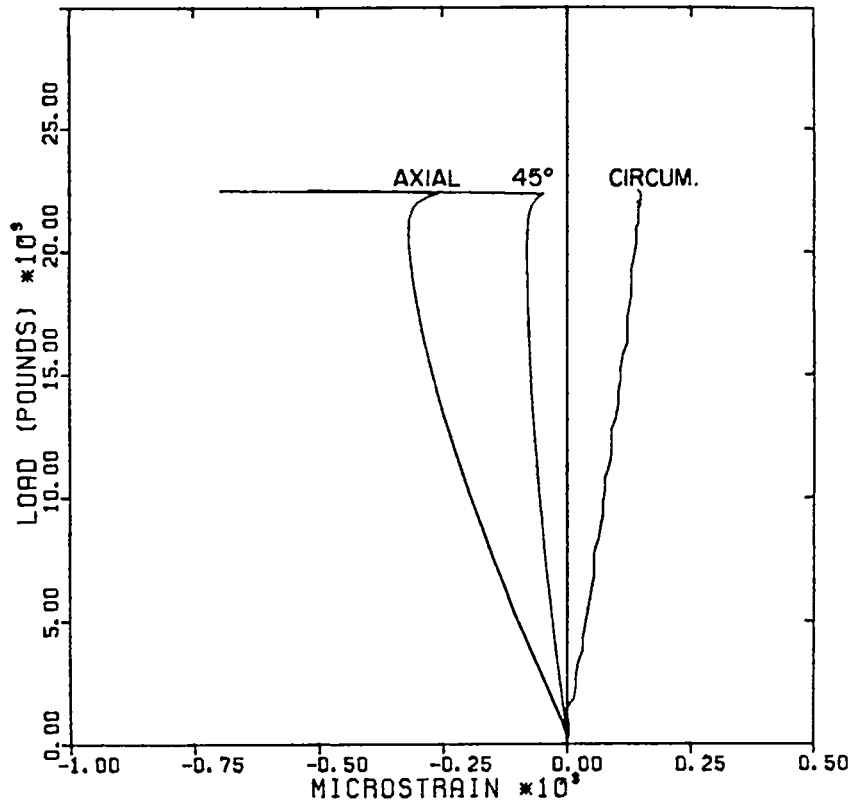


Fig. 19. Strains at rosette 63 inside.

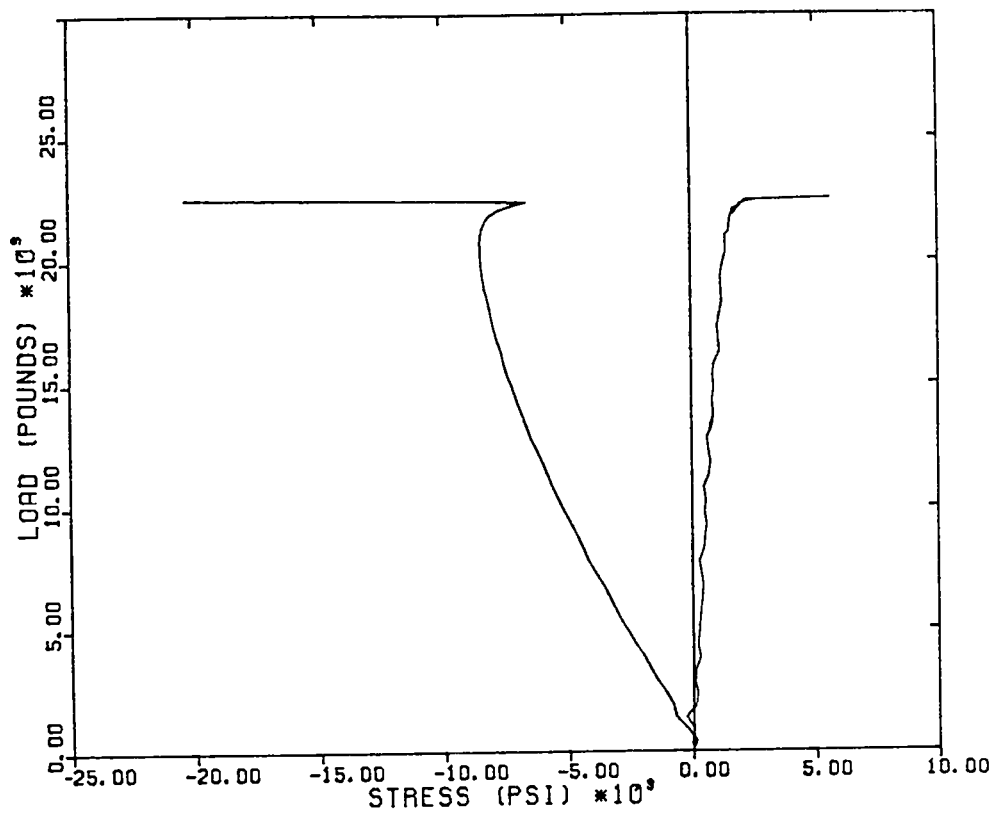


Fig. 20. Principal stresses at rosette 63 inside.

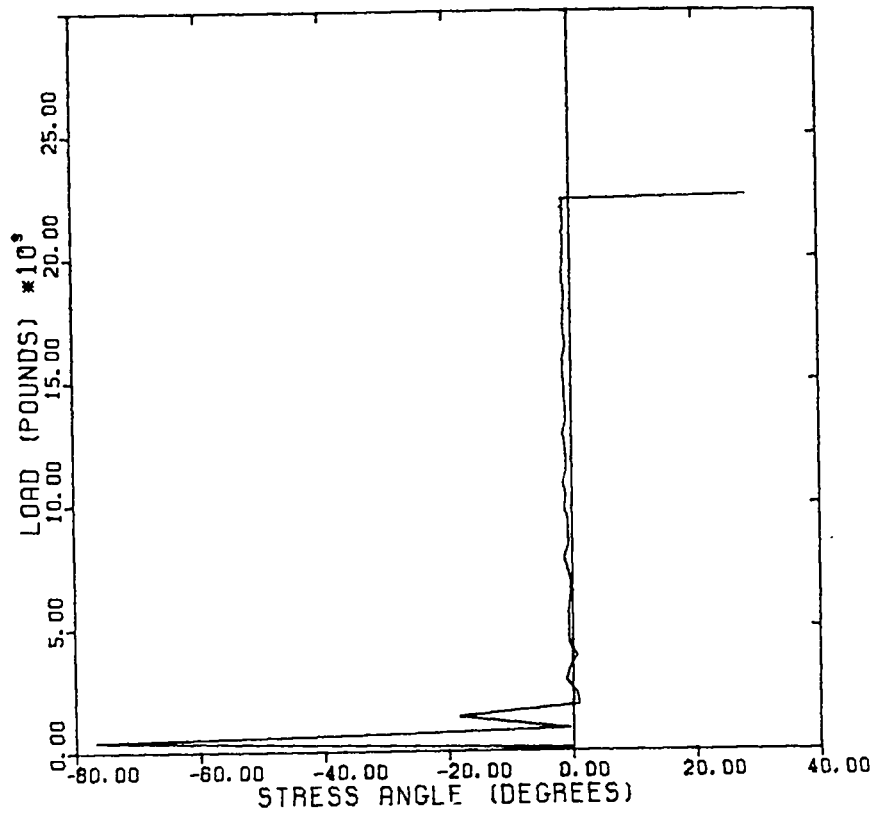


Fig. 21. Principal stress direction at rosette 63 inside.

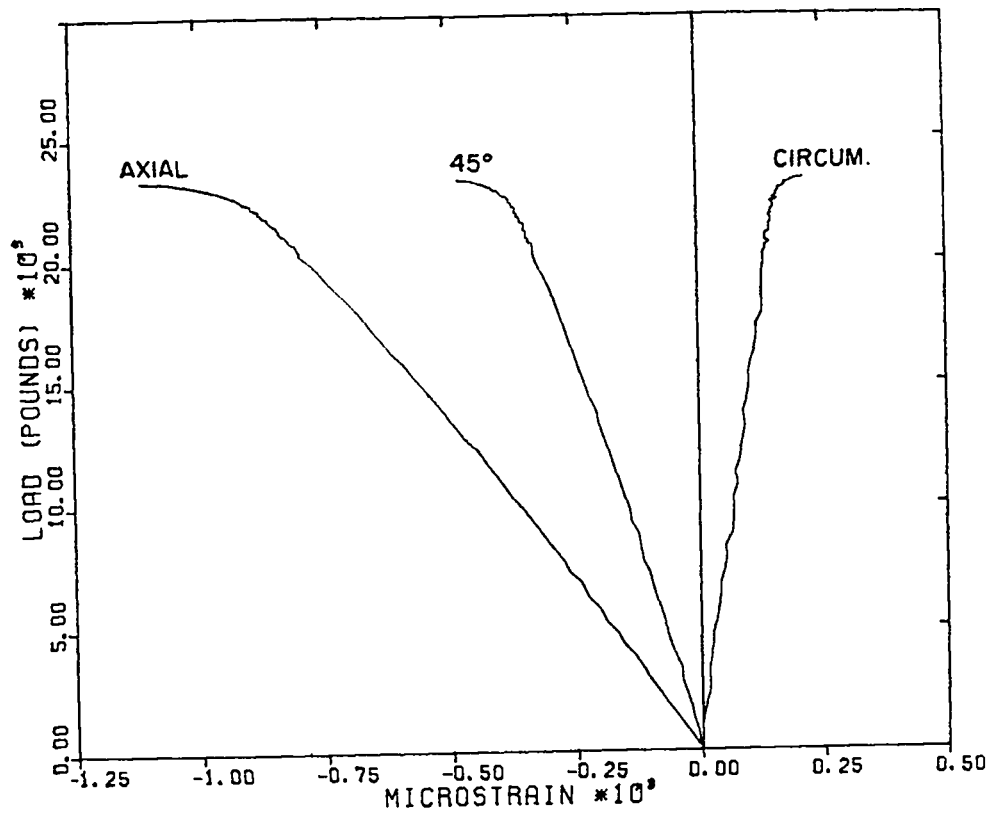


Fig. 22. Strains at rosette 63 outside.

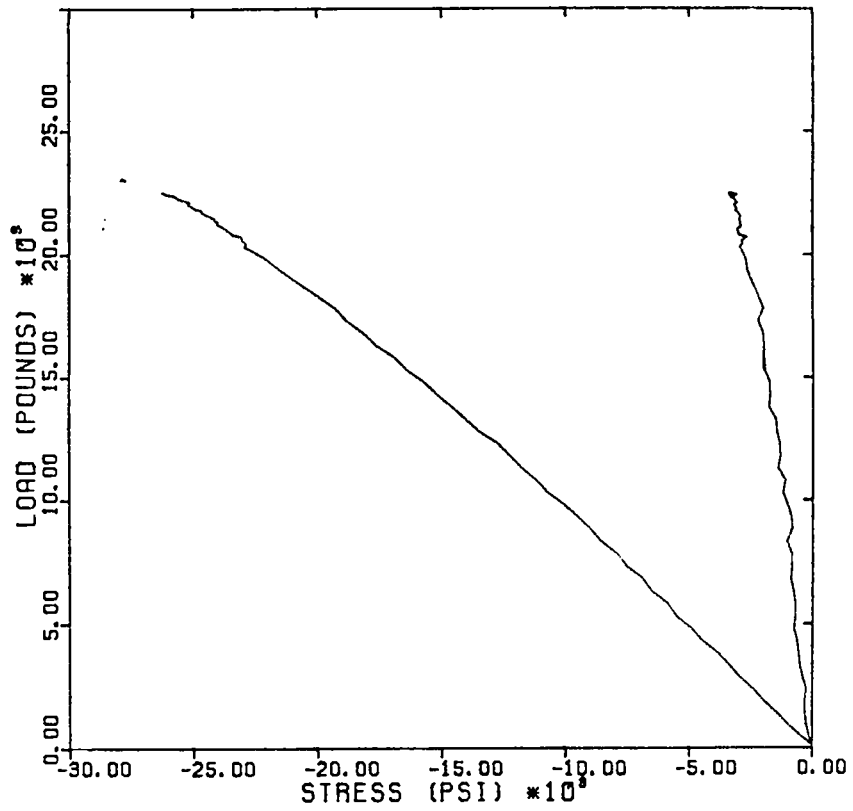


Fig. 23. Principal stresses at rosette 63 outside.

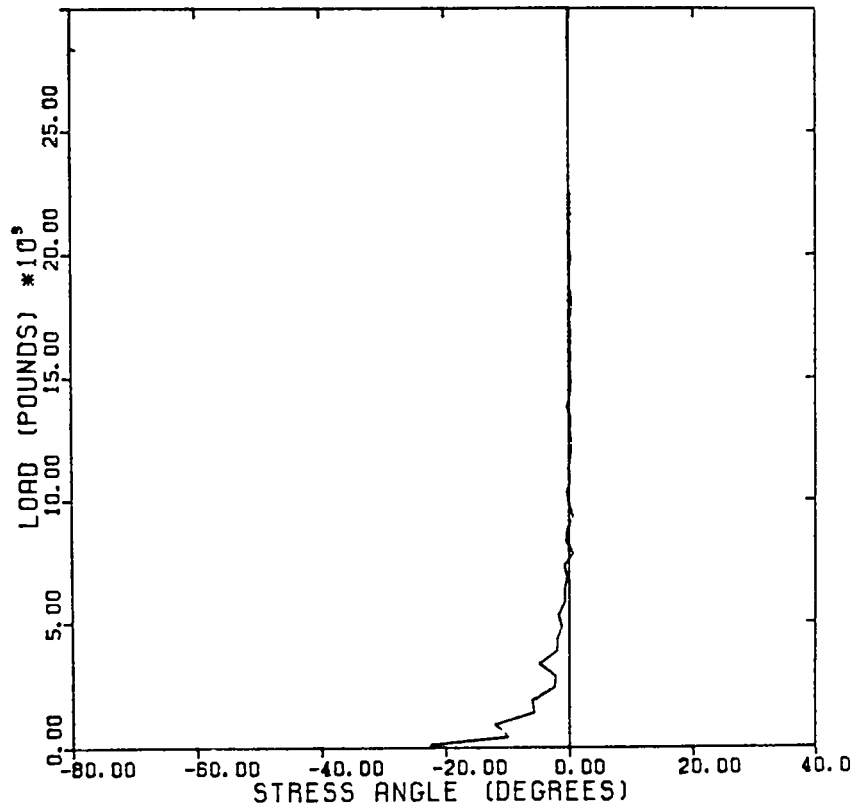


Fig. 24. Principal stress direction at rosette 63 outside.

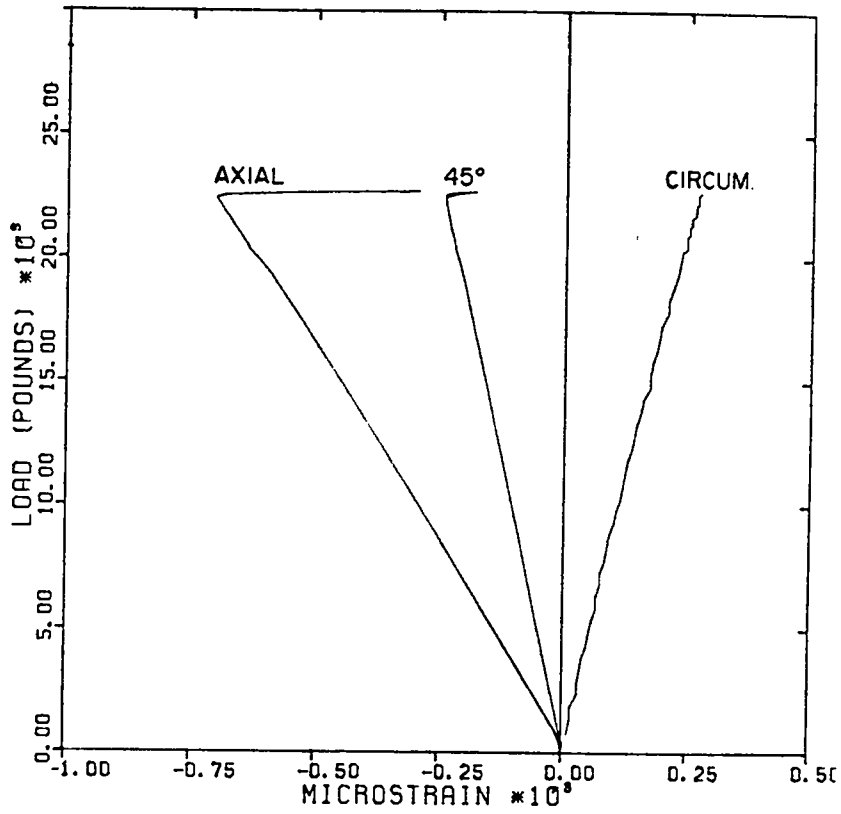


Fig. 25. Strains at rosette 13 inside.

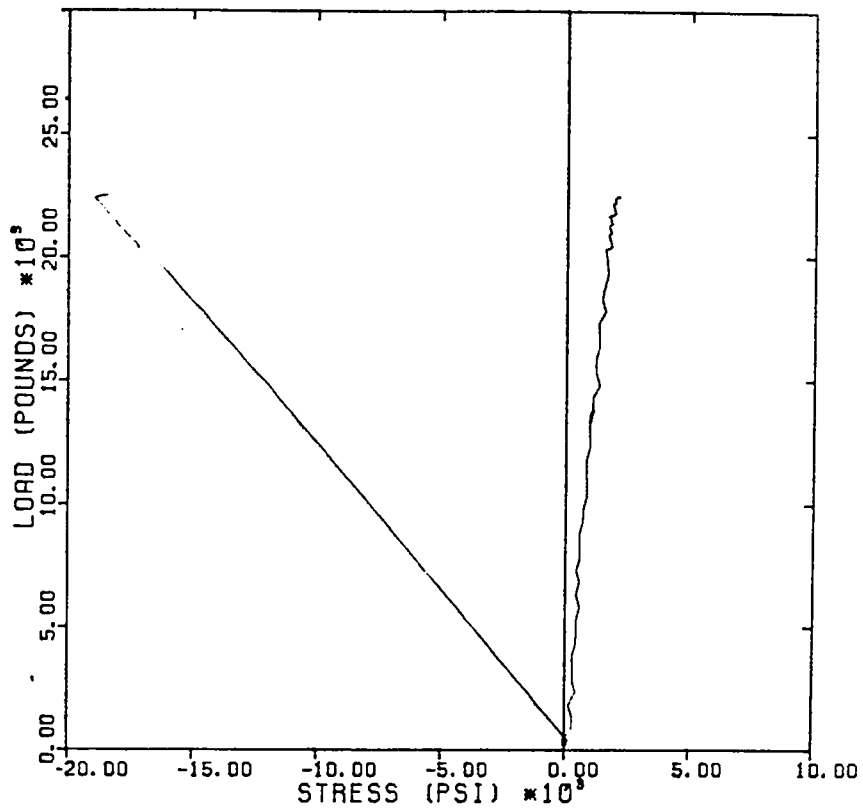


Fig. 26. Principal stresses at rosette 13 inside.

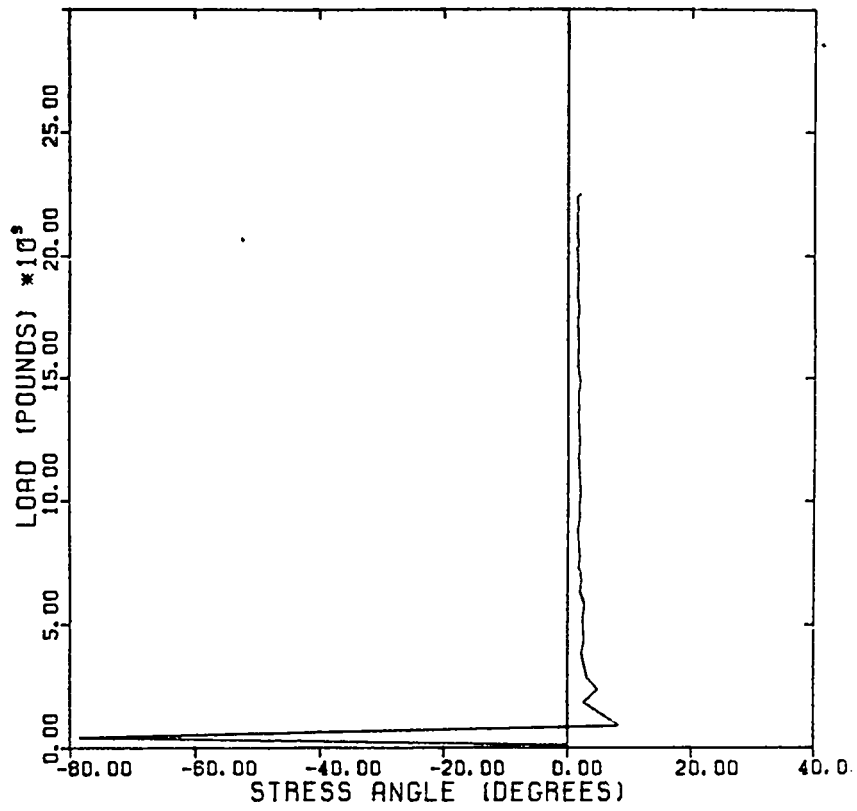


Fig. 27. Principal stress direction at rosette 13 inside.

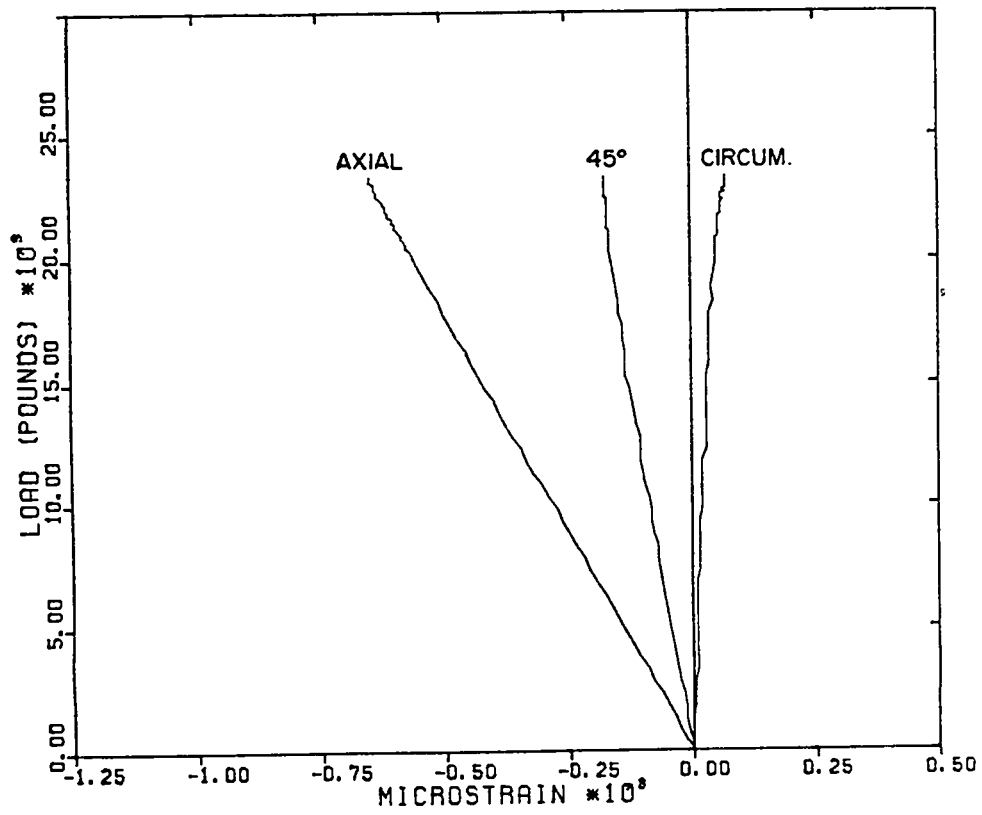


Fig. 28. Strains at rosette 13 outside.

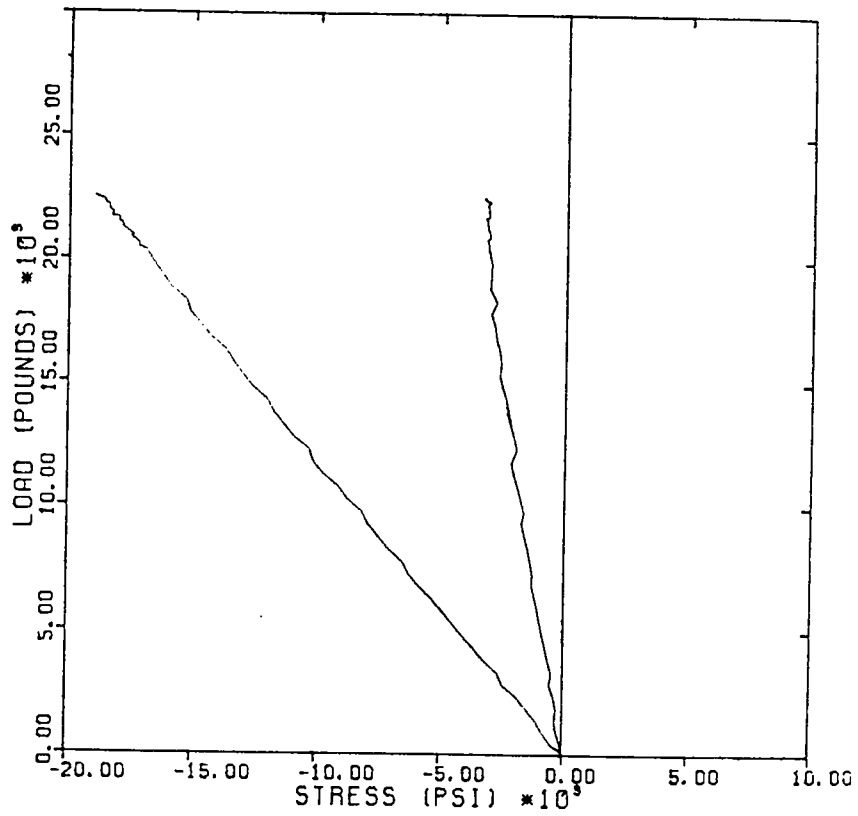


Fig. 29. Principal stresses at rosette 13 outside.

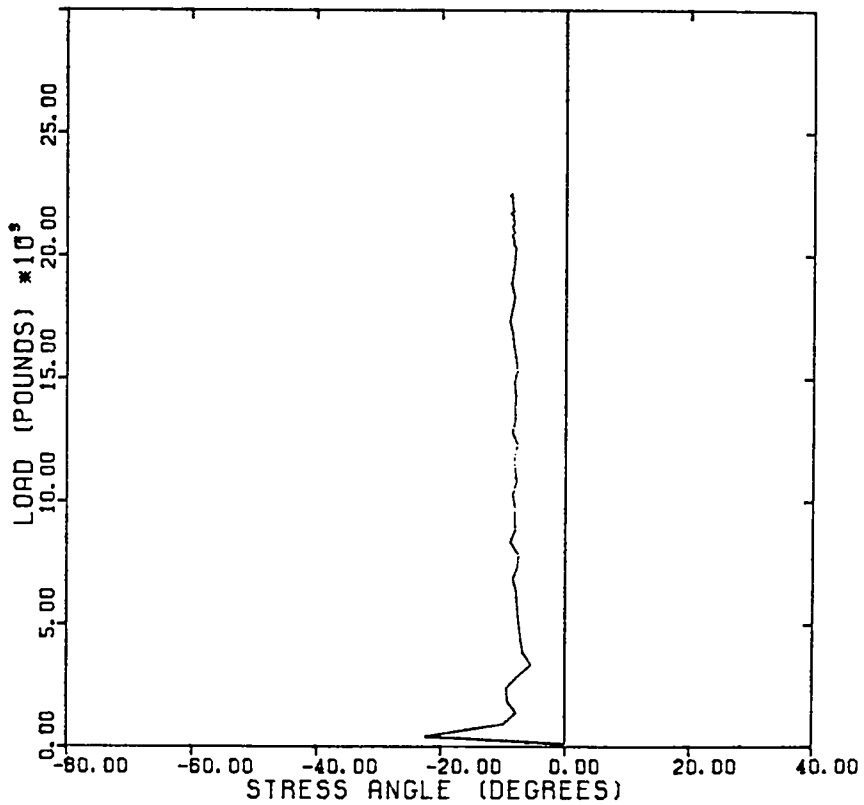


Fig. 30. Principal stress direction at rosette 13 outside.

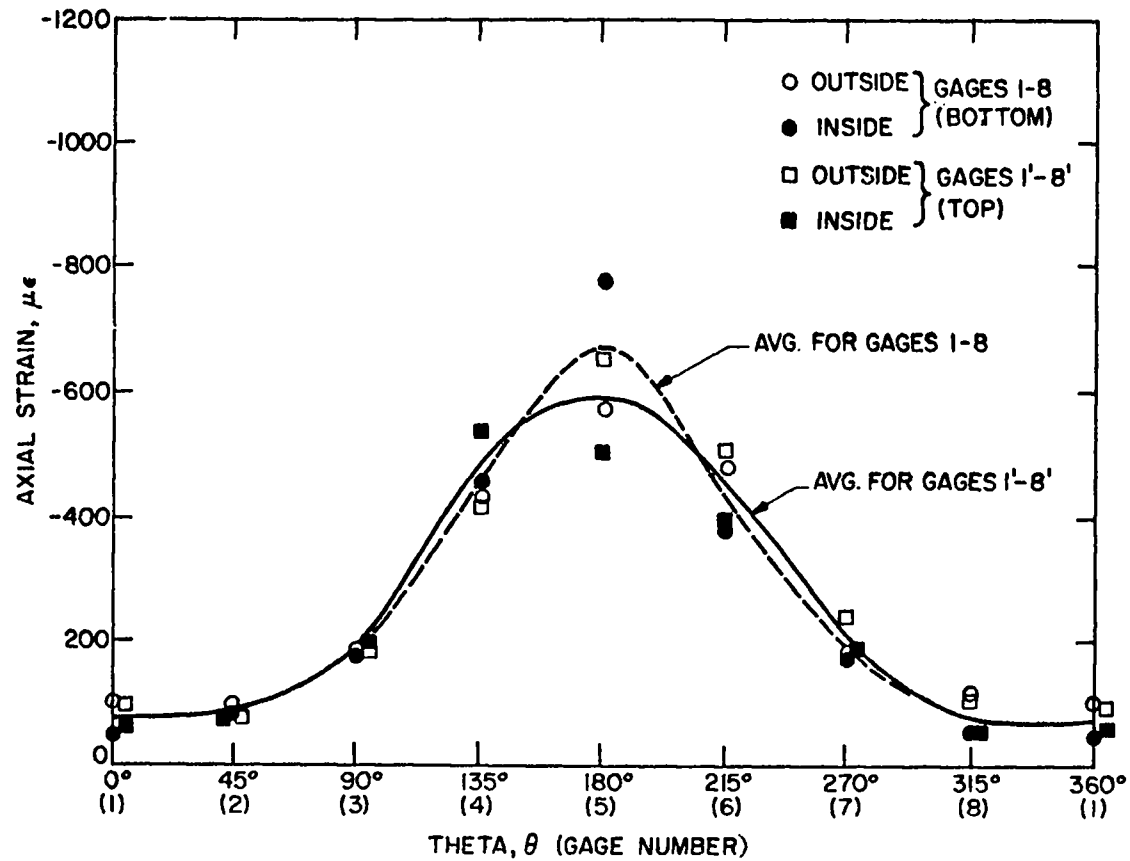


Fig. 31. Axial strain distribution around cylinder 1 at 23 000-1b load.



Fig. 32. Cylinder 2 buckle.



Fig. 33. Cylinder 2 buckle.

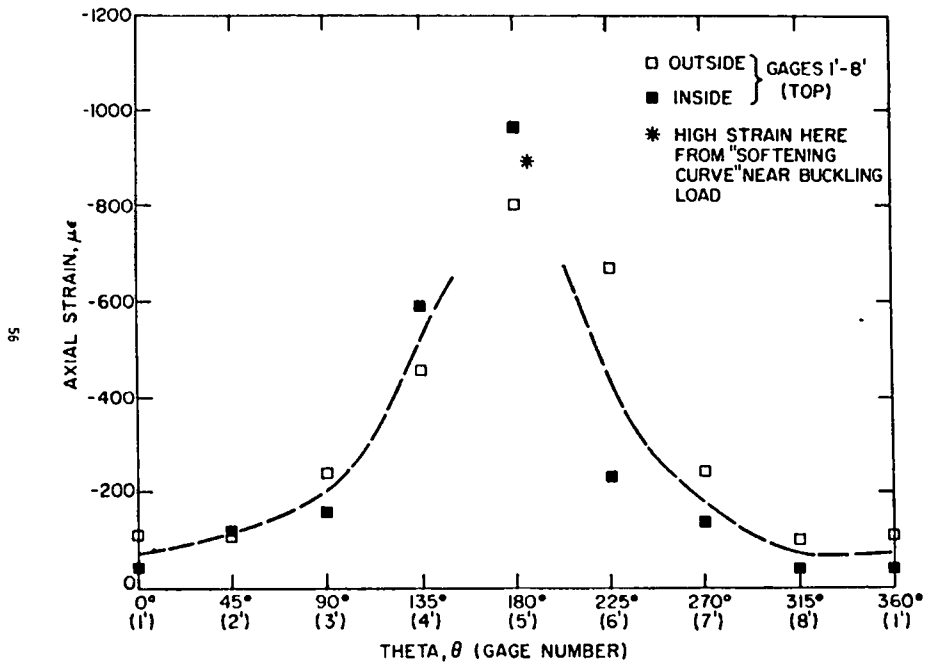


Fig. 34. Axial strain distribution around cylinder 2 at 26 900-lb load.

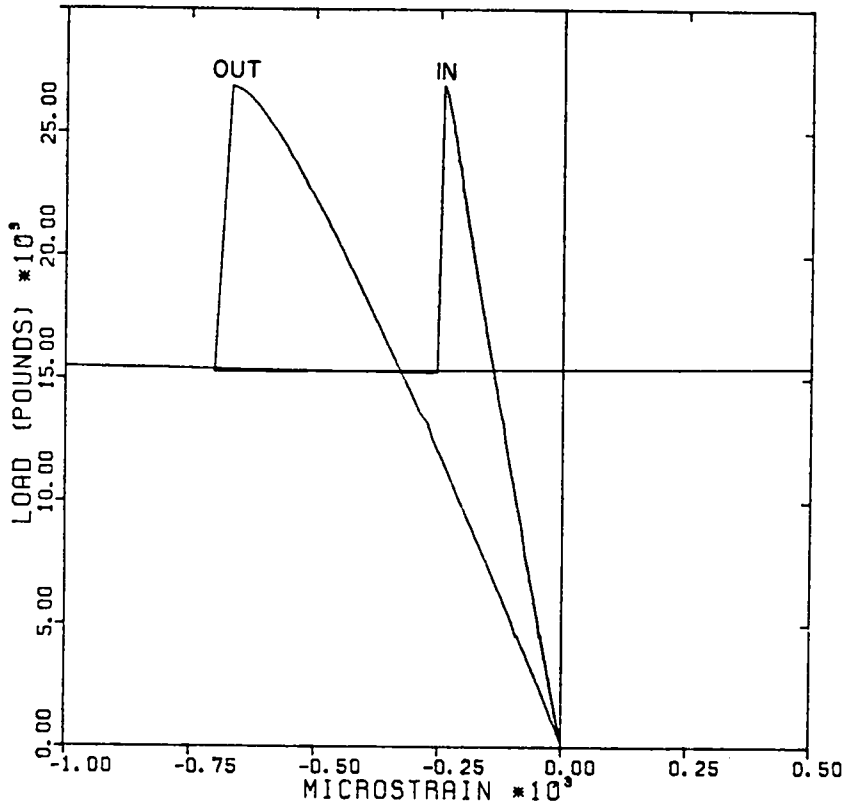


Fig. 35. Strain data at location 4 for cylinder 2.

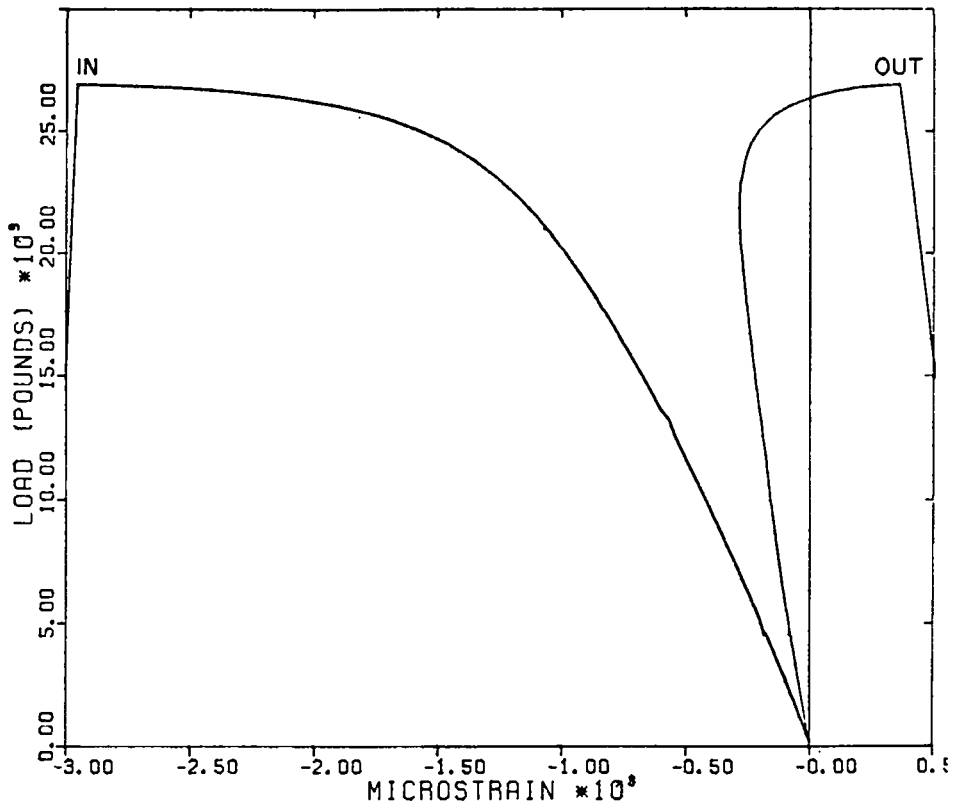


Fig. 36. Strain data at location 5 for cylinder 2.

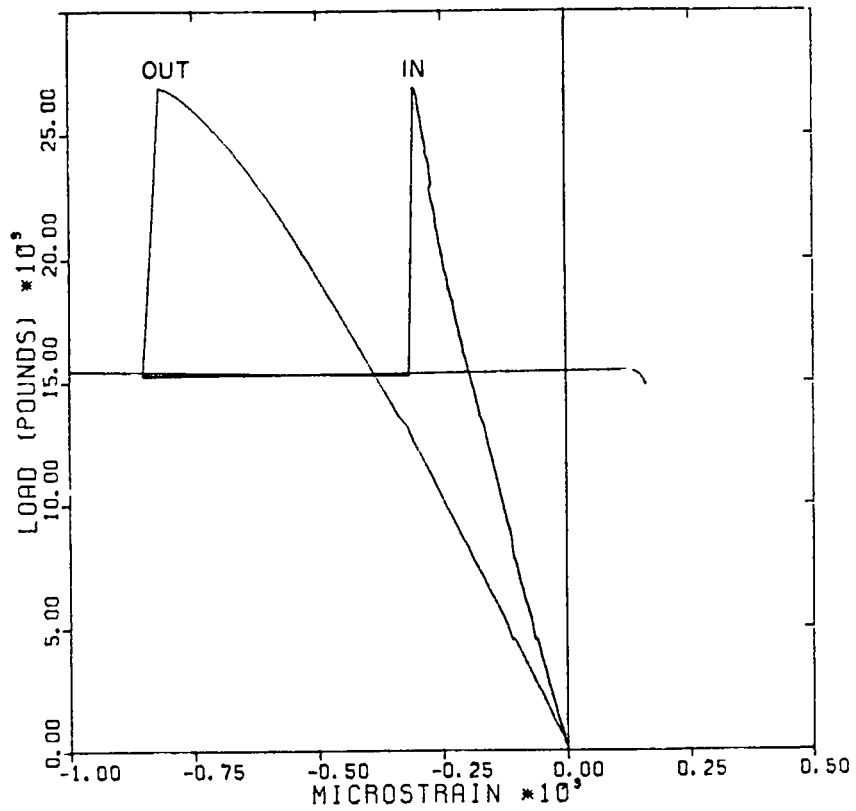


Fig. 37. Strain data at location 6 for cylinder 2.

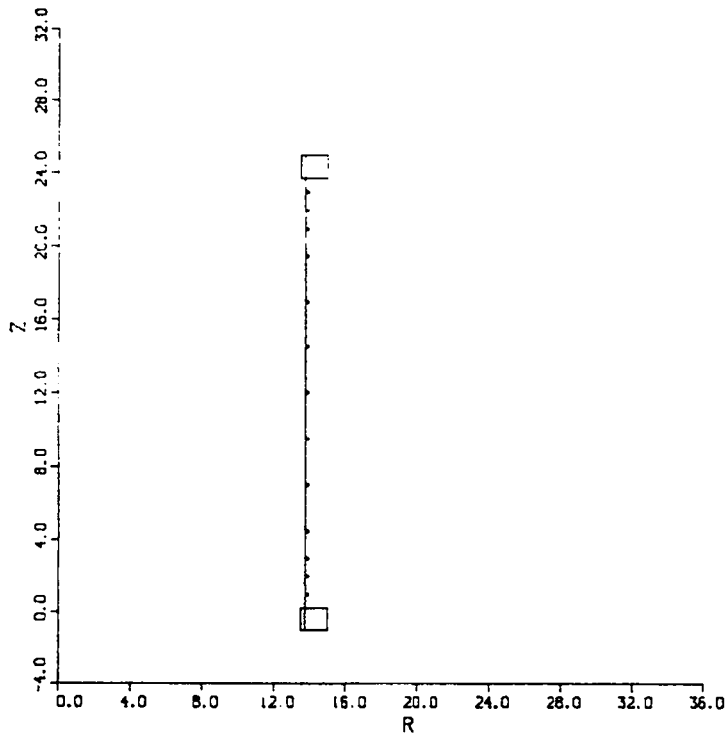


Fig. 38. Undeformed finite element mesh.

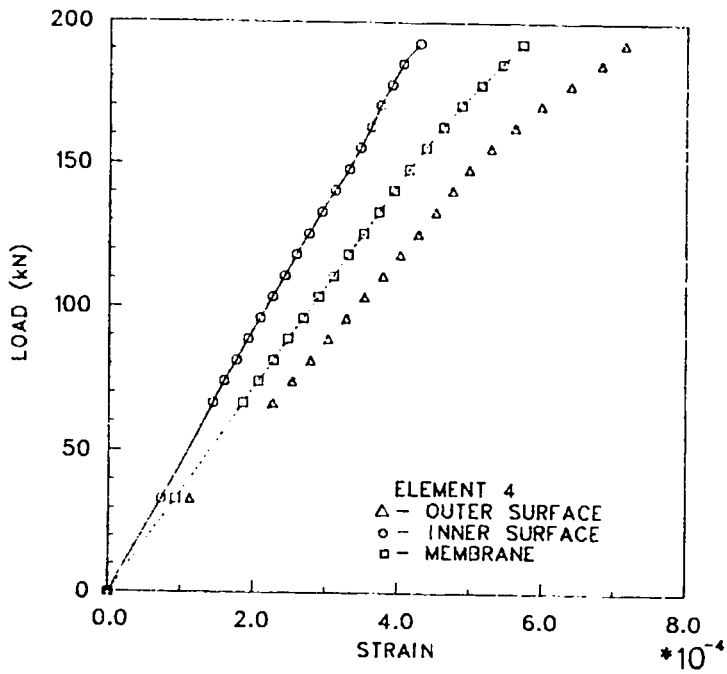


Fig. 39. Calculated load vs strain at location of strain gage 9'.

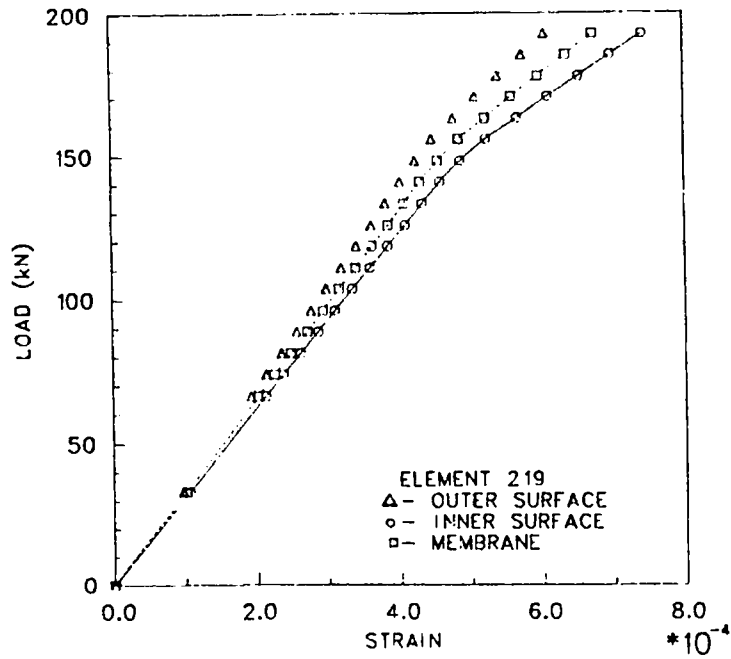


Fig. 40. Calculated load vs strain at location of strain gage 63.

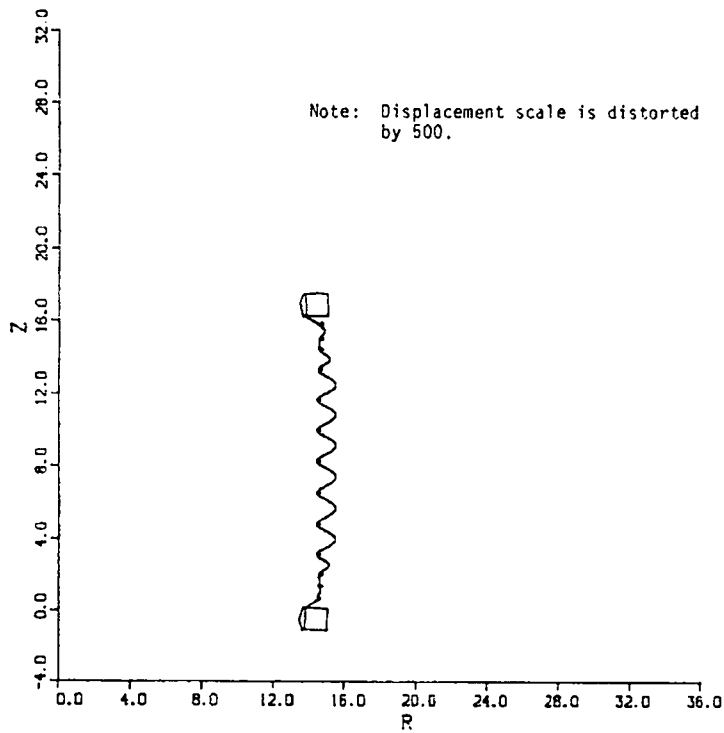
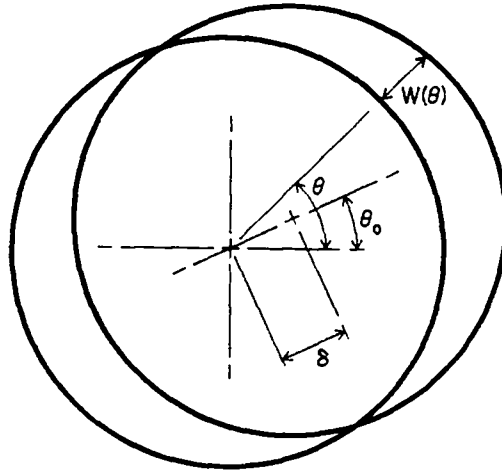


Fig. 41. Deformed mesh at buckling for the ADINA model.



$$W(\theta) = \delta \cos(\theta - \theta_0)$$

$$W(\theta) = (\delta \cos \theta_0) \cos \theta + (\delta \sin \theta_0) \sin \theta$$

Fig. 42. Rigid body translation in a circular section.

APPENDIX A

CHORD GAGE DATA AND RESULTS FOR MODEL 1

CYLINDER NUMBER 1

ST. NO.	C.S. NO.	RECORDED DATA	LOCAL RADIUS	DELTA RHO
ST. NO. 1	C.S. NO. 1	.2111	13.8532	.1122
ST. NO. 1	C.S. NO. 2	.2108	13.8730	.1320
ST. NO. 1	C.S. NO. 3	.2106	13.8862	.1452
ST. NO. 1	C.S. NO. 4	.2110	13.8598	.1188
ST. NO. 1	C.S. NO. 5	.2094	13.9660	.2250
ST. NO. 1	C.S. NO. 6	.2092	13.9794	.2384
ST. NO. 1	C.S. NO. 7	.2086	14.0197	.2787
ST. NO. 1	C.S. NO. 8	.2104	13.8994	.1584
ST. NO. 1	C.S. NO. 9	.2136	13.6906	-.0504
ST. NO. 1	C.S. NO. 10	.2149	13.6076	-.1334
ST. NO. 1	C.S. NO. 11	.2121	13.7877	.0467
ST. NO. 1	C.S. NO. 12	.2155	13.5696	-.1714

ST. NO.	C.S. NO.	RECORDED DATA	LOCAL RADIUS	DELTA RHO
ST. NO. 4	C.S. NO. 1	.2146	13.6266	-.1143
ST. NO. 4	C.S. NO. 2	.2159	13.5444	-.1966
ST. NO. 4	C.S. NO. 3	.2150	13.6012	-.1398
ST. NO. 4	C.S. NO. 4	.2144	13.6394	-.1016
ST. NO. 4	C.S. NO. 5	.2138	13.6778	-.0632
ST. NO. 4	C.S. NO. 6	.2138	13.6778	-.0632
ST. NO. 4	C.S. NO. 7	.2132	13.7164	-.0246
ST. NO. 4	C.S. NO. 8	.2134	13.7035	-.0375
ST. NO. 4	C.S. NO. 9	.2123	13.7747	.0337
ST. NO. 4	C.S. NO. 10	.2130	13.7293	-.0117
ST. NO. 4	C.S. NO. 11	.2135	13.6970	-.0439
ST. NO. 4	C.S. NO. 12	.2138	13.6778	-.0632

ST. NO.	C.S. NO.	RECORDED DATA	LOCAL RADIUS	DELTA RHO
ST. NO. 2	C.S. NO. 1	.2122	13.7812	.0402
ST. NO. 2	C.S. NO. 2	.2122	13.7812	.0402
ST. NO. 2	C.S. NO. 3	.2128	13.7422	.0012
ST. NO. 2	C.S. NO. 4	.2124	13.7682	.0272
ST. NO. 2	C.S. NO. 5	.2127	13.7487	.0077
ST. NO. 2	C.S. NO. 6	.2142	13.6522	-.0888
ST. NO. 2	C.S. NO. 7	.2134	13.7035	-.0375
ST. NO. 2	C.S. NO. 8	.2126	13.7552	.0142
ST. NO. 2	C.S. NO. 9	.2116	13.8204	.0794
ST. NO. 2	C.S. NO. 10	.2122	13.7812	.0402
ST. NO. 2	C.S. NO. 11	.2147	13.5203	-.1207
ST. NO. 2	C.S. NO. 12	.2116	13.8204	.0794

ST. NO.	C.S. NO.	RECORDED DATA	LOCAL RADIUS	DELTA RHO
ST. NO. 5	C.S. NO. 1	.2117	13.8138	.0728
ST. NO. 5	C.S. NO. 2	.2112	13.8466	.1056
ST. NO. 5	C.S. NO. 3	.2130	13.7293	-.0117
ST. NO. 5	C.S. NO. 4	.2123	13.7747	.0337
ST. NO. 5	C.S. NO. 5	.2116	13.8204	.0794
ST. NO. 5	C.S. NO. 6	.2111	13.8532	.1122
ST. NO. 5	C.S. NO. 7	.2119	13.8007	.0598
ST. NO. 5	C.S. NO. 8	.2123	13.7747	.0337
ST. NO. 5	C.S. NO. 9	.2121	13.7877	.0467
ST. NO. 5	C.S. NO. 10	.2114	13.8335	.0925
ST. NO. 5	C.S. NO. 11	.2101	13.9193	.1783
ST. NO. 5	C.S. NO. 12	.2098	13.9393	.1983

ST. NO.	C.S. NO.	RECORDED DATA	LOCAL RADIUS	DELTA RHO
ST. NO. 3	C.S. NO. 1	.2119	13.8007	.0598
ST. NO. 3	C.S. NO. 2	.2105	13.8928	.1518
ST. NO. 3	C.S. NO. 3	.2103	13.9060	.1650
ST. NO. 3	C.S. NO. 4	.2117	13.8138	.0728
ST. NO. 3	C.S. NO. 5	.2130	13.7293	-.0117
ST. NO. 3	C.S. NO. 6	.2119	13.8007	.0598
ST. NO. 3	C.S. NO. 7	.2127	13.7487	.0077
ST. NO. 3	C.S. NO. 8	.2130	13.7293	-.0117
ST. NO. 3	C.S. NO. 9	.2120	13.7942	.0532
ST. NO. 3	C.S. NO. 10	.2112	13.8466	.1056
ST. NO. 3	C.S. NO. 11	.2093	13.9727	.2317
ST. NO. 3	C.S. NO. 12	.2105	13.8928	.1518

ST. NO.	C.S. NO.	RECORDED DATA	LOCAL RADIUS	DELTA RHO
ST. NO. 6	C.S. NO. 1	.2121	13.7877	.0467
ST. NO. 6	C.S. NO. 2	.2138	13.6778	-.0632
ST. NO. 6	C.S. NO. 3	.2126	13.7552	.0142
ST. NO. 6	C.S. NO. 4	.2135	13.6970	-.0439
ST. NO. 6	C.S. NO. 5	.2140	13.6649	-.0760
ST. NO. 6	C.S. NO. 6	.2154	13.5759	-.1651
ST. NO. 6	C.S. NO. 7	.2118	13.8073	.0663
ST. NO. 6	C.S. NO. 8	.2105	13.8928	.1518
ST. NO. 6	C.S. NO. 9	.2127	13.7487	.0077
ST. NO. 6	C.S. NO. 10	.2134	13.7035	-.0375
ST. NO. 6	C.S. NO. 11	.2125	13.7617	.0207
ST. NO. 6	C.S. NO. 12	.2118	13.8073	.0663

			RECORDED	LOCAL	DELTA				RECORDED	LOCAL	DELTA
			DATA	RADIUS	RHO				DATA	RADIUS	RHO
ST. NO.	7	C.S. NO. 1	.2103	13.9060	.1650	ST. NO.	10	C.S. NO. 1	.2146	13.6266	-.1143
ST. NO.	7	C.S. NO. 2	.2087	14.0130	.2720	ST. NO.	10	C.S. NO. 2	.2154	13.5759	-.1651
ST. NO.	7	C.S. NO. 3	.2085	14.0264	.2855	ST. NO.	10	C.S. NO. 3	.2160	13.5381	-.2029
ST. NO.	7	C.S. NO. 4	.2082	14.0467	.3057	ST. NO.	10	C.S. NO. 4	.2149	13.6076	-.1334
ST. NO.	7	C.S. NO. 5	.2089	13.9995	.2585	ST. NO.	10	C.S. NO. 5	.2143	13.6458	-.0952
ST. NO.	7	C.S. NO. 6	.2072	14.1147	.3737	ST. NO.	10	C.S. NO. 6	.2157	13.5570	-.1840
ST. NO.	7	C.S. NO. 7	.2124	13.7682	.0272	ST. NO.	10	C.S. NO. 7	.2158	13.5507	-.1903
ST. NO.	7	C.S. NO. 8	.2126	13.7552	.0142	ST. NO.	10	C.S. NO. 8	.2147	13.6203	-.1207
ST. NO.	7	C.S. NO. 9	.2094	13.9660	.2250	ST. NO.	10	C.S. NO. 9	.2143	13.6458	-.0952
ST. NO.	7	C.S. NO. 10	.2093	13.9727	.2317	ST. NO.	10	C.S. NO. 10	.2138	13.6778	-.0632
ST. NO.	7	C.S. NO. 11	.2113	13.8400	.0991	ST. NO.	10	C.S. NO. 11	.2138	13.6778	-.0632
ST. NO.	7	C.S. NO. 12	.2136	13.6906	-.0504	ST. NO.	10	C.S. NO. 12	.2139	13.6713	-.0696
			RECORDED	LOCAL	DELTA				RECORDED	LOCAL	DELTA
			DATA	RADIUS	RHO				DATA	RADIUS	RHO
ST. NO.	8	C.S. NO. 1	.2140	13.6649	-.0760	ST. NO.	11	C.S. NO. 1	.2117	13.8138	.0728
ST. NO.	8	C.S. NO. 2	.2156	13.5633	-.1777	ST. NO.	11	C.S. NO. 2	.2107	13.8796	.1386
ST. NO.	8	C.S. NO. 3	.2150	13.6012	-.1398	ST. NO.	11	C.S. NO. 3	.2109	13.8664	.1254
ST. NO.	8	C.S. NO. 4	.2128	13.7422	.0012	ST. NO.	11	C.S. NO. 4	.2121	13.7877	.0467
ST. NO.	8	C.S. NO. 5	.2128	13.7422	.0012	ST. NO.	11	C.S. NO. 5	.2120	13.7942	.0532
ST. NO.	8	C.S. NO. 6	.2134	13.7035	-.0375	ST. NO.	11	C.S. NO. 6	.2122	13.7812	.0402
ST. NO.	8	C.S. NO. 7	.2104	13.8994	.1584	ST. NO.	11	C.S. NO. 7	.2117	13.8138	.0728
ST. NO.	8	C.S. NO. 8	.2116	13.8204	.0794	ST. NO.	11	C.S. NO. 8	.2120	13.7942	.0532
ST. NO.	8	C.S. NO. 9	.2133	13.7099	-.0311	ST. NO.	11	C.S. NO. 9	.2136	13.6906	-.0504
ST. NO.	8	C.S. NO. 10	.2134	13.7035	-.0375	ST. NO.	11	C.S. NO. 10	.2147	13.6203	-.1207
ST. NO.	8	C.S. NO. 11	.2126	13.7552	.0142	ST. NO.	11	C.S. NO. 11	.2148	13.6139	-.1271
ST. NO.	8	C.S. NO. 12	.2107	13.8796	.1386	ST. NO.	11	C.S. NO. 12	.2145	13.6330	-.1080
			RECORDED	LOCAL	DELTA				RECORDED	LOCAL	DELTA
			DATA	RADIUS	RHO				DATA	RADIUS	RHO
ST. NO.	9	C.S. NO. 1	.2147	13.6203	-.1207	ST. NO.	12	C.S. NO. 1	.2142	13.6522	-.0888
ST. NO.	9	C.S. NO. 2	.2135	13.6970	-.0439	ST. NO.	12	C.S. NO. 2	.2154	13.5759	-.1651
ST. NO.	9	C.S. NO. 3	.2146	13.6266	-.1143	ST. NO.	12	C.S. NO. 3	.2152	13.5885	-.1524
ST. NO.	9	C.S. NO. 4	.2168	13.4880	-.2530	ST. NO.	12	C.S. NO. 4	.2128	13.7422	.0012
ST. NO.	9	C.S. NO. 5	.2158	13.5507	-.1903	ST. NO.	12	C.S. NO. 5	.2127	13.7487	.0077
ST. NO.	9	C.S. NO. 6	.2159	13.5444	-.1966	ST. NO.	12	C.S. NO. 6	.2115	13.8269	.0859
ST. NO.	9	C.S. NO. 7	.2148	13.6139	-.1271	ST. NO.	12	C.S. NO. 7	.2135	13.6970	-.0439
ST. NO.	9	C.S. NO. 8	.2158	13.5507	-.1903	ST. NO.	12	C.S. NO. 8	.2138	13.6778	-.0632
ST. NO.	9	C.S. NO. 9	.2157	13.5570	-.1840	ST. NO.	12	C.S. NO. 9	.2124	13.7682	.0272
ST. NO.	9	C.S. NO. 10	.2159	13.5444	-.1966	ST. NO.	12	C.S. NO. 10	.2110	13.8598	.1188
ST. NO.	9	C.S. NO. 11	.2156	13.5633	-.1777	ST. NO.	12	C.S. NO. 11	.2109	13.8664	.1254
ST. NO.	9	C.S. NO. 12	.2162	13.5255	-.2154	ST. NO.	12	C.S. NO. 12	.2124	13.7682	.0272

			RECORDED DATA	LOCAL RADIUS	DELTA RHO				RECORDED DATA	LOCAL RADIUS	DELTA RHO
ST. NO. 13	C.S. NO. 1		.2122	13.7812	.0402	ST. NO. 16	C.S. NO. 1		.2126	13.7552	.0142
ST. NO. 13	C.S. NO. 2		.2127	13.7487	.0077	ST. NO. 16	C.S. NO. 2		.2122	13.7812	.0402
ST. NO. 13	C.S. NO. 3		.2134	13.7035	-.0375	ST. NO. 16	C.S. NO. 3		.2119	13.8007	.0598
ST. NO. 13	C.S. NO. 4		.2157	13.3570	-.1840	ST. NO. 16	C.S. NO. 4		.2108	13.8730	.1320
ST. NO. 13	C.S. NO. 5		.2150	13.6012	-.1398	ST. NO. 16	C.S. NO. 5		.2104	13.8994	.1584
ST. NO. 13	C.S. NO. 6		.2167	13.4943	-.2467	ST. NO. 16	C.S. NO. 6		.2093	13.9727	.2317
ST. NO. 13	C.S. NO. 7		.2152	13.5885	-.1524	ST. NO. 16	C.S. NO. 7		.2085	14.0264	.2855
ST. NO. 13	C.S. NO. 8		.2143	13.6458	-.0952	ST. NO. 16	C.S. NO. 8		.2081	14.0535	.3125
ST. NO. 13	C.S. NO. 9		.2152	13.5885	-.1524	ST. NO. 16	C.S. NO. 9		.2071	14.1215	.3806
ST. NO. 13	C.S. NO. 10		.2161	13.5318	-.2092	ST. NO. 16	C.S. NO. 10		.2075	14.0942	.3533
ST. NO. 13	C.S. NO. 11		.2164	13.5130	-.2280	ST. NO. 16	C.S. NO. 11		.2085	14.0264	.2855
ST. NO. 13	C.S. NO. 12		.2145	13.6330	-.1080	ST. NO. 16	C.S. NO. 12		.2093	13.9727	.2317
			RECORDED DATA	LOCAL RADIUS	DELTA RHO				RECORDED DATA	LOCAL RADIUS	DELTA RHO
ST. NO. 14	C.S. NO. 1		.2123	13.7747	.0337	ST. NO. 17	C.S. NO. 1		.2158	13.5507	-.1903
ST. NO. 14	C.S. NO. 2		.2109	13.8664	.1254	ST. NO. 17	C.S. NO. 2		.2148	13.6139	-.1271
ST. NO. 14	C.S. NO. 3		.2107	13.8796	.1386	ST. NO. 17	C.S. NO. 3		.2135	13.6970	-.0439
ST. NO. 14	C.S. NO. 4		.2105	13.8928	.1518	ST. NO. 17	C.S. NO. 4		.2139	13.6713	-.0696
ST. NO. 14	C.S. NO. 5		.2122	13.7812	.0402	ST. NO. 17	C.S. NO. 5		.2141	13.6585	-.0824
ST. NO. 14	C.S. NO. 6		.2115	13.8269	.0859	ST. NO. 17	C.S. NO. 6		.2151	13.5949	-.1461
ST. NO. 14	C.S. NO. 7		.2125	13.7617	.0207	ST. NO. 17	C.S. NO. 7		.2159	13.5444	-.1966
ST. NO. 14	C.S. NO. 8		.2139	13.6713	-.0696	ST. NO. 17	C.S. NO. 8		.2160	13.5381	-.2029
ST. NO. 14	C.S. NO. 9		.2132	13.7164	-.0246	ST. NO. 17	C.S. NO. 9		.2158	13.5507	-.1903
ST. NO. 14	C.S. NO. 10		.2128	13.7422	.0012	ST. NO. 17	C.S. NO. 10		.2149	13.6076	-.1334
ST. NO. 14	C.S. NO. 11		.2118	13.8073	.0663	ST. NO. 17	C.S. NO. 11		.2137	13.6842	-.0568
ST. NO. 14	C.S. NO. 12		.2128	13.7422	.0012	ST. NO. 17	C.S. NO. 12		.2132	13.7164	-.0246
			RECORDED DATA	LOCAL RADIUS	DELTA RHO				RECORDED DATA	LOCAL RADIUS	DELTA RHO
ST. NO. 15	C.S. NO. 1		.2127	13.7487	.0077	ST. NO. 18	C.S. NO. 1		.2061	14.1903	.4493
ST. NO. 15	C.S. NO. 2		.2142	13.6522	-.0888	ST. NO. 18	C.S. NO. 2		.2066	14.1558	.4148
ST. NO. 15	C.S. NO. 3		.2140	13.6649	-.0760	ST. NO. 18	C.S. NO. 3		.2109	13.8664	.1254
ST. NO. 15	C.S. NO. 4		.2134	13.7035	-.0375	ST. NO. 18	C.S. NO. 4		.2114	13.8335	.0925
ST. NO. 15	C.S. NO. 5		.2113	13.8400	.0991	ST. NO. 18	C.S. NO. 5		.2136	13.6906	-.0504
ST. NO. 15	C.S. NO. 6		.2114	13.8335	.0925	ST. NO. 18	C.S. NO. 6		.2140	13.6649	-.0760
ST. NO. 15	C.S. NO. 7		.2106	13.8862	.1452	ST. NO. 18	C.S. NO. 7		.2140	13.6649	-.0760
ST. NO. 15	C.S. NO. 8		.2096	13.9526	.2116	ST. NO. 18	C.S. NO. 8		.2144	13.6394	-.1016
ST. NO. 15	C.S. NO. 9		.2103	13.9060	.1650	ST. NO. 18	C.S. NO. 9		.2149	13.6076	-.1334
ST. NO. 15	C.S. NO. 10		.2102	13.9127	.1717	ST. NO. 18	C.S. NO. 10		.2159	13.5444	-.1966
ST. NO. 15	C.S. NO. 11		.2107	13.8796	.1386	ST. NO. 18	C.S. NO. 11		.2163	13.5193	-.2217
ST. NO. 15	C.S. NO. 12		.2105	13.8928	.1518	ST. NO. 18	C.S. NO. 12		.2161	13.5318	-.2092

ST. NO.	C.S. NO.	RECORDED DATA	LOCAL RADIUS	DELTA RHO	ST. NO.	C.S. NO.	RECORDED DATA	LOCAL RADIUS	DELTA RHO
19	1	.2162	13.5255	-.2154	22	1	.2131	13.7228	-.0182
19	2	.2163	13.5193	-.2217	22	2	.2126	13.7552	.0142
19	3	.2137	13.6842	-.0568	22	3	.2144	13.6394	-.1016
19	4	.2142	13.6522	-.0888	22	4	.2144	13.6394	-.1016
19	5	.2127	13.7487	.0077	22	5	.2135	13.6970	-.0439
19	6	.2105	13.8928	.1518	22	6	.2147	13.6203	-.1207
19	7	.2124	13.7682	.0272	22	7	.2127	13.7487	.0077
19	8	.2135	13.6970	-.0439	22	8	.2118	13.8073	.0663
19	9	.2141	13.6585	-.0824	22	9	.2101	13.9193	.1783
19	10	.2147	13.6203	-.1207	22	10	.2113	13.8400	.0991
19	11	.2152	13.5885	-.1524	22	11	.2141	13.6585	-.0824
19	12	.2151	13.5949	-.1461	22	12	.2139	13.6713	-.0696

ST. NO.	C.S. NO.	RECORDED DATA	LOCAL RADIUS	DELTA RHO	ST. NO.	C.S. NO.	RECORDED DATA	LOCAL RADIUS	DELTA RHO
20	1	.2115	13.8269	.0859	23	1	.2094	13.9660	.2250
20	2	.2115	13.8269	.0859	23	2	.2109	13.8664	.1254
20	3	.2129	13.7357	-.0052	23	3	.2101	13.9193	.1783
20	4	.2117	13.8138	.0728	23	4	.2097	13.9459	.2050
20	5	.2133	13.7099	-.0311	23	5	.2122	13.7812	.0402
20	6	.2164	13.5130	-.2280	23	6	.2124	13.7682	.0272
20	7	.2152	13.5885	-.1524	23	7	.2126	13.7552	.0142
20	8	.2122	13.7812	.0402	23	8	.2108	13.8730	.1320
20	9	.2118	13.8073	.0663	23	9	.2114	13.8335	.0925
20	10	.2100	13.9260	.1850	23	10	.2110	13.8598	.1188
20	11	.2098	13.9393	.1983	23	11	.2078	14.0738	.3328
20	12	.2096	13.9526	.2116	23	12	.2078	14.0738	.3328

ST. NO.	C.S. NO.	RECORDED DATA	LOCAL RADIUS	DELTA RHO	ST. NO.	C.S. NO.	RECORDED DATA	LOCAL RADIUS	DELTA RHO
21	1	.2152	13.5885	-.1524	24	1	.2146	13.6266	-.1143
21	2	.2153	13.5822	-.1588	24	2	.2128	13.7422	.0012
21	3	.2132	13.7164	-.0246	24	3	.2134	13.7035	-.0375
21	4	.2142	13.6522	-.0888	24	4	.2125	13.7617	.0207
21	5	.2116	13.8204	.0794	24	5	.2105	13.8928	.1518
21	6	.2102	13.9127	.1717	24	6	.2104	13.8994	.1584
21	7	.2096	13.9526	.2116	24	7	.2168	13.4880	-.2530
21	8	.2128	13.7422	.0012	24	8	.2145	13.6330	-.1080
21	9	.2132	13.7164	-.0246	24	9	.2161	13.5318	-.2092
21	10	.2140	13.6649	-.0760	24	10	.2152	13.5885	-.1524
21	11	.2129	13.7357	-.0052	24	11	.2168	13.4880	-.2530
21	12	.2141	13.6585	-.0824	24	12	.2174	13.4507	-.2903

			RECORDED DATA	LOCAL RADIUS	DELTA RHO
ST. NO. 25	C.S. NO. 1		.2149	13.6076	-.1334
ST. NO. 25	C.S. NO. 2		.2157	13.5570	-.1840
ST. NO. 25	C.S. NO. 3		.2138	13.6778	-.0632
ST. NO. 25	C.S. NO. 4		.2150	13.6012	-.1398
ST. NO. 25	C.S. NO. 5		.2127	13.7487	.0077
ST. NO. 25	C.S. NO. 6		.2147	13.6203	-.1207
ST. NO. 25	C.S. NO. 7		.2157	13.5570	-.1840
ST. NO. 25	C.S. NO. 8		.2145	13.6330	-.1080
ST. NO. 25	C.S. NO. 9		.2130	13.7293	-.0117
ST. NO. 25	C.S. NO. 10		.2137	13.6842	-.0568
ST. NO. 25	C.S. NO. 11		.2134	13.7035	-.0375
ST. NO. 25	C.S. NO. 12		.2145	13.6330	-.1080

			RECORDED DATA	LOCAL RADIUS	DELTA RHO
ST. NO. 28	C.S. NO. 1		.2094	13.9660	.2250
ST. NO. 28	C.S. NO. 2		.2091	13.9861	.2451
ST. NO. 28	C.S. NO. 3		.2103	13.9060	.1650
ST. NO. 28	C.S. NO. 4		.2089	13.9995	.2585
ST. NO. 28	C.S. NO. 5		.2098	13.9393	.1983
ST. NO. 28	C.S. NO. 6		.2123	13.7747	.0337
ST. NO. 28	C.S. NO. 7		.2114	13.8335	.0925
ST. NO. 28	C.S. NO. 8		.2116	13.8204	.0794
ST. NO. 28	C.S. NO. 9		.2109	13.8664	.1254
ST. NO. 28	C.S. NO. 10		.2112	13.8466	.1056
ST. NO. 28	C.S. NO. 11		.2116	13.8204	.0794
ST. NO. 28	C.S. NO. 12		.2130	13.7293	-.0117

			RECORDED DATA	LOCAL RADIUS	DELTA RHO
ST. NO. 26	C.S. NO. 1		.2109	13.8664	.1254
ST. NO. 26	C.S. NO. 2		.2121	13.7877	.0467
ST. NO. 26	C.S. NO. 3		.2130	13.7293	-.0117
ST. NO. 26	C.S. NO. 4		.2143	13.6458	-.0952
ST. NO. 26	C.S. NO. 5		.2102	13.9127	.1717
ST. NO. 26	C.S. NO. 6		.2159	13.5444	-.1966
ST. NO. 26	C.S. NO. 7		.2122	13.7812	.0402
ST. NO. 26	C.S. NO. 8		.2115	13.8269	.0859
ST. NO. 26	C.S. NO. 9		.2125	13.7617	.0207
ST. NO. 26	C.S. NO. 10		.2126	13.7552	.0142
ST. NO. 26	C.S. NO. 11		.2133	13.7099	-.0311
ST. NO. 26	C.S. NO. 12		.2117	13.8138	.0728

			RECORDED DATA	LOCAL RADIUS	DELTA RHO
ST. NO. 29	C.S. NO. 1		.2123	13.7747	.0337
ST. NO. 29	C.S. NO. 2		.2137	13.6842	-.0568
ST. NO. 29	C.S. NO. 3		.2126	13.7552	.0142
ST. NO. 29	C.S. NO. 4		.2130	13.7293	-.0117
ST. NO. 29	C.S. NO. 5		.2113	13.8400	.0991
ST. NO. 29	C.S. NO. 6		.2089	13.9995	.2585
ST. NO. 29	C.S. NO. 7		.2079	14.0670	.3261
ST. NO. 29	C.S. NO. 8		.2081	14.0535	.3125
ST. NO. 29	C.S. NO. 9		.2088	14.0062	.2652
ST. NO. 29	C.S. NO. 10		.2095	13.9593	.2183
ST. NO. 29	C.S. NO. 11		.2107	13.8796	.1386
ST. NO. 29	C.S. NO. 12		.2090	13.9928	.2518

			RECORDED DATA	LOCAL RADIUS	DELTA RHO
ST. NO. 27	C.S. NO. 1		.2158	13.5507	-.1903
ST. NO. 27	C.S. NO. 2		.2148	13.6139	-.1271
ST. NO. 27	C.S. NO. 3		.2144	13.6394	-.1016
ST. NO. 27	C.S. NO. 4		.2141	13.6585	-.0824
ST. NO. 27	C.S. NO. 5		.2095	13.9593	.2183
ST. NO. 27	C.S. NO. 6		.2120	13.7942	.0532
ST. NO. 27	C.S. NO. 7		.2158	13.5507	-.1903
ST. NO. 27	C.S. NO. 8		.2168	13.4880	-.2530
ST. NO. 27	C.S. NO. 9		.2166	13.5005	-.2405
ST. NO. 27	C.S. NO. 10		.2163	13.5193	-.2217
ST. NO. 27	C.S. NO. 11		.2147	13.6203	-.1207
ST. NO. 27	C.S. NO. 12		.2146	13.6266	-.1143

			RECORDED DATA	LOCAL RADIUS	DELTA RHO
ST. NO. 30	C.S. NO. 1		.2148	13.6139	-.1271
ST. NO. 30	C.S. NO. 2		.2130	13.7293	-.0117
ST. NO. 30	C.S. NO. 3		.2134	13.7035	-.0375
ST. NO. 30	C.S. NO. 4		.2139	13.6713	-.0696
ST. NO. 30	C.S. NO. 5		.2165	13.5067	-.2342
ST. NO. 30	C.S. NO. 6		.2169	13.4818	-.2592
ST. NO. 30	C.S. NO. 7		.2175	13.4445	-.2965
ST. NO. 30	C.S. NO. 8		.2144	13.6394	-.1016
ST. NO. 30	C.S. NO. 9		.2140	13.6649	-.0760
ST. NO. 30	C.S. NO. 10		.2135	13.6970	-.0439
ST. NO. 30	C.S. NO. 11		.2126	13.7552	.0142
ST. NO. 30	C.S. NO. 12		.2141	13.6585	-.0824

			RECORDED	LOCAL	DELTA				RECORDED	LOCAL	DELTA
			DATA	RADIUS	RHO				DATA	RADIUS	RHO
ST. NO. 31	C.S. NO. 1		.2157	13.5570	-.1840	ST. NO. 34	C.S. NO. 1		.2150	13.6012	-.1398
ST. NO. 31	C.S. NO. 2		.2159	13.5444	-.1966	ST. NO. 34	C.S. NO. 2		.2136	13.6906	-.0504
ST. NO. 31	C.S. NO. 3		.2136	13.6906	-.0504	ST. NO. 34	C.S. NO. 3		.2145	13.6330	-.1080
ST. NO. 31	C.S. NO. 4		.2125	13.7617	.0207	ST. NO. 34	C.S. NO. 4		.2167	13.4943	-.2467
ST. NO. 31	C.S. NO. 5		.2115	13.8269	.0859	ST. NO. 34	C.S. NO. 5		.2172	13.4631	-.2779
ST. NO. 31	C.S. NO. 6		.2116	13.8204	.0794	ST. NO. 34	C.S. NO. 6		.2161	13.5318	-.2092
ST. NO. 31	C.S. NO. 7		.2110	13.8598	.1188	ST. NO. 34	C.S. NO. 7		.2145	13.6330	-.1080
ST. NO. 31	C.S. NO. 8		.2140	13.6649	-.0760	ST. NO. 34	C.S. NO. 8		.2130	13.7293	-.0117
ST. NO. 31	C.S. NO. 9		.2137	13.6842	-.0568	ST. NO. 34	C.S. NO. 9		.2140	13.6649	-.0760
ST. NO. 31	C.S. NO. 10		.2119	13.8007	.0598	ST. NO. 34	C.S. NO. 10		.2145	13.6330	-.1080
ST. NO. 31	C.S. NO. 11		.2107	13.8796	.1386	ST. NO. 34	C.S. NO. 11		.2142	13.6522	-.0888
ST. NO. 31	C.S. NO. 12		.2109	13.8664	.1254	ST. NO. 34	C.S. NO. 12		.2139	13.6713	-.0696
			RECORDED	LOCAL	DELTA				RECORDED	LOCAL	DELTA
			DATA	RADIUS	RHO				DATA	RADIUS	RHO
ST. NO. 32	C.S. NO. 1		.2092	13.9794	.2384	ST. NO. 35	C.S. NO. 1		.2093	13.9727	.2317
ST. NO. 32	C.S. NO. 2		.2093	13.9727	.2317	ST. NO. 35	C.S. NO. 2		.2086	14.0197	.2787
ST. NO. 32	C.S. NO. 3		.2118	13.8073	.0663	ST. NO. 35	C.S. NO. 3		.2097	13.9459	.2050
ST. NO. 32	C.S. NO. 4		.2123	13.7747	.0337	ST. NO. 35	C.S. NO. 4		.2081	14.0535	.3125
ST. NO. 32	C.S. NO. 5		.2109	13.8664	.1254	ST. NO. 35	C.S. NO. 5		.2099	13.9326	.1916
ST. NO. 32	C.S. NO. 6		.2103	13.9060	.1650	ST. NO. 35	C.S. NO. 6		.2109	13.8664	.1254
ST. NO. 32	C.S. NO. 7		.2085	14.0264	.2855	ST. NO. 35	C.S. NO. 7		.2131	13.7228	-.0182
ST. NO. 32	C.S. NO. 8		.2072	14.1147	.3737	ST. NO. 35	C.S. NO. 8		.2135	13.6970	-.0439
ST. NO. 32	C.S. NO. 9		.2073	14.1079	.3669	ST. NO. 35	C.S. NO. 9		.2133	13.7099	-.0311
ST. NO. 32	C.S. NO. 10		.2105	13.8928	.1518	ST. NO. 35	C.S. NO. 10		.2142	13.6522	-.0888
ST. NO. 32	C.S. NO. 11		.2121	13.7877	.0467	ST. NO. 35	C.S. NO. 11		.2142	13.6522	-.0888
ST. NO. 32	C.S. NO. 12		.2125	13.7617	.0207	ST. NO. 35	C.S. NO. 12		.2171	13.4693	-.2717
			RECORDED	LOCAL	DELTA				RECORDED	LOCAL	DELTA
			DATA	RADIUS	RHO				DATA	RADIUS	RHO
ST. NO. 33	C.S. NO. 1		.2132	13.7164	-.0246	ST. NO. 36	C.S. NO. 1		.2175	13.4445	-.2965
ST. NO. 33	C.S. NO. 2		.2146	13.6266	-.1143	ST. NO. 36	C.S. NO. 2		.2188	13.3644	-.3766
ST. NO. 33	C.S. NO. 3		.2135	13.6970	-.0439	ST. NO. 36	C.S. NO. 3		.2171	13.4693	-.2717
ST. NO. 33	C.S. NO. 4		.2127	13.7487	.0077	ST. NO. 36	C.S. NO. 4		.2177	13.4321	-.3089
ST. NO. 33	C.S. NO. 5		.2130	13.7293	-.0117	ST. NO. 36	C.S. NO. 5		.2163	13.5193	-.2217
ST. NO. 33	C.S. NO. 6		.2138	13.6778	-.0632	ST. NO. 36	C.S. NO. 6		.2166	13.5005	-.2405
ST. NO. 33	C.S. NO. 7		.2161	13.5318	-.2092	ST. NO. 36	C.S. NO. 7		.2158	13.5507	-.1903
ST. NO. 33	C.S. NO. 8		.2178	13.4259	-.3150	ST. NO. 36	C.S. NO. 8		.2158	13.5507	-.1903
ST. NO. 33	C.S. NO. 9		.2169	13.4818	-.2592	ST. NO. 36	C.S. NO. 9		.2139	13.6713	-.0696
ST. NO. 33	C.S. NO. 10		.2151	13.5949	-.1461	ST. NO. 36	C.S. NO. 10		.2125	13.7617	.0207
ST. NO. 33	C.S. NO. 11		.2149	13.6076	-.1334	ST. NO. 36	C.S. NO. 11		.2142	13.6522	-.0888
ST. NO. 33	C.S. NO. 12		.2136	13.6906	-.0504	ST. NO. 36	C.S. NO. 12		.2109	13.8664	.1254

AVERAGE CHORD	GAGE RADIUS OF CURVATURE AT CROSS SECTION 1 IS =	13.74040
AVERAGE CHORD	GAGE RADIUS OF CURVATURE AT CROSS SECTION 2 IS =	13.73908
AVERAGE CHORD	GAGE RADIUS OF CURVATURE AT CROSS SECTION 3 IS =	13.73700
AVERAGE CHORD	GAGE RADIUS OF CURVATURE AT CROSS SECTION 4 IS =	13.73705
AVERAGE CHORD	GAGE RADIUS OF CURVATURE AT CROSS SECTION 5 IS =	13.76259
AVERAGE CHORD	GAGE RADIUS OF CURVATURE AT CROSS SECTION 6 IS =	13.73827
AVERAGE CHORD	GAGE RADIUS OF CURVATURE AT CROSS SECTION 7 IS =	13.73530
AVERAGE CHORD	GAGE RADIUS OF CURVATURE AT CROSS SECTION 8 IS =	13.74031
AVERAGE CHORD	GAGE RADIUS OF CURVATURE AT CROSS SECTION 9 IS =	13.74333
AVERAGE CHORD	GAGE RADIUS OF CURVATURE AT CROSS SECTION 10 IS =	13.73914
AVERAGE CHORD	GAGE RADIUS OF CURVATURE AT CROSS SECTION 11 IS =	13.74191
AVERAGE CHORD	GAGE RADIUS OF CURVATURE AT CROSS SECTION 12 IS =	13.73738

AVERAGE RADIUS FROM ALL DATA POINTS = 13.74098

APPENDIX B

CHORD GAGE DATA AND RESULTS FOR MODEL 2

CYLINDER NUMBER 2

ST. NO.	C.S. NO.	RECORDED DATA	LOCAL RADIUS	DELTA RHO
ST. NO. 1	C.S. NO. 1	.2130	13.7293	.0010
ST. NO. 1	C.S. NO. 2	.2111	13.8532	-.1249
ST. NO. 1	C.S. NO. 3	.2101	13.9193	-.1910
ST. NO. 1	C.S. NO. 4	.2081	14.0535	-.3252
ST. NO. 1	C.S. NO. 5	.2093	13.9727	-.2444
ST. NO. 1	C.S. NO. 6	.2075	14.0942	-.3660
ST. NO. 1	C.S. NO. 7	.2096	13.9526	-.2243
ST. NO. 1	C.S. NO. 8	.2112	13.8466	-.1183
ST. NO. 1	C.S. NO. 9	.2117	13.8138	-.0855
ST. NO. 1	C.S. NO. 10	.2103	13.9060	-.1778
ST. NO. 1	C.S. NO. 11	.2089	13.9995	-.2712
ST. NO. 1	C.S. NO. 12	.2085	14.0264	-.2982

ST. NO.	C.S. NO.	RECORDED DATA	LOCAL RADIUS	DELTA RHO
ST. NO. 4	C.S. NO. 1	.2140	13.6649	-.0633
ST. NO. 4	C.S. NO. 2	.2143	13.6458	-.0825
ST. NO. 4	C.S. NO. 3	.2139	13.6713	-.0569
ST. NO. 4	C.S. NO. 4	.2129	13.7357	-.0075
ST. NO. 4	C.S. NO. 5	.2152	13.5885	-.1397
ST. NO. 4	C.S. NO. 6	.2148	13.6139	-.1144
ST. NO. 4	C.S. NO. 7	.2156	13.5633	-.1650
ST. NO. 4	C.S. NO. 8	.2158	13.5507	-.1776
ST. NO. 4	C.S. NO. 9	.2137	13.6842	-.0441
ST. NO. 4	C.S. NO. 10	.2139	13.6713	-.0569
ST. NO. 4	C.S. NO. 11	.2118	13.8073	-.0790
ST. NO. 4	C.S. NO. 12	.2119	13.8007	-.0725

ST. NO.	C.S. NO.	RECORDED DATA	LOCAL RADIUS	DELTA RHO
ST. NO. 2	C.S. NO. 1	.2145	13.6330	-.0953
ST. NO. 2	C.S. NO. 2	.2149	13.6076	-.1207
ST. NO. 2	C.S. NO. 3	.2151	13.5949	-.1334
ST. NO. 2	C.S. NO. 4	.2163	13.5193	-.2090
ST. NO. 2	C.S. NO. 5	.2160	13.5381	-.1902
ST. NO. 2	C.S. NO. 6	.2152	13.5885	-.1397
ST. NO. 2	C.S. NO. 7	.2146	13.6266	-.1016
ST. NO. 2	C.S. NO. 8	.2126	13.7552	.0269
ST. NO. 2	C.S. NO. 9	.2120	13.7942	.0659
ST. NO. 2	C.S. NO. 10	.2125	13.7617	.0334
ST. NO. 2	C.S. NO. 11	.2137	13.6842	-.0441
ST. NO. 2	C.S. NO. 12	.2155	13.5696	-.1587

ST. NO.	C.S. NO.	RECORDED DATA	LOCAL RADIUS	DELTA RHO
ST. NO. 5	C.S. NO. 1	.2124	13.7682	.0399
ST. NO. 5	C.S. NO. 2	.2122	13.7812	.0529
ST. NO. 5	C.S. NO. 3	.2132	13.7164	-.0119
ST. NO. 5	C.S. NO. 4	.2141	13.6585	-.0697
ST. NO. 5	C.S. NO. 5	.2119	13.8007	.0725
ST. NO. 5	C.S. NO. 6	.2124	13.7682	.0399
ST. NO. 5	C.S. NO. 7	.2112	13.8466	.1183
ST. NO. 5	C.S. NO. 8	.2112	13.8466	.1183
ST. NO. 5	C.S. NO. 9	.2116	13.8204	.0921
ST. NO. 5	C.S. NO. 10	.2133	13.7099	-.0184
ST. NO. 5	C.S. NO. 11	.2156	13.5633	-.1650
ST. NO. 5	C.S. NO. 12	.2159	13.5444	-.1839

ST. NO.	C.S. NO.	RECORDED DATA	LOCAL RADIUS	DELTA RHO
ST. NO. 3	C.S. NO. 1	.2147	13.6203	-.1080
ST. NO. 3	C.S. NO. 2	.2147	13.6203	-.1080
ST. NO. 3	C.S. NO. 3	.2163	13.5193	-.2090
ST. NO. 3	C.S. NO. 4	.2163	13.5193	-.2090
ST. NO. 3	C.S. NO. 5	.2149	13.6076	-.1207
ST. NO. 3	C.S. NO. 6	.2160	13.5381	-.1902
ST. NO. 3	C.S. NO. 7	.2149	13.5076	-.1207
ST. NO. 3	C.S. NO. 8	.2146	13.6266	-.1016
ST. NO. 3	C.S. NO. 9	.2160	13.5381	-.1902
ST. NO. 3	C.S. NO. 10	.2150	13.6012	-.1271
ST. NO. 3	C.S. NO. 11	.2160	13.5381	-.1902
ST. NO. 3	C.S. NO. 12	.2143	13.6458	-.0825

ST. NO.	C.S. NO.	RECORDED DATA	LOCAL RADIUS	DELTA RHO
ST. NO. 6	C.S. NO. 1	.2124	13.7682	.0399
ST. NO. 6	C.S. NO. 2	.2121	13.7877	.0594
ST. NO. 6	C.S. NO. 3	.2103	13.9060	.1778
ST. NO. 6	C.S. NO. 4	.2086	14.0197	.2914
ST. NO. 6	C.S. NO. 5	.2109	13.8664	.1381
ST. NO. 6	C.S. NO. 6	.2107	13.8796	.1513
ST. NO. 6	C.S. NO. 7	.2130	13.7293	.0010
ST. NO. 6	C.S. NO. 8	.2135	13.6970	-.0312
ST. NO. 6	C.S. NO. 9	.2135	13.6970	-.0312
ST. NO. 6	C.S. NO. 10	.2129	13.7357	.0075
ST. NO. 6	C.S. NO. 11	.2104	13.8994	.1711
ST. NO. 6	C.S. NO. 12	.2098	13.9393	.2110

ST. NO.	C.S. NO.	RECORDED DATA	LOCAL RADIUS	DELTA RHO	ST. NO.	C.S. NO.	RECORDED DATA	LOCAL RADIUS	DELTA RHO
7	1	.2093	13.9727	.2444	10	1	.2140	13.6649	-.0633
7	2	.2087	14.0130	.2847	10	2	.2127	13.7487	.0204
7	3	.2122	13.7812	.0529	10	3	.2117	13.8138	.0855
7	4	.2135	13.6970	-.0312	10	4	.2120	13.7942	.0659
7	5	.2130	13.7293	.0010	10	5	.2136	13.6906	-.0377
7	6	.2138	13.6778	-.0505	10	6	.2146	13.6266	-.1016
7	7	.2133	13.7099	-.0184	10	7	.2139	13.6713	-.0569
7	8	.2123	13.7747	.0464	10	8	.2132	13.7164	-.0119
7	9	.2114	13.8335	.1052	10	9	.2119	13.8007	.0725
7	10	.2118	13.8073	.0790	10	10	.2125	13.7617	.0334
7	11	.2143	13.6458	-.0825	10	11	.2136	13.6906	-.0377
7	12	.2150	13.6012	-.1271	10	12	.2142	13.6522	-.0761
ST. NO.	C.S. NO.	RECORDED DATA	LOCAL RADIUS	DELTA RHO	ST. NO.	C.S. NO.	RECORDED DATA	LOCAL RADIUS	DELTA RHO
8	1	.2142	13.6522	-.0761	11	1	.2112	13.8466	.1183
8	2	.2146	13.6266	-.1016	11	2	.2114	13.8335	.1052
8	3	.2116	13.8204	.0921	11	3	.2119	13.8007	.0725
8	4	.2117	13.8138	.0855	11	4	.2130	13.7293	.0010
8	5	.2119	13.8007	.0725	11	5	.2140	13.6649	-.0633
8	6	.2105	13.8928	.1645	11	6	.2138	13.6778	-.0505
8	7	.2104	13.8994	.1711	11	7	.2165	13.5067	-.2215
8	8	.2113	13.8400	.1118	11	8	.2160	13.5381	-.1902
8	9	.2138	13.6778	-.0505	11	9	.2166	13.5005	-.2278
8	10	.2143	13.6458	-.0825	11	10	.2165	13.5067	-.2215
8	11	.2141	13.6585	-.0697	11	11	.2158	13.5507	-.1776
8	12	.2141	13.6585	-.0697	11	12	.2145	13.6330	-.0953
ST. NO.	C.S. NO.	RECORDED DATA	LOCAL RADIUS	DELTA RHO	ST. NO.	C.S. NO.	RECORDED DATA	LOCAL RADIUS	DELTA RHO
9	1	.2138	13.6778	-.0505	12	1	.2133	13.7099	-.0184
9	2	.2150	13.6012	-.1271	12	2	.2135	13.6970	-.0312
9	3	.2162	13.5255	-.2027	12	3	.2140	13.6649	-.0633
9	4	.2156	13.5633	-.1650	12	4	.2128	13.7422	.0139
9	5	.2137	13.6842	-.0441	12	5	.2111	13.8532	.1249
9	6	.2142	13.6522	-.0761	12	6	.2104	13.8994	.1711
9	7	.2146	13.6266	-.1016	12	7	.2083	14.0399	.3117
9	8	.2142	13.6522	-.0761	12	8	.2088	14.0062	.2779
9	9	.2133	13.7099	-.0184	12	9	.2093	13.9727	.2444
9	10	.2122	13.7812	.0529	12	10	.2099	13.9326	.2043
9	11	.2110	13.8598	.1315	12	11	.2096	13.9526	.2243
9	12	.2112	13.8466	.1183	12	12	.2110	13.8598	.1315

ST. NO.	C.S. NO.	RECORDED DATA	LOCAL RADIUS	DELTA RHO
ST. NO. 13	C.S. NO. 1	.2127	13.7487	.0204
ST. NO. 13	C.S. NO. 2	.2118	13.8073	.0790
ST. NO. 13	C.S. NO. 3	.2115	13.8269	.0986
ST. NO. 13	C.S. NO. 4	.2115	13.8269	.0986
ST. NO. 13	C.S. NO. 5	.2126	13.7552	.0269
ST. NO. 13	C.S. NO. 6	.2136	13.6906	-.0377
ST. NO. 13	C.S. NO. 7	.2145	13.6330	-.0953
ST. NO. 13	C.S. NO. 8	.2149	13.6076	-.1207
ST. NO. 13	C.S. NO. 9	.2144	13.6394	-.0889
ST. NO. 13	C.S. NO. 10	.2152	13.5885	-.1397
ST. NO. 13	C.S. NO. 11	.2162	13.5255	-.2027
ST. NO. 13	C.S. NO. 12	.2156	13.5633	-.1650

ST. NO.	C.S. NO.	RECORDED DATA	LOCAL RADIUS	DELTA RHO
ST. NO. 16	C.S. NO. 1	.2140	13.6649	-.0633
ST. NO. 16	C.S. NO. 2	.2126	13.7552	.0269
ST. NO. 16	C.S. NO. 3	.2102	13.9127	.1844
ST. NO. 16	C.S. NO. 4	.2116	13.8204	.0921
ST. NO. 16	C.S. NO. 5	.2134	13.7035	-.0248
ST. NO. 16	C.S. NO. 6	.2130	13.7293	.0010
ST. NO. 16	C.S. NO. 7	.2175	13.4445	-.2838
ST. NO. 16	C.S. NO. 8	.2157	13.5570	-.1713
ST. NO. 16	C.S. NO. 9	.2154	13.5759	-.1524
ST. NO. 16	C.S. NO. 10	.2146	13.6266	-.1016
ST. NO. 16	C.S. NO. 11	.2151	13.5949	-.1334
ST. NO. 16	C.S. NO. 12	.2146	13.6266	-.1016

ST. NO.	C.S. NO.	RECORDED DATA	LOCAL RADIUS	DELTA RHO
ST. NO. 14	C.S. NO. 1	.2140	13.6649	-.0633
ST. NO. 14	C.S. NO. 2	.2139	13.6713	-.0569
ST. NO. 14	C.S. NO. 3	.2139	13.6713	-.0569
ST. NO. 14	C.S. NO. 4	.2145	13.6330	-.0953
ST. NO. 14	C.S. NO. 5	.2147	13.6203	-.1080
ST. NO. 14	C.S. NO. 6	.2124	13.7682	.0399
ST. NO. 14	C.S. NO. 7	.2134	13.7035	-.0248
ST. NO. 14	C.S. NO. 8	.2122	13.7812	.0529
ST. NO. 14	C.S. NO. 9	.2129	13.7357	.0075
ST. NO. 14	C.S. NO. 10	.2105	13.8928	.1645
ST. NO. 14	C.S. NO. 11	.2103	13.9060	.1778
ST. NO. 14	C.S. NO. 12	.2102	13.9127	.1844

ST. NO.	C.S. NO.	RECORDED DATA	LOCAL RADIUS	DELTA RHO
ST. NO. 17	C.S. NO. 1	.2147	13.6203	-.1080
ST. NO. 17	C.S. NO. 2	.2156	13.5633	-.1650
ST. NO. 17	C.S. NO. 3	.2172	13.4631	-.2652
ST. NO. 17	C.S. NO. 4	.2155	13.5696	-.1587
ST. NO. 17	C.S. NO. 5	.2133	13.7099	-.0184
ST. NO. 17	C.S. NO. 6	.2132	13.7164	-.0119
ST. NO. 17	C.S. NO. 7	.2101	13.9193	.1910
ST. NO. 17	C.S. NO. 8	.2113	13.8400	.1118
ST. NO. 17	C.S. NO. 9	.2120	13.7942	.0659
ST. NO. 17	C.S. NO. 10	.2132	13.7164	-.0119
ST. NO. 17	C.S. NO. 11	.2126	13.7552	.0269
ST. NO. 17	C.S. NO. 12	.2142	13.6522	-.0761

ST. NO.	C.S. NO.	RECORDED DATA	LOCAL RADIUS	DELTA RHO
ST. NO. 15	C.S. NO. 1	.2127	13.7487	.0204
ST. NO. 15	C.S. NO. 2	.2130	13.7293	.0010
ST. NO. 15	C.S. NO. 3	.2136	13.6906	-.0377
ST. NO. 15	C.S. NO. 4	.2125	13.7617	.0334
ST. NO. 15	C.S. NO. 5	.2109	13.8664	.1381
ST. NO. 15	C.S. NO. 6	.2123	13.7747	.0464
ST. NO. 15	C.S. NO. 7	.2087	14.0130	.2847
ST. NO. 15	C.S. NO. 8	.2103	13.9060	.1778
ST. NO. 15	C.S. NO. 9	.2095	13.9593	.2310
ST. NO. 15	C.S. NO. 10	.2110	13.8598	.1315
ST. NO. 15	C.S. NO. 11	.2106	13.8862	.1579
ST. NO. 15	C.S. NO. 12	.2102	13.9127	.1844

ST. NO.	C.S. NO.	RECORDED DATA	LOCAL RADIUS	DELTA RHO
ST. NO. 18	C.S. NO. 1	.2121	13.7877	.0594
ST. NO. 18	C.S. NO. 2	.2127	13.7487	.0204
ST. NO. 18	C.S. NO. 3	.2125	13.7617	.0334
ST. NO. 18	C.S. NO. 4	.2142	13.6522	-.0761
ST. NO. 18	C.S. NO. 5	.2169	13.4818	-.2465
ST. NO. 18	C.S. NO. 6	.2169	13.4818	-.2465
ST. NO. 18	C.S. NO. 7	.2174	13.4507	-.2776
ST. NO. 18	C.S. NO. 8	.2164	13.5130	-.2153
ST. NO. 18	C.S. NO. 9	.2160	13.5381	-.1902
ST. NO. 18	C.S. NO. 10	.2138	13.6778	-.0505
ST. NO. 18	C.S. NO. 11	.2139	13.6713	-.0569
ST. NO. 18	C.S. NO. 12	.2126	13.7552	.0269

			RECORDED	LOCAL	DELTA				RECORDED	LOCAL	DELTA
			DATA	RADIUS	RHO				DATA	RADIUS	RHO
ST. NO. 19	C.S. NO. 1		.2147	13.6203	-.1080	ST. NO. 22	C.S. NO. 1		.2166	13.5005	-.2278
ST. NO. 19	C.S. NO. 2		.2136	13.6906	-.0377	ST. NO. 22	C.S. NO. 2		.2167	13.4943	-.2340
ST. NO. 19	C.S. NO. 3		.2130	13.7293	.0010	ST. NO. 22	C.S. NO. 3		.2155	13.5696	-.1587
ST. NO. 19	C.S. NO. 4		.2120	13.7942	.0659	ST. NO. 22	C.S. NO. 4		.2153	13.5822	-.1461
ST. NO. 19	C.S. NO. 5		.2096	13.9526	.2243	ST. NO. 22	C.S. NO. 5		.2140	13.6649	-.0633
ST. NO. 19	C.S. NO. 6		.2100	13.9260	.1977	ST. NO. 22	C.S. NO. 6		.2125	13.7617	.0334
ST. NO. 19	C.S. NO. 7		.2104	13.8994	.1711	ST. NO. 22	C.S. NO. 7		.2140	13.6649	-.0633
ST. NO. 19	C.S. NO. 8		.2115	13.8269	.0986	ST. NO. 22	C.S. NO. 8		.2162	13.5255	-.2027
ST. NO. 19	C.S. NO. 9		.2121	13.7877	.0594	ST. NO. 22	C.S. NO. 9		.2174	13.4507	-.2776
ST. NO. 19	C.S. NO. 10		.2138	13.6778	-.0505	ST. NO. 22	C.S. NO. 10		.2163	13.5193	-.2090
ST. NO. 19	C.S. NO. 11		.2135	13.6970	-.0312	ST. NO. 22	C.S. NO. 11		.2159	13.5444	-.1839
ST. NO. 19	C.S. NO. 12		.2134	13.7035	-.0248	ST. NO. 22	C.S. NO. 12		.2170	13.4756	-.2527
			RECORDED	LOCAL	DELTA				RECORDED	LOCAL	DELTA
			DATA	RADIUS	RHO				DATA	RADIUS	RHO
ST. NO. 20	C.S. NO. 1		.2110	13.8598	.1315	ST. NO. 23	C.S. NO. 1		.2100	13.9260	.1977
ST. NO. 20	C.S. NO. 2		.2111	13.8532	.1249	ST. NO. 23	C.S. NO. 2		.2117	13.8138	.0855
ST. NO. 20	C.S. NO. 3		.2126	13.7552	.0269	ST. NO. 23	C.S. NO. 3		.2130	13.7293	.0010
ST. NO. 20	C.S. NO. 4		.2127	13.7487	.0204	ST. NO. 23	C.S. NO. 4		.2127	13.7487	.0204
ST. NO. 20	C.S. NO. 5		.2142	13.6522	-.0761	ST. NO. 23	C.S. NO. 5		.2139	13.6713	-.0569
ST. NO. 20	C.S. NO. 6		.2139	13.6713	-.0569	ST. NO. 23	C.S. NO. 6		.2157	13.5570	-.1713
ST. NO. 20	C.S. NO. 7		.2155	13.5696	-.1587	ST. NO. 23	C.S. NO. 7		.2152	13.5885	-.1397
ST. NO. 20	C.S. NO. 8		.2154	13.5759	-.1524	ST. NO. 23	C.S. NO. 8		.2136	13.6906	-.0377
ST. NO. 20	C.S. NO. 9		.2153	13.5822	-.1461	ST. NO. 23	C.S. NO. 9		.2133	13.7099	-.0184
ST. NO. 20	C.S. NO. 10		.2143	13.6458	-.0825	ST. NO. 23	C.S. NO. 10		.2146	13.6266	-.1016
ST. NO. 20	C.S. NO. 11		.2140	13.6649	-.0633	ST. NO. 23	C.S. NO. 11		.2137	13.6842	-.0441
ST. NO. 20	C.S. NO. 12		.2142	13.6522	-.0761	ST. NO. 23	C.S. NO. 12		.2119	13.8007	.0725
			RECORDED	LOCAL	DELTA				RECORDED	LOCAL	DELTA
			DATA	RADIUS	RHO				DATA	RADIUS	RHO
ST. NO. 21	C.S. NO. 1		.2136	13.6906	-.0377	ST. NO. 24	C.S. NO. 1		.2145	13.6330	-.0953
ST. NO. 21	C.S. NO. 2		.2130	13.7293	.0010	ST. NO. 24	C.S. NO. 2		.2124	13.7682	.0399
ST. NO. 21	C.S. NO. 3		.2124	13.7682	.0399	ST. NO. 24	C.S. NO. 3		.2120	13.7942	.0659
ST. NO. 21	C.S. NO. 4		.2127	13.7487	.0204	ST. NO. 24	C.S. NO. 4		.2128	13.7422	.0139
ST. NO. 21	C.S. NO. 5		.2125	13.7617	.0334	ST. NO. 24	C.S. NO. 5		.2135	13.6970	-.0312
ST. NO. 21	C.S. NO. 6		.2132	13.7164	-.0119	ST. NO. 24	C.S. NO. 6		.2129	13.7357	.0075
ST. NO. 21	C.S. NO. 7		.2104	13.8994	.1711	ST. NO. 24	C.S. NO. 7		.2125	13.7617	.0334
ST. NO. 21	C.S. NO. 8		.2092	13.9794	.2511	ST. NO. 24	C.S. NO. 8		.2134	13.7035	-.0248
ST. NO. 21	C.S. NO. 9		.2081	14.0535	.3252	ST. NO. 24	C.S. NO. 9		.2136	13.6906	-.0377
ST. NO. 21	C.S. NO. 10		.2095	13.9593	.2310	ST. NO. 24	C.S. NO. 10		.2117	13.8138	.0855
ST. NO. 21	C.S. NO. 11		.2107	13.8796	.1513	ST. NO. 24	C.S. NO. 11		.2114	13.8335	.1052
ST. NO. 21	C.S. NO. 12		.2113	13.8400	.1118	ST. NO. 24	C.S. NO. 12		.2120	13.7942	.0659

ST. NO.	C.S. NO.	RECORDED DATA	LOCAL RADIUS	DELTA RHO	ST. NO.	C.S. NO.	RECORDED DATA	LOCAL RADIUS	DELTA RHO
25	1	.2111	13.8532	.1249	28	1	.2135	13.6970	-.0312
25	2	.2122	13.7812	.0529	28	2	.2156	13.5633	-.1650
25	3	.2115	13.8269	.0986	28	3	.2155	13.5696	-.1587
25	4	.2107	13.8796	.1513	28	4	.2120	13.7942	.0659
25	5	.2103	13.9060	.1778	28	5	.2113	13.8400	.1118
25	6	.2096	13.9526	.2243	28	6	.2127	13.7487	.0204
25	7	.2120	13.7942	.0659	28	7	.2149	13.6076	-.1207
25	8	.2114	13.8335	.1052	28	8	.2146	13.6266	-.1016
25	9	.2099	13.9326	.2043	28	9	.2163	13.5193	-.2090
25	10	.2116	13.8204	.0921	28	10	.2159	13.5444	-.1839
25	11	.2121	13.7877	.0594	28	11	.2156	13.5633	-.1650
25	12	.2117	13.8138	.0855	28	12	.2144	13.6394	-.0889

ST. NO.	C.S. NO.	RECORDED DATA	LOCAL RADIUS	DELTA RHO	ST. NO.	C.S. NO.	RECORDED DATA	LOCAL RADIUS	DELTA RHO
26	1	.2125	13.7617	.0334	29	1	.2125	13.7617	.0334
26	2	.2136	13.6906	-.0377	29	2	.2126	13.7552	.0269
26	3	.2152	13.5885	-.1397	29	3	.2148	13.6139	-.1144
26	4	.2136	13.6906	-.0377	29	4	.2150	13.6012	-.1271
26	5	.2118	13.8073	.0790	29	5	.2147	13.6203	-.1080
26	6	.2121	13.7877	.0594	29	6	.2141	13.6585	-.0697
26	7	.2094	13.9660	.2377	29	7	.2136	13.6906	-.0377
26	8	.2092	13.9794	.2511	29	8	.2146	13.6266	-.1016
26	9	.2097	13.9459	.2177	29	9	.2121	13.7877	.0594
26	10	.2096	13.9526	.2243	29	10	.2123	13.7747	.0464
26	11	.2112	13.8466	-.1183	29	11	.2139	13.6713	-.0569
26	12	.2106	13.8862	.1579	29	12	.2147	13.6203	-.1080

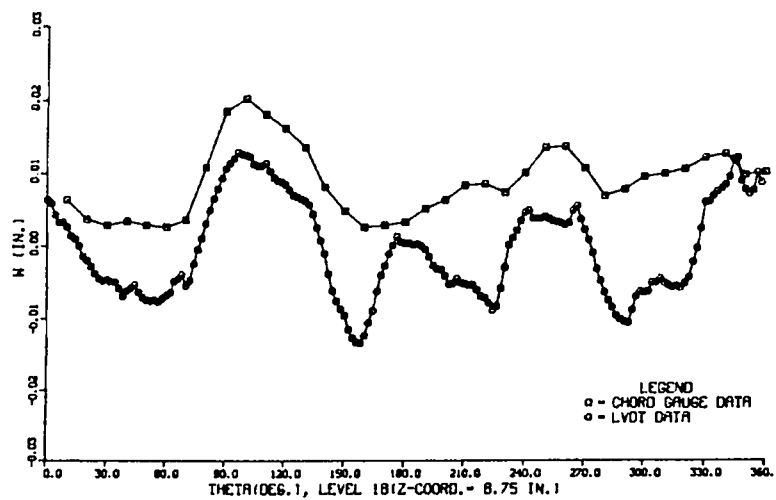
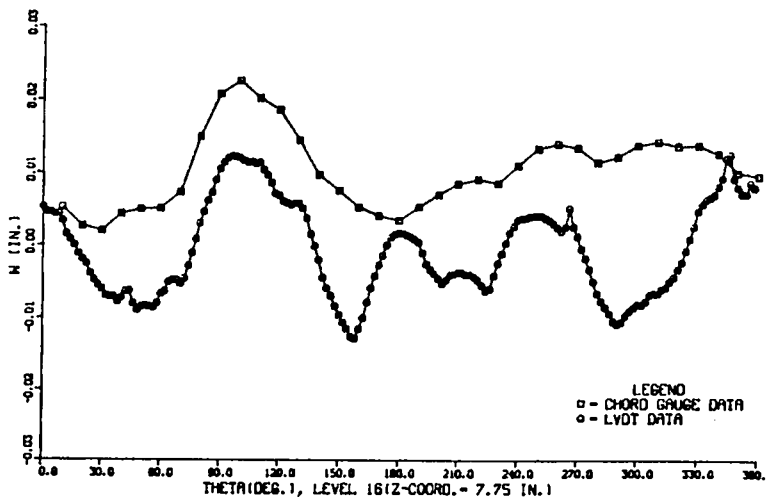
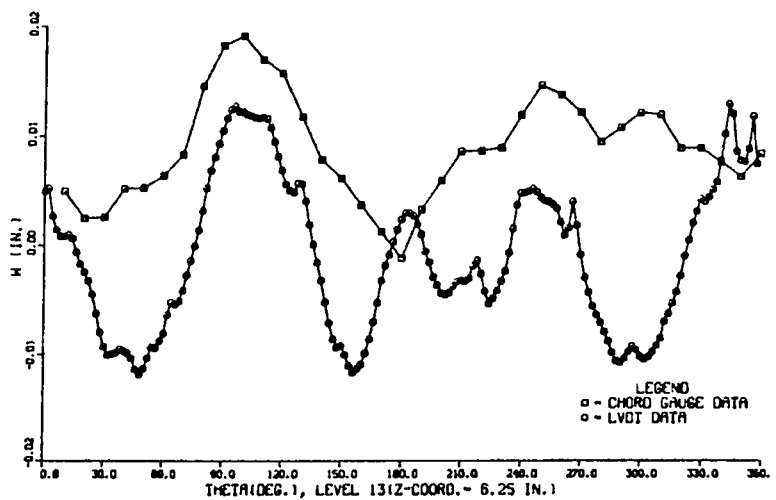
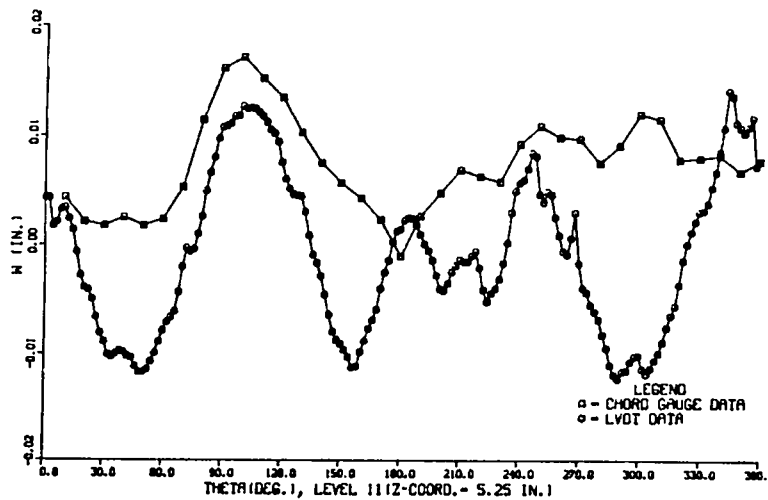
ST. NO.	C.S. NO.	RECORDED DATA	LOCAL RADIUS	DELTA RHO	ST. NO.	C.S. NO.	RECORDED DATA	LOCAL RADIUS	DELTA RHO
27	1	.2118	13.8073	.0790	30	1	.2149	13.6076	-.1207
27	2	.2080	14.0603	.3320	30	2	.2142	13.6522	-.0761
27	3	.2064	14.1696	.4413	30	3	.2136	13.6906	-.0377
27	4	.2105	13.8928	.1645	30	4	.2147	13.6203	-.1080
27	5	.2133	13.7099	-.0184	30	5	.2152	13.5885	-.1397
27	6	.2132	13.7164	-.0119	30	6	.2146	13.6266	-.1016
27	7	.2131	13.7228	-.0055	30	7	.2138	13.6778	-.0505
27	8	.2134	13.7035	-.0248	30	8	.2121	13.7877	.0594
27	9	.2132	13.7164	-.0119	30	9	.2150	13.6012	-.1271
27	10	.2136	13.6906	-.0377	30	10	.2152	13.5885	-.1397
27	11	.2119	13.8007	.0725	30	11	.2130	13.7293	.0010
27	12	.2135	13.6970	-.0312	30	12	.2130	13.7293	.0010

			RECORDED DATA	LOCAL RADIUS	DELTA RHO				RECORDED DATA	LOCAL RADIUS	DELTA RHO		
ST. NO.	31	C.S. NO.	1	.2150	13.6012	-.1271	ST. NO.	34	C.S. NO.	1	.2144	13.6394	-.0889
ST. NO.	31	C.S. NO.	2	.2157	13.5570	-.1713	ST. NO.	34	C.S. NO.	2	.2157	13.5570	-.1713
ST. NO.	31	C.S. NO.	3	.2158	13.5507	-.1776	ST. NO.	34	C.S. NO.	3	.2167	13.4943	-.2340
ST. NO.	31	C.S. NO.	4	.2135	13.6970	-.0312	ST. NO.	34	C.S. NO.	4	.2169	13.4818	-.2465
ST. NO.	31	C.S. NO.	5	.2130	13.7293	.0010	ST. NO.	34	C.S. NO.	5	.2149	13.6076	-.1207
ST. NO.	31	C.S. NO.	6	.2136	13.6906	-.0377	ST. NO.	34	C.S. NO.	6	.2133	13.7099	-.0184
ST. NO.	31	C.S. NO.	7	.2158	13.5507	-.1776	ST. NO.	34	C.S. NO.	7	.2110	13.8598	.1315
ST. NO.	31	C.S. NO.	8	.2158	13.5507	-.1776	ST. NO.	34	C.S. NO.	8	.2132	13.7164	-.0119
ST. NO.	31	C.S. NO.	9	.2129	13.7357	.0075	ST. NO.	34	C.S. NO.	9	.2104	13.8994	.1711
ST. NO.	31	C.S. NO.	10	.2120	13.7942	.0659	ST. NO.	34	C.S. NO.	10	.2102	13.9127	.1844
ST. NO.	31	C.S. NO.	11	.2152	13.5885	-.1397	ST. NO.	34	C.S. NO.	11	.2083	14.0399	.3117
ST. NO.	31	C.S. NO.	12	.2138	13.6778	-.0505	ST. NO.	34	C.S. NO.	12	.2072	14.1147	.3864
			RECORDED DATA	LOCAL RADIUS	DELTA RHO				RECORDED DATA	LOCAL RADIUS	DELTA RHO		
ST. NO.	32	C.S. NO.	1	.2114	13.8335	.1052	ST. NO.	35	C.S. NO.	1	.2108	13.8730	.1447
ST. NO.	32	C.S. NO.	2	.2112	13.8466	.1183	ST. NO.	35	C.S. NO.	2	.2114	13.8335	.1052
ST. NO.	32	C.S. NO.	3	.2119	13.8007	.0725	ST. NO.	35	C.S. NO.	3	.2121	13.7877	.0594
ST. NO.	32	C.S. NO.	4	.2133	13.7099	-.0184	ST. NO.	35	C.S. NO.	4	.2129	13.7357	.0075
ST. NO.	32	C.S. NO.	5	.2129	13.7357	.0075	ST. NO.	35	C.S. NO.	5	.2147	13.6203	-.1080
ST. NO.	32	C.S. NO.	6	.2121	13.7877	.0594	ST. NO.	35	C.S. NO.	6	.2132	13.7164	-.0119
ST. NO.	32	C.S. NO.	7	.2113	13.8400	.1118	ST. NO.	35	C.S. NO.	7	.2169	13.4818	-.2465
ST. NO.	32	C.S. NO.	8	.2136	13.6906	-.0377	ST. NO.	35	C.S. NO.	8	.2133	13.7099	-.0184
ST. NO.	32	C.S. NO.	9	.2145	13.6330	-.0953	ST. NO.	35	C.S. NO.	9	.2155	13.5696	-.1587
ST. NO.	32	C.S. NO.	10	.2145	13.6330	-.0953	ST. NO.	35	C.S. NO.	10	.2133	13.7099	-.0184
ST. NO.	32	C.S. NO.	11	.2122	13.7812	.0529	ST. NO.	35	C.S. NO.	11	.2172	13.4631	-.2652
ST. NO.	32	C.S. NO.	12	.2131	13.7228	-.0055	ST. NO.	35	C.S. NO.	12	.2155	13.5696	-.1587
			RECORDED DATA	LOCAL RADIUS	DELTA RHO				RECORDED DATA	LOCAL RADIUS	DELTA RHO		
ST. NO.	33	C.S. NO.	1	.2140	13.6649	-.0633	ST. NO.	36	C.S. NO.	1	.2135	13.6970	-.0312
ST. NO.	33	C.S. NO.	2	.2120	13.7942	.0659	ST. NO.	36	C.S. NO.	2	.2135	13.6970	-.0312
ST. NO.	33	C.S. NO.	3	.2111	13.8532	.1249	ST. NO.	36	C.S. NO.	3	.2117	13.8138	.0855
ST. NO.	33	C.S. NO.	4	.2103	13.9060	.1778	ST. NO.	36	C.S. NO.	4	.2107	13.8796	.1513
ST. NO.	33	C.S. NO.	5	.2126	13.7552	.0269	ST. NO.	36	C.S. NO.	5	.2089	13.9995	.2712
ST. NO.	33	C.S. NO.	6	.2143	13.6458	-.0825	ST. NO.	36	C.S. NO.	6	.2123	13.7747	.0464
ST. NO.	33	C.S. NO.	7	.2151	13.5949	-.1334	ST. NO.	36	C.S. NO.	7	.2084	14.0332	.3049
ST. NO.	33	C.S. NO.	8	.2130	13.7293	.0010	ST. NO.	36	C.S. NO.	8	.2105	13.8928	.1645
ST. NO.	33	C.S. NO.	9	.2141	13.6585	-.0697	ST. NO.	36	C.S. NO.	9	.2090	13.9928	.2645
ST. NO.	33	C.S. NO.	10	.2151	13.5949	-.1334	ST. NO.	36	C.S. NO.	10	.2124	13.7682	.0399
ST. NO.	33	C.S. NO.	11	.2152	13.5885	-.1397	ST. NO.	36	C.S. NO.	11	.2104	13.8994	.1711
ST. NO.	33	C.S. NO.	12	.2170	13.4756	-.2527	ST. NO.	36	C.S. NO.	12	.2118	13.8073	.0790

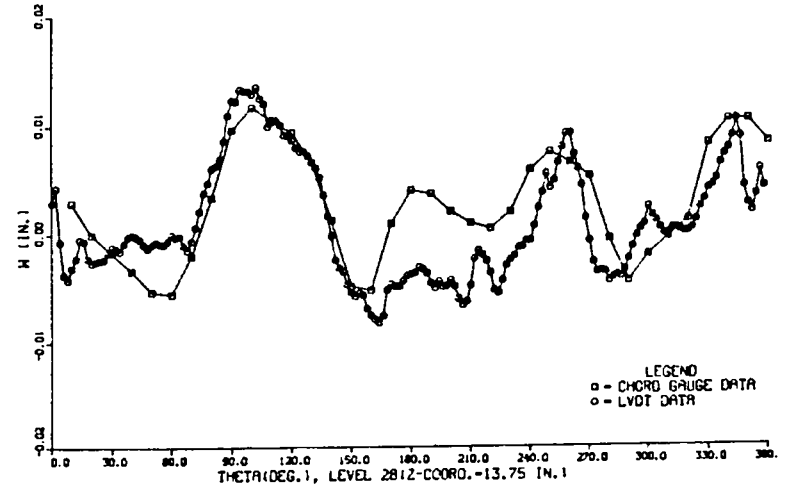
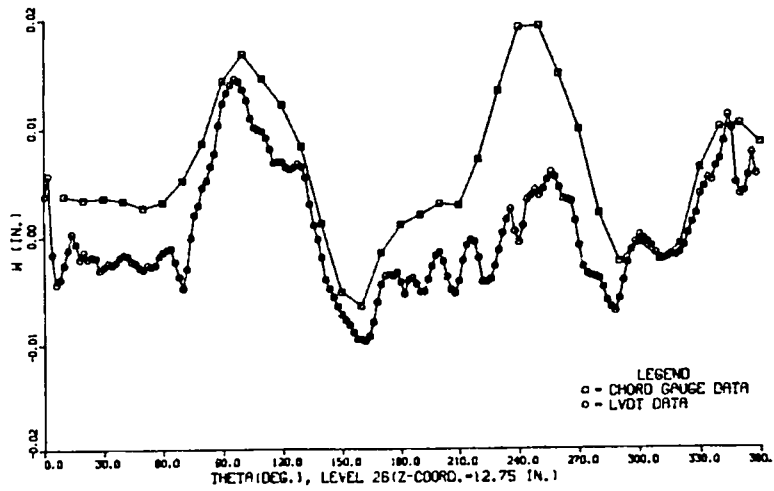
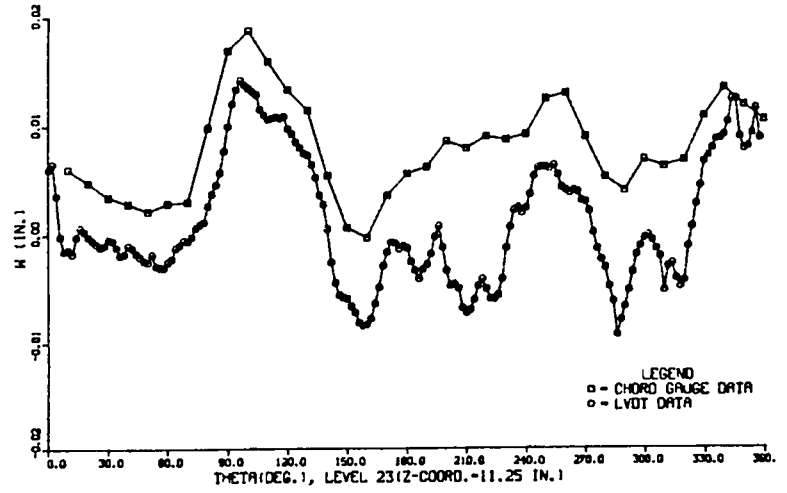
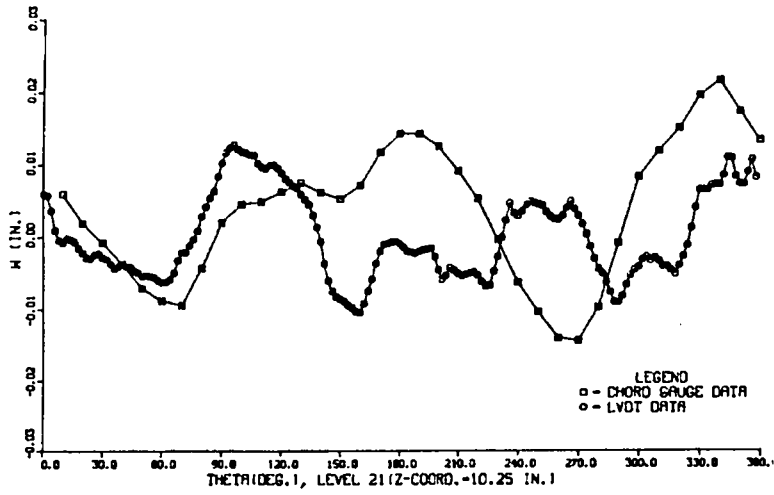
AVERAGE CHORD GAGE RADIUS OF CURVATURE AT CROSS SECTION 1 IS = 13.72140
AVERAGE CHORD GAGE RADIUS OF CURVATURE AT CROSS SECTION 2 IS = 13.72855
AVERAGE CHORD GAGE RADIUS OF CURVATURE AT CROSS SECTION 3 IS = 13.72681
AVERAGE CHORD GAGE RADIUS OF CURVATURE AT CROSS SECTION 4 IS = 13.73230
AVERAGE CHORD GAGE RADIUS OF CURVATURE AT CROSS SECTION 5 IS = 13.72925
AVERAGE CHORD GAGE RADIUS OF CURVATURE AT CROSS SECTION 6 IS = 13.72926
AVERAGE CHORD GAGE RADIUS OF CURVATURE AT CROSS SECTION 7 IS = 13.72630
AVERAGE CHORD GAGE RADIUS OF CURVATURE AT CROSS SECTION 8 IS = 13.72788
AVERAGE CHORD GAGE RADIUS OF CURVATURE AT CROSS SECTION 9 IS = 13.73200
AVERAGE CHORD GAGE RADIUS OF CURVATURE AT CROSS SECTION 10 IS = 13.72804
AVERAGE CHORD GAGE RADIUS OF CURVATURE AT CROSS SECTION 11 IS = 13.72922
AVERAGE CHORD GAGE RADIUS OF CURVATURE AT CROSS SECTION 12 IS = 13.72833

AVERAGE RADIUS FROM ALL DATA POINTS = 13.72828

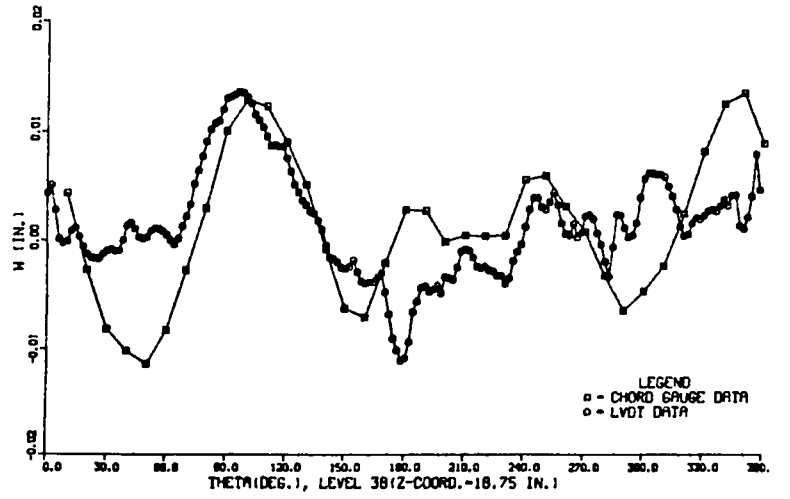
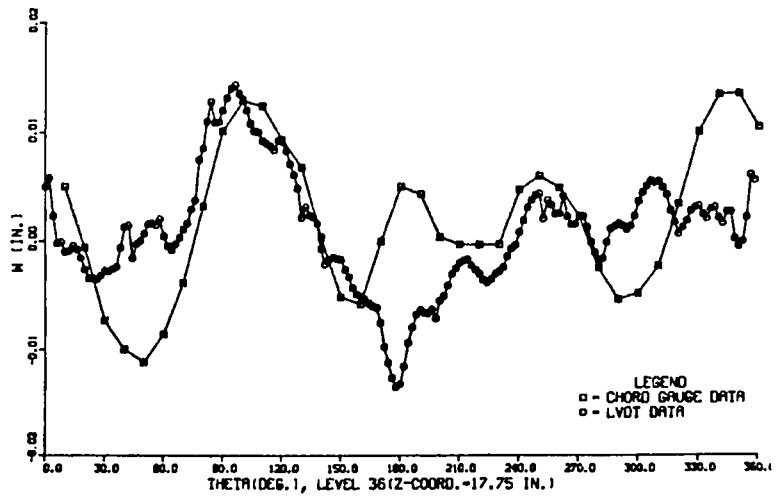
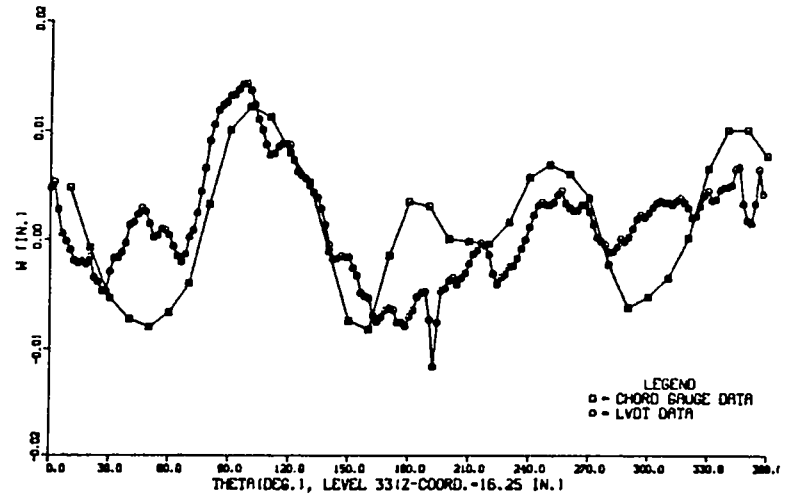
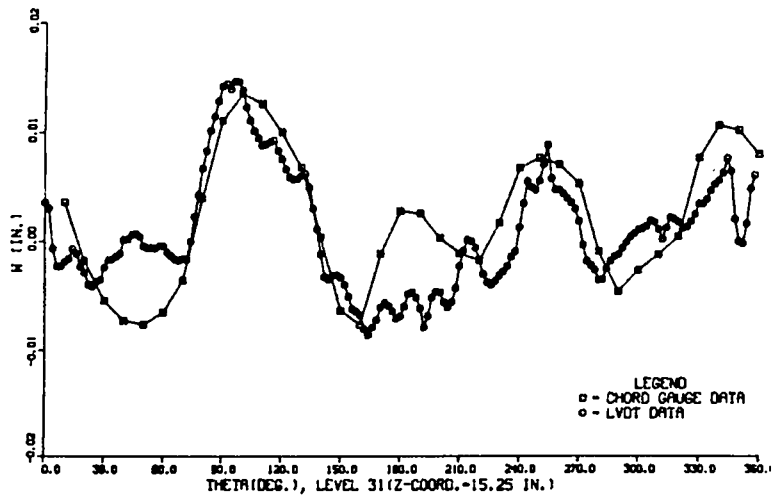
APPENDIX C
COMPARISON OF LVDT AND CHORD GAGE RESULTS



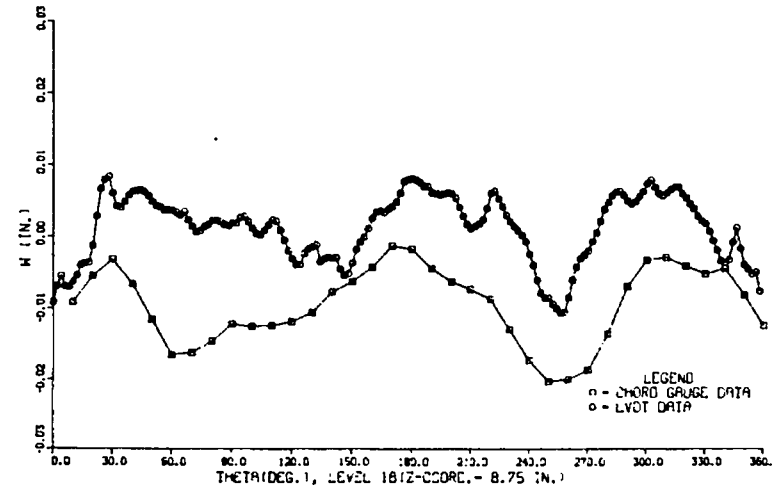
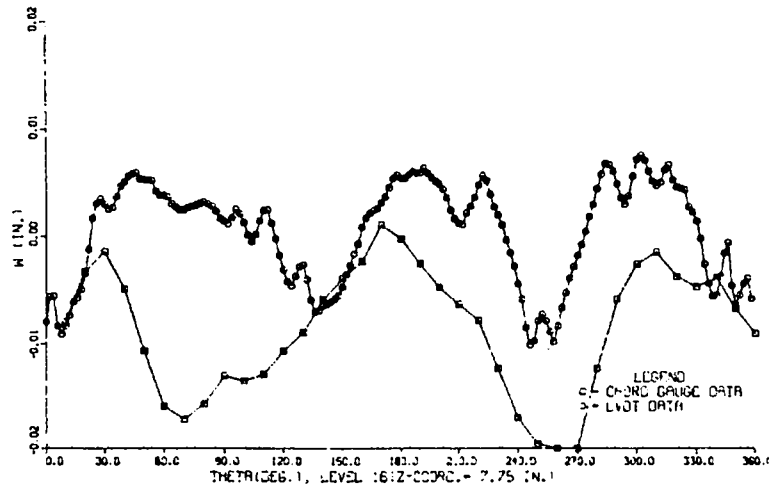
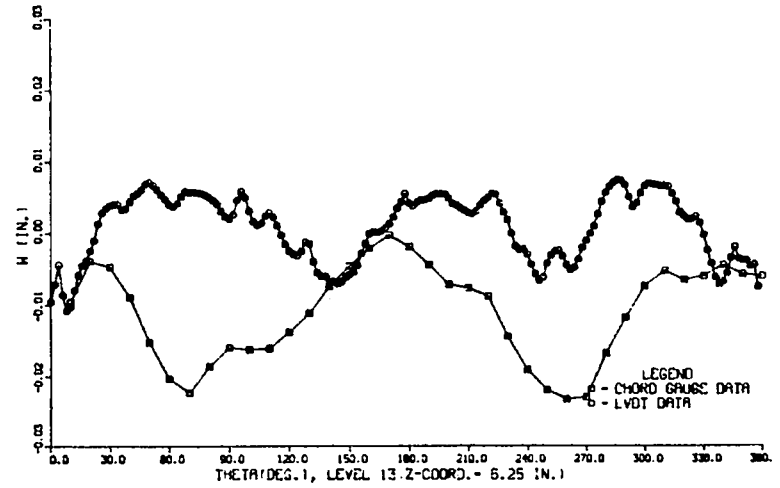
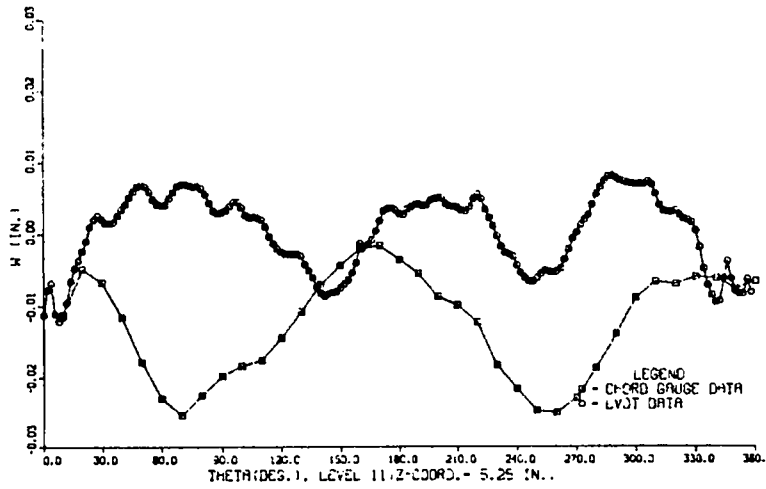
Cylinder 1



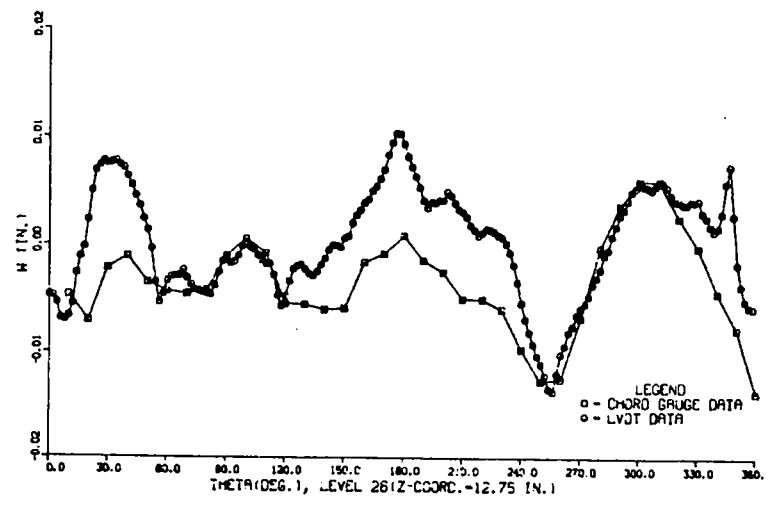
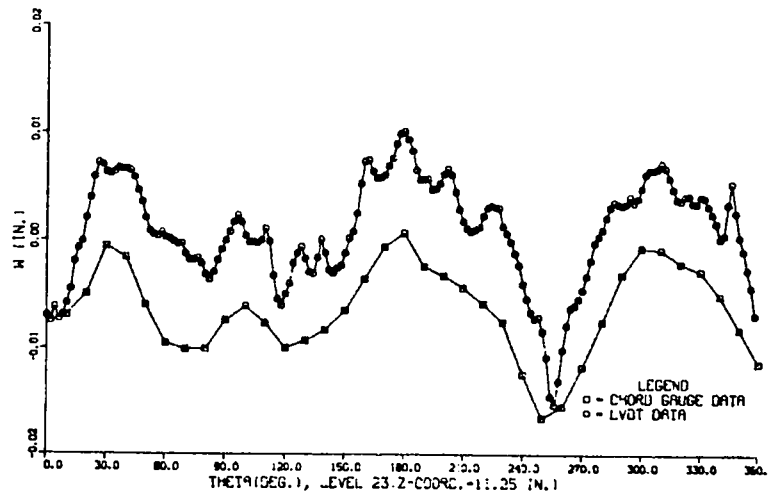
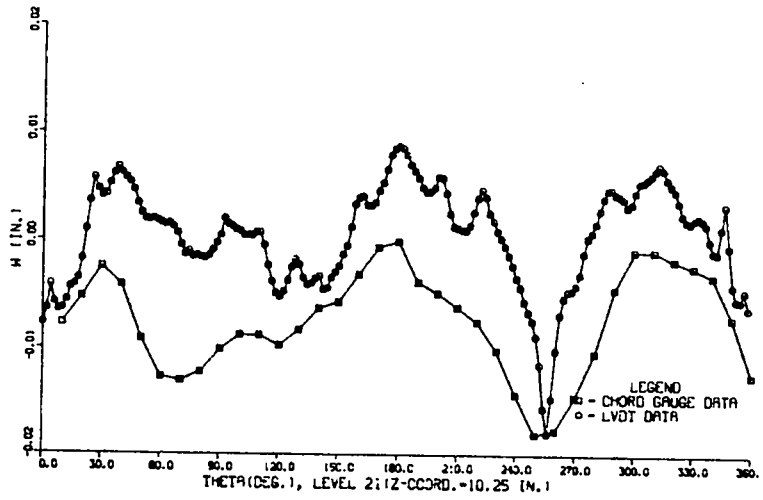
Cylinder 1



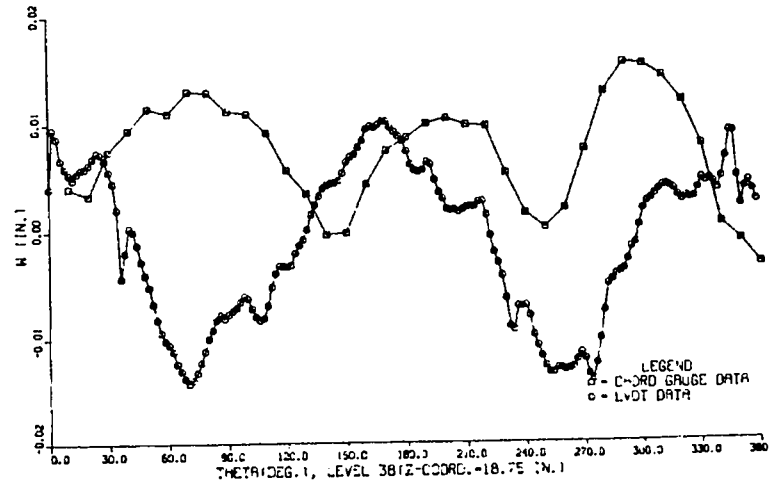
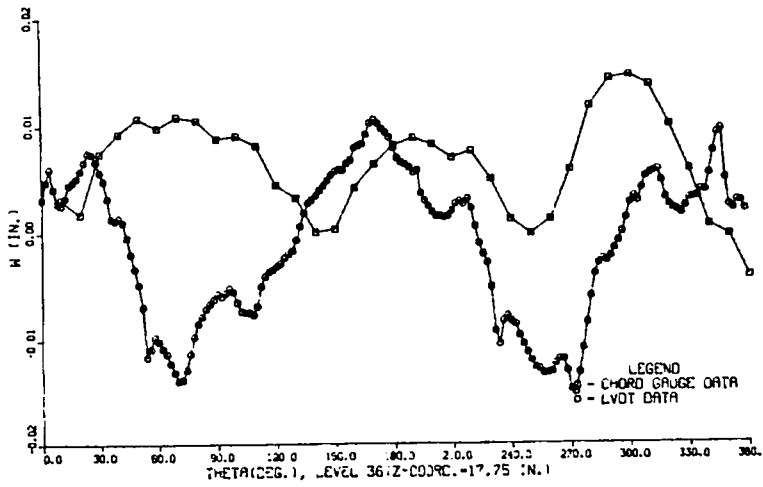
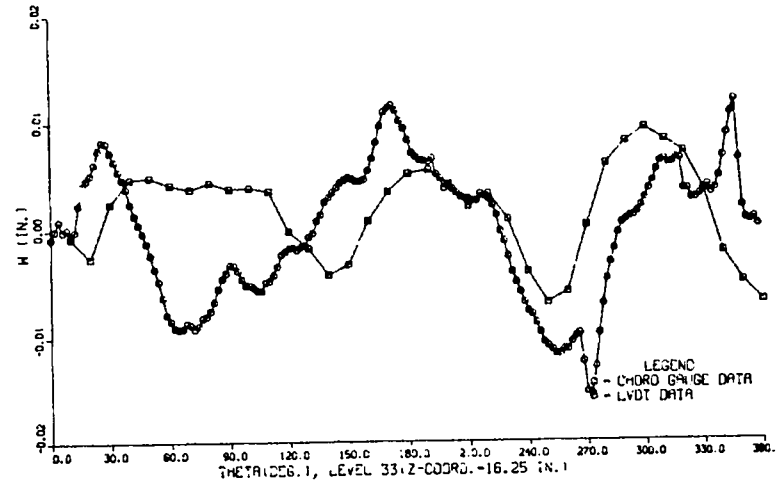
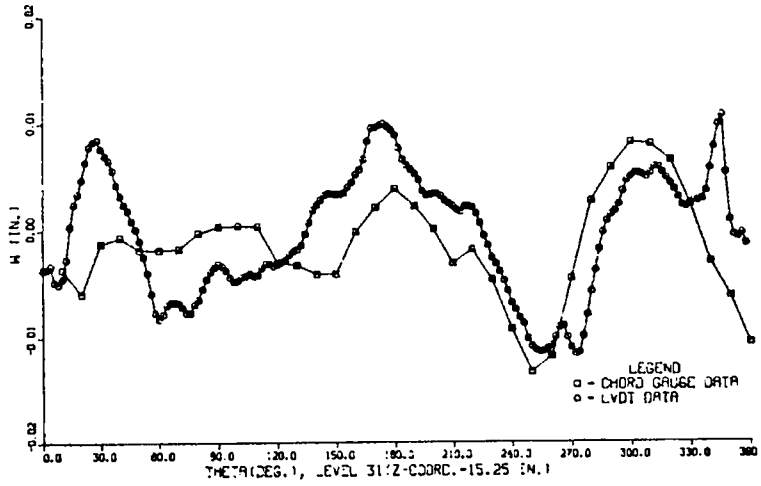
Cylinder 1



Cylinder 2



Cylinder 2



Cylinder 2

DISTRIBUTION

	<u>Copies</u>
Nuclear Regulatory Commission, RF, Bethesda, Maryland	288
Technical Information Center, Oak Ridge,	2
Los Alamos National Laboratory, Los Alamos, New Mexico	<u>50</u>
	340

Available from
GPO Sales Program
Division of Technical Information and Document Control
US Nuclear Regulatory Commission
Washington, DC 20555
and
National Technical Information Service
Springfield, VA 22161

Los Alamos